

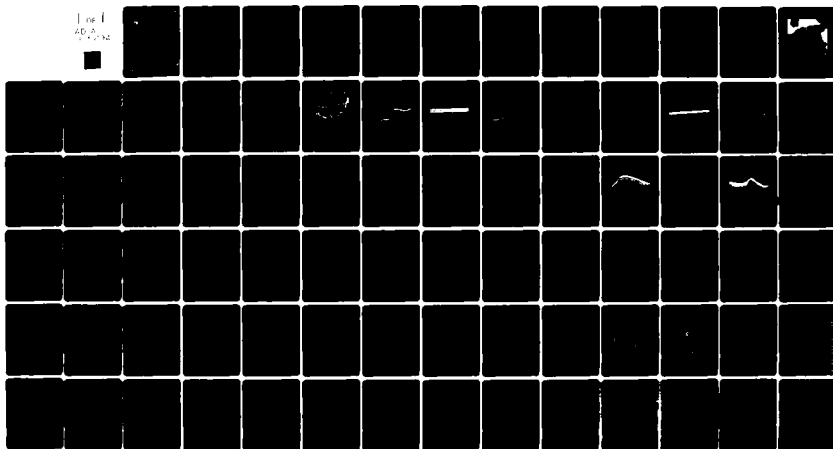
AD-A115 290

NAVAL OCEAN RESEARCH AND DEVELOPMENT ACTIVITY NSTL 5--ETC F/G 20/1  
GEOACOUSTIC MODELS FOR THE STRAITS OF SICILY AND SARDINIA-TUNIS--ETC(U)  
APR 82 J E MATTHEWS  
NORDA-TN-99

UNCLASSIFIED

NL

1 of 1  
AD-A115 290



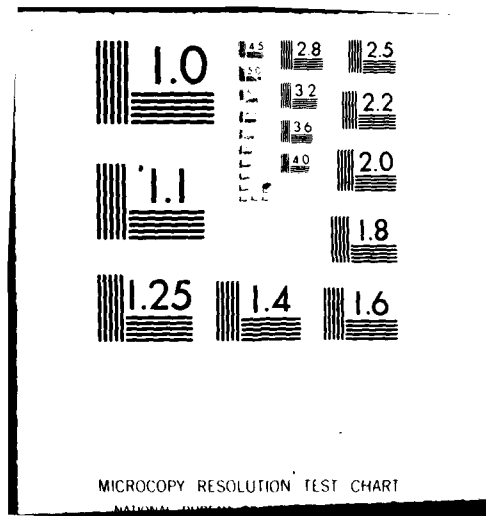
END

DATE

FILED

7-82

DTIC



13

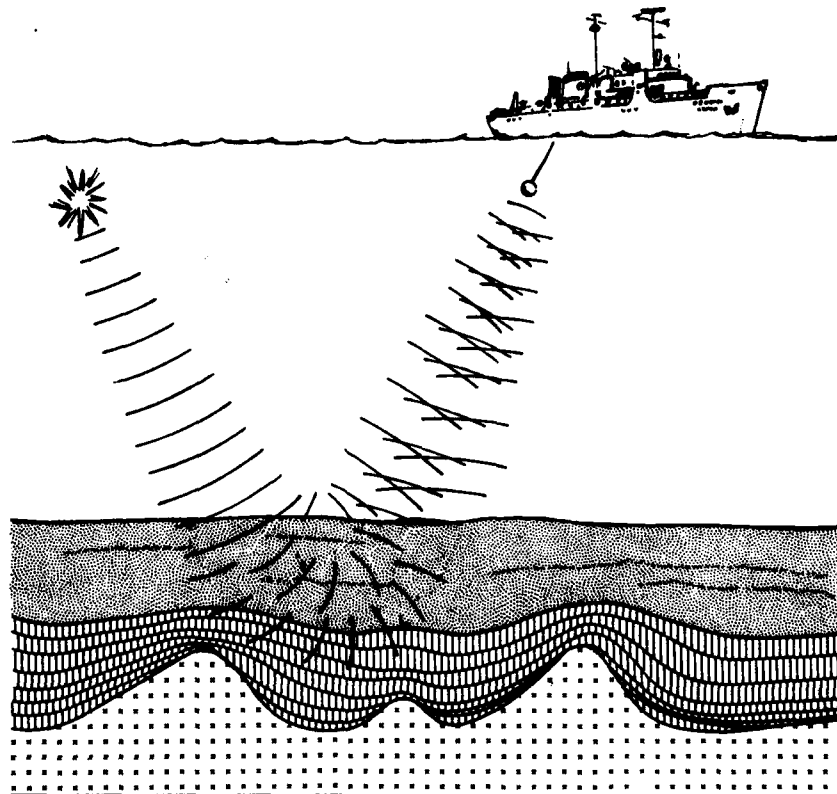
NORDA Technical Note 99

Naval Ocean Research and  
Development Activity  
NSTL Station, Mississippi 39529



## Geoacoustic Models for the Straits of Sicily and Sardinia-Tunisia

AD A115294



DTIC FILE COPY

J.E. Matthews

Sea Floor Division  
Ocean Science and Technology Laboratory

April 1982

DISTRIBUTION STATEMENT A

Approved for public release;  
Distribution Unlimited

DTIC  
ELECTE

JUN 9 1982

D

82 000 001

# EXECUTIVE SUMMARY

This publication documents the derivation of geoacoustic models for the Straits of Sicily and Sardinia-Tunisia. The geologic description of the region is based upon published geological/geophysical papers and archive data. The zone of primary concern is the first few hundred meters below the sea floor, which, in the present case, consists of unlithified Quaternary-Pliocene sediments. Lying below this upper layer is acoustic basement, which consists of Miocene chalks and limestones or evaporites. The modeling procedures developed by E. L. Hamilton were then used to estimate the physical properties of these sediment types. Finally, bottom loss as a function of grazing angle at a variety of frequencies was computed for the sea floor models.

Accession For	
NTIS GRA&I	<input checked="" type="checkbox"/>
DTIC TAB	<input type="checkbox"/>
Unannounced	<input type="checkbox"/>
Justification	
By	
Distribution/	
Availability Codes	
Dist	Avail and/or Special
A	



#### ACKNOWLEDGEMENTS

I am greatly indebted to E. L. Hamilton of the Naval Ocean Systems Center (NOSC) for his valuable discussions over the past few years on geoacoustic modeling. K. E. Gilbert of NORDA provided computer programs for the computation of bottom loss. H. C. Eppert and J. A. Green of NORDA critically read the manuscript, and L. H. McRaney of NORDA provided editorial assistance. R. A. Edman of NORDA did the illustrations, including the bathymetry. Funding was provided by the Navy Scientific Assistance Program, and the Naval Electronics System Command, and NORDA's Environmental Requirements and Program Analysis Group.

## CONTENTS

	Page
I. INTRODUCTION	1
II. REGIONAL GEOLOGIC SETTING	2
III. REGIONAL OCEANOGRAPHIC SETTING	6
IV. STRAIT OF SICILY	10
A. PHYSIOGRAPHY AND GEOLOGY	10
B. SEISMIC STRATIGRAPHY	11
C. DISTRIBUTION OF QUATERNARY-PLIOCENE SEDIMENTS	22
D. GEOACOUSTIC MODELS	23
V. STRAIT OF SARDINIA-TUNISIA	30
A. PHYSIOGRAPHY AND GEOLOGY	30
B. SEISMIC STRATIGRAPHY	31
C. DISTRIBUTION OF QUATERNARY-PLIOCENE SEDIMENTS	34
D. GEOACOUSTIC MODELS	36
VI. BOTTOM LOSS CALCULATIONS	36
VII. REFERENCES	69
BACK POCKET	

PLATE I - Bathymetry of the Straits of Sicily and  
Sardinia-Tunisia; with Acoustic Bottom  
Interaction Province Classification

## GEOACOUSTIC MODELS FOR THE STRAITS OF SICILY AND SARDINIA-TUNISIA

### I. INTRODUCTION

Many active and passive sonar systems are, to some extent, dependent upon sound energy that has interacted with the sea floor. During much of the 1960's, interest in acoustic bottom interaction was directed toward high-frequency (kilohertz range) active sonars, and requirements were met by global bottom loss measurement programs. During the 1970's interest in bottom interactive acoustic energy was expanded to other frequency ranges, to environments other than just the deep ocean basins, and to systems which were sometimes best supported by physical descriptions of the sea floor rather than bottom loss measurements alone. Much of this interest was generated by the undersea surveillance community. The geoacoustic model came into existence with this increased interest in acoustic bottom interaction. The concept of the geoacoustic model is defined by its developer (Hamilton, 1980) as: "a model of the real sea floor with emphasis on measured, extrapolated, and predicted values of those properties important in underwater acoustics and those aspects of geophysics involving sound transmission."

This report presents the development of a geoacoustic model for an area of the central Mediterranean Sea, specifically, the Straits of Sicily and Sardinia-Tunisia. Continuous seismic reflection profiles, 3.5 kHz bathymetry, sediment cores, and published geological/geophysical reports are used to ascertain the sediment types and stratigraphic units present beneath the sea floor. Published empirical relationships between sediment type and sediment physical properties are then used to construct geoacoustic models. Theoretical bottom loss curves were then computed from the geoacoustic models. The general conclusion is that the shallow water regions are predominantly calcium carbonate sands, which are predicted to have the response of a high-velocity (greater than bottom water) semi-infinite half-space. This would suggest a reflective bottom at all frequencies. The deeper water regions are generally covered with fine-grained, stratified sediments (terrigenous and hemipelagic). The estimated velocity gradient for these sediments is  $1.5 \text{ s}^{-1}$ . These would sustain the diving wave refraction, producing low loss at low frequency, and the layering would produce a reflective bottom at high frequency. Thus, the sea floor in the entire region of study would be expected to have relatively low bottom loss at all frequencies.

A second, significantly different approach to determining sea floor parameters is also commonly used. This second approach consists of modeling measured acoustic data (usually bottom loss or transmission loss), while varying sea floor parameters until a fit is achieved. The sea floor parameters determined in this manner are not necessarily in agreement with direct measurements of these parameters, nor do they constitute a unique solution. The author therefore suggests the terms "acoustically equivalent" or "equivalent" bottom model to distinguish this second type of sea floor parameterization from what is presented here and defined in the literature as a geoacoustical model. Equivalent models are very useful; however, if the parameters determined in this manner differ significantly from the known range for physical properties, some propagation mechanism has not been properly accounted for in the equivalent model determination. On the other hand the conversion of a geologic description into a geoacoustic model can also result in error, but for different reasons. Thus, a clear distinction between these approaches and their shortcomings should be maintained.

## II. REGIONAL GEOLOGIC SETTING

From a geological/geophysical point of view, the Mediterranean Sea is highly complex, being composed of several distinct oceanic basins and land masses. The tectonic and sedimentary histories of the region have long been the subject of debate, as discussed at length in Nairn et al. (1977, 1978) and Stanley (1972). It is not the purpose here to enter this debate, but merely to summarize the descriptive geologic data and theory relevant to acoustic interaction with the sea floor. Such descriptions, however, are often inseparable from a plate tectonic context.

The Strait of Sicily and the Strait of Sardinia-Tunisia\* are in the central Mediterranean Sea, between the African Continent and the Islands of Sicily and Sardinia (Fig. 1). Figure 2 shows the limits of the bathymetry chart (Plate I) and outlines the specific area of interest. The sea floors of the Strait of Sicily and the Strait of Sardinia-Tunisia, however, are not generally believed to have a common origin. The present-day plate boundary runs down the Italian peninsula, through the Island of Sicily, and across to northern Tunisia. This zone is well-delineated by present-day seismic and volcanic activity and contrasting structural provinces (Fig. 3). Most of the Strait of Sicily is on the same crustal plate as Africa and is generally believed to represent a submerged portion of the African Continent. This submergence was probably related to the Alpine orogeny and was essentially completed by Late Miocene time. Gravimetric, magnetic, and reflection seismic data (Finetti and Morelli, 1973) support the interpretation that the strait is underlain by thick continental crust. Drill data in the strait (Finetti and Morelli, 1973) indicate that much of this thick section is Tertiary, shallow-water limestone.

The islands of Sardinia and Corsica are generally believed to have separated from the European continent during the Tertiary and moved to the southeast (relative to a stationary Europe), and rotated counter-clockwise to their present position. The crust between Sardinia and Africa is thus related to the origin of the Tyrrhenian and the Algerian Basins.

The origin of the Tyrrhenian Basin is not well understood. The deeper portions of the basin have Bouguer gravity anomalies in excess of +200 milligals, indicating relatively thin crust (Allen and Morelli, 1971). Magnetic anomalies (Finetti and Morelli, 1973) reflect only the numerous seamounts of the basin which have yielded dredge samples of Paleozoic and Triassic age (Heezen et al., 1971). Seismic wide-angle reflection data (Finetti and Morelli, 1973) indicate a mantle of 8.2 km/sec velocity at a depth of 12 kilometers (km), a depth in agreement with the gravity data. Continuous seismic reflection profiles reveal approximately 200 meters (m) of unconsolidated sediment over evaporites (Ryan et al., 1965, 1970), and wide-angle reflection data (Finetti and Morelli, 1973) indicate a kilometer of evaporites and approximately two kilometers of pre-evaporite sedimentary rock. All theories that have been proposed for the origin of the basin (Permian-age basin, founded continental craton, back-arc basin) suggest "marginal sea" or "back-arc" type origins (Hsu, 1977) as opposed to a "typical" ocean basin formed by rifting (similarly to the North Atlantic).

\*NOTE: The term Strait of Sardinia-Tunisia is neither an official nor recognized name and is not found on Department of Defense maps or charts. It is used purely as a convenience when referring to the region lying between the Island of Sardinia and the African Continent.

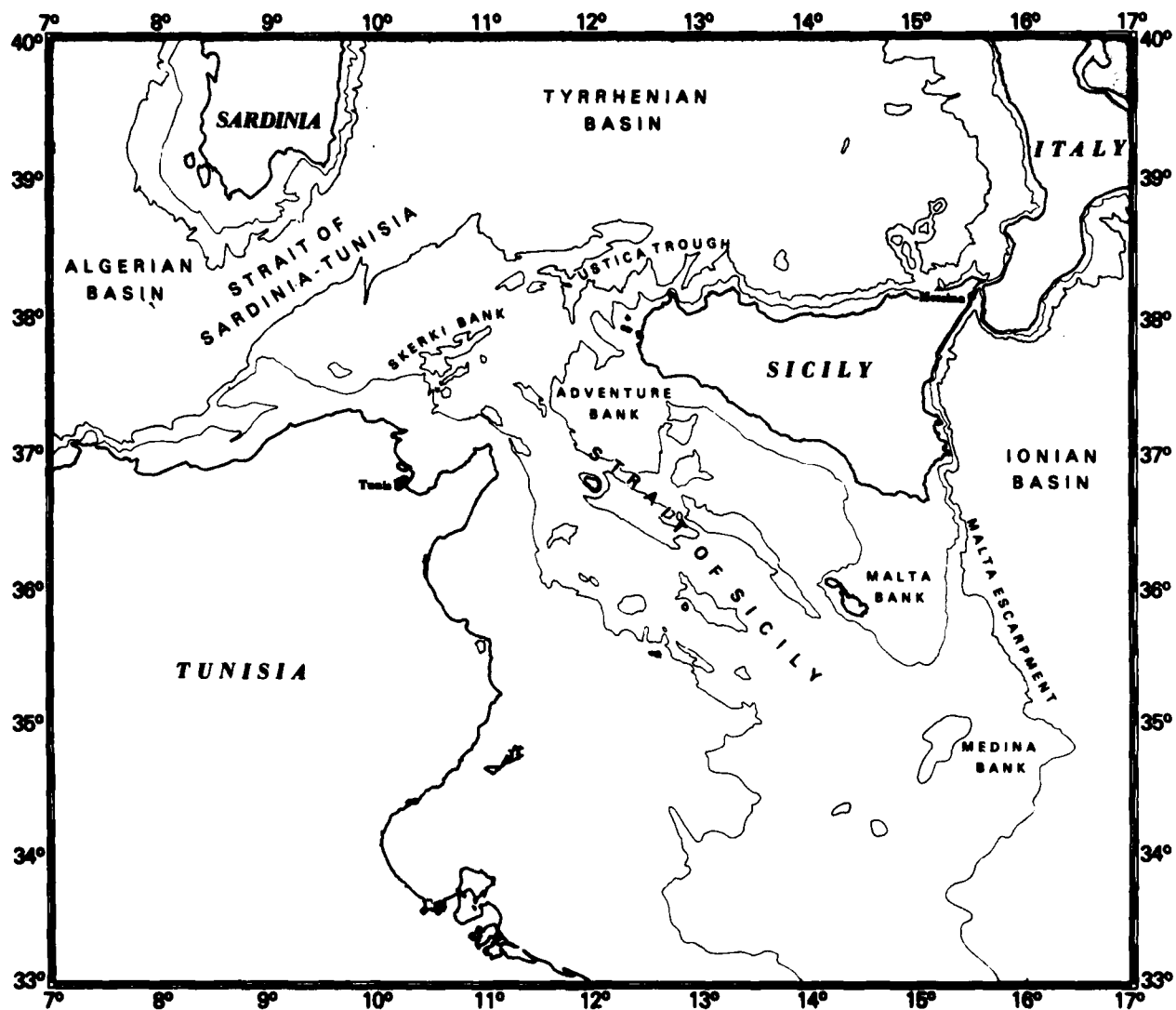


Figure 1. Geographic names of the central Mediterranean Sea

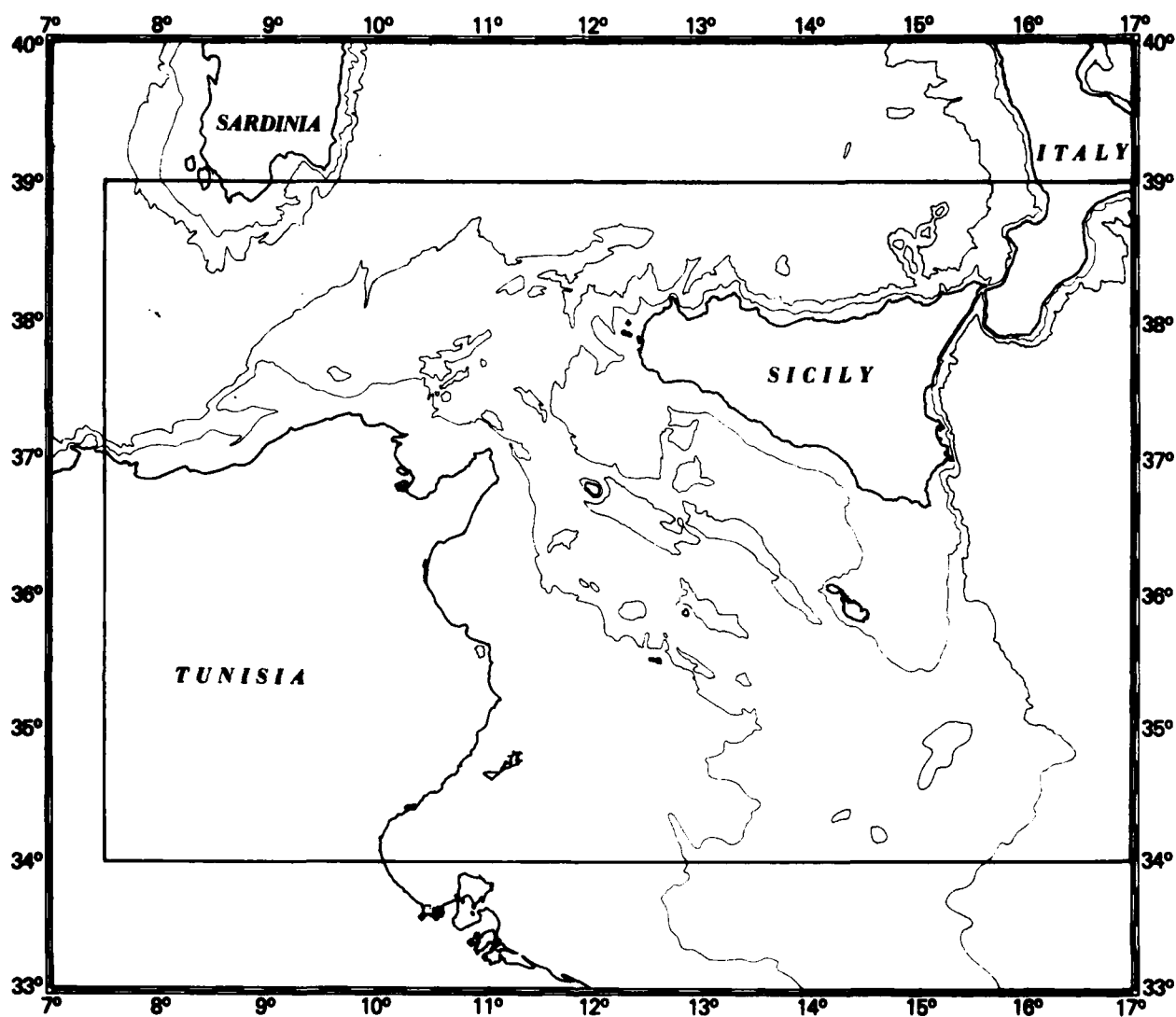


Figure 2. Regional map of the Straits of Sicily and Sardinia-Tunisia, showing the limits of Plate 1

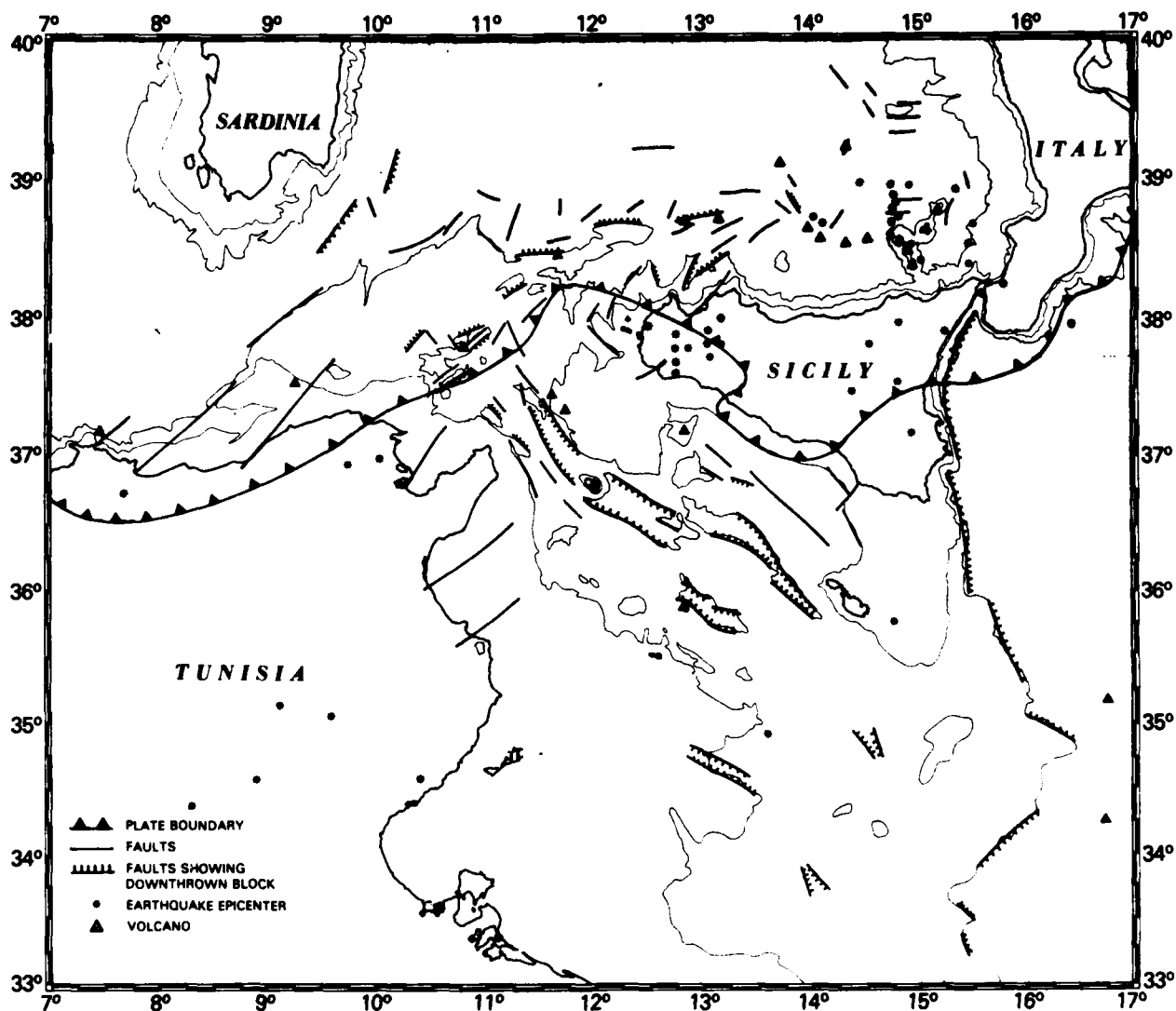


Figure 3. Tectonic map of the Straits of Sicily and Sardinia-Tunisia illustrating the plate boundary, volcanoes, earthquake epicenters, and major faults. Modified from Finetti and Morelli (1973), Lort (1977), Boccaletti and Manetti (1978).

The Algerian Basin, on the other hand, is generally considered to have been formed by rifting and creation of crust between what is now France/Spain on the one side and Sardinia/Corsica/Africa on the other. Lort (1977) summarizes and references the theories that have been proposed. The models for opening vary, but generally propose an opening of the Provencal Basin in Middle to Upper Oligocene, and a Lower to Middle Miocene age for initial opening of the Algerian Basin. Seismic reflection profiles indicate thicknesses of unconsolidated Quaternary-Pliocene sediment in excess of a kilometer (Stanley, 1977), and seismic refraction and wide-angle reflection data indicate a total sediment thickness of at least 13 km (Finetti and Morelli, 1973). Seismic reflection profiles in the Strait of Sardinia (Auzende et al., 1971) indicate continuity of Paleocene basement between Sardinia and Tunisia. Therefore, it is likely that the crustal material in the Strait of Sardinia-Tunisia may be more kindred to the Tyrrhenian Basin and is not of simple oceanic origin, but represents part of a pre-Oligocene basin and includes the continental margins of Africa and Sardinia (previously European continental margin). Seismic reflection profiles do indicate the presence of the Miocene evaporite sequence in the strait. The origin of the evaporites is also a subject of debate (Sonnenfeld, 1975 and Curzi et al., 1980), but their presence is characteristic of the Mediterranean basins that existed in Miocene time, and is very thin or absent on the continental and insular shelves, such as the Strait of Sicily. Whatever the early history of these straits, by Late Miocene time the Strait of Sicily was tensionally faulted and formed the submerged portion of the Tunisian Shelf, and the Strait of Sardinia-Tunisia was a faulted remnant of a pre-Oligocene basin which bordered the continental margins of Sardinia and Tunisia.

Throughout the area of interest there are several prominent seismic reflecting horizons and sequences of reflectors, but there is some discrepancy as to nomenclature. Tables 1 and 2 show some of the designations used in the published literature. Seismic illustrations and discussion included in this report will use the nomenclature of Table 1.

At frequencies above 50 Hz, acoustic energy significant to sonars probably does not interact with materials more than a few hundred meters below the water-sediment interface. Thus, the sediment zone of primary acoustic interest in the Straits of Sardinia-Tunisia and Sicily are the Quaternary-Pliocene unconsolidated sediments above seismic Horizon A. The lithified Miocene and older sediments below Horizon A will, for the purpose of this report, be considered acoustic basement. It should be noted, however, that acoustic basement for the Strait of Sardinia-Tunisia is therefore the evaporite sequence, and acoustic basement in the Strait of Sicily is limestone. Figure 4 shows the areal extent of evaporites in the central Mediterranean region. Note that their occurrence is essentially confined to the deep-water regions. The top of both of these acoustic basements, however, is designated as seismic Horizon A. Figure 5 is an isopach map of the Quaternary-Pliocene sediments above Horizon A. It is this upper sequence of sediments which will dominate the remaining discussion.

### III. REGIONAL OCEANOGRAPHIC SETTING

North Atlantic water flows on the surface through the Strait of Gibraltar and along the southern margin of the Mediterranean Sea forming the North African Current. This surface water usually extends to a depth of 200-300 m and has an approximate salinity of 37.4 ‰, with a temperature range of 13°- 23°C. After this water mass flows between Sardinia and Tunisia, it turns to the southeast and flows through the Strait of Sicily. At the eastern end of the Strait of Sicily, this cool, lower salinity water encounters the warmer, more saline water of the Eastern

TABLE 1. Correlation of seismic reflectors from Finetti and Morelli (1973)

<u>Mediterranean Sea in General</u>	<u>Strait of Sicily Only</u>
Horizon A - Base of Quaternary-Pliocene or top of evaporite	----- Horizon A - Base of the Quaternary-Pliocene
Horizon B - Base of Miocene evaporite	----- Horizon B - In the Miocene
	----- Horizon C - In the Eocene
Horizon K - Top of Mesozoic	----- Horizon K - Top of Mesozoic
Horizon S - Acoustic basement	-----
	----- Horizon E - Near top of Jurassic
	----- Horizon F - Near top of Triassic

TABLE 2. Seismic stratigraphic sequences (From Stanley (1977), Mauffret et al. (1973), Morelli (1975), and Ryan et al. (1970, 1973))

Mediterranean Sea in General

- Sequence A - Lower Pliocene to Recent group of reflectors
- Sequence B - Upper Miocene interbedded evaporites top is Horizon H or M
- Sequence C - Upper Miocene salt, top is Horizon K, base is Horizon L
- Sequence D - Upper Miocene to Oligocene infrasalt series includes Horizon N
- Horizon S - Acoustic basement

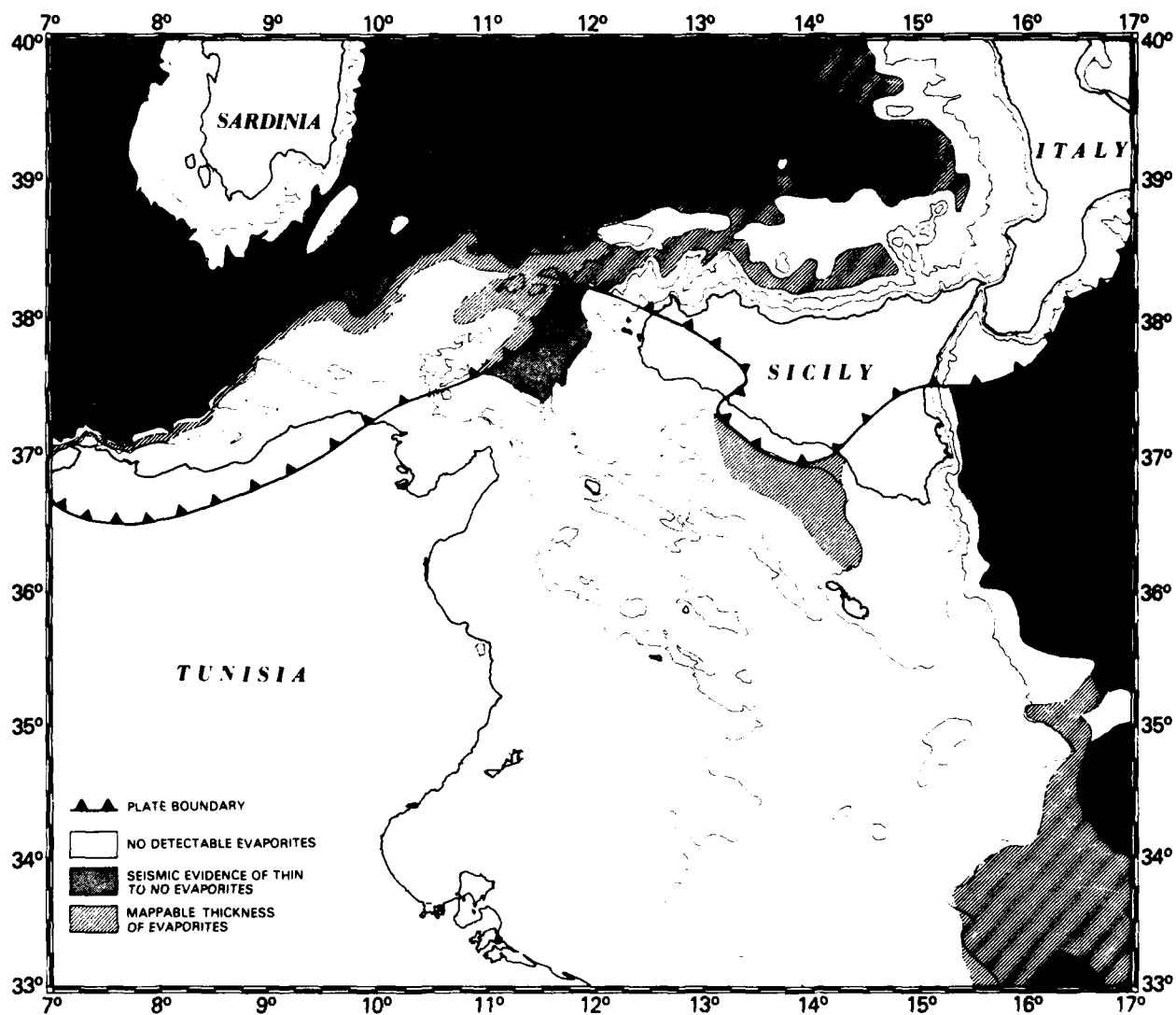


Figure 4. Map of the Straits of Sicily and Sardinia-Tunisia illustrating the plate boundary and the distribution of Upper Miocene evaporites. Modified from Finetti and Morelli (1973)

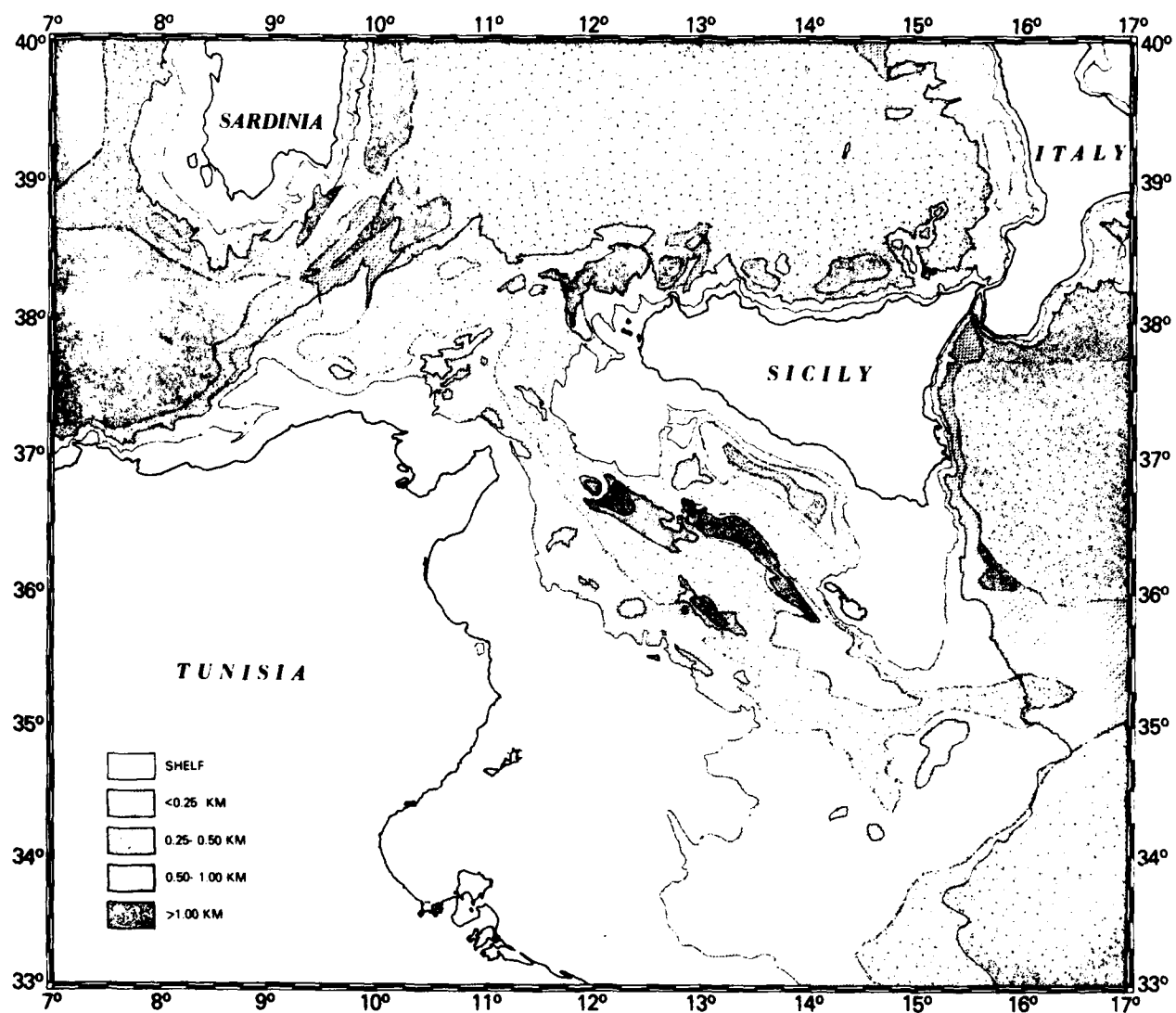


Figure 5. Map showing the thickness of Quaternary-Pliocene sediments in the Straits of Sicily and Sardinia-Tunisia. Modified from Stanley (1977)

Mediterranean Sea to form the Maltese Front. Both the intensity and position of the front vary considerably, but it is generally found in the vicinity of the Strait of Messina south to the African continental margin.

Below this easterly flowing surface current is a counter-current of colder, more saline water (38.7 ‰ salinity and a temperature of approximately 14°C). This counter-current, called the Levantine Intermediate Current, has a core depth of 400-500 m. The water mass is formed during the winter months in the Northern Levantine Basin.

Below a depth of about 1500 m, Mediterranean Deep Water is found. This water mass is located in the Sardinia-Tunisia Strait between the Algerian and Tyrrhenian Basins, but the isolated deep troughs of the Strait of Sicily (Linosa, Pantelleria, and Malta Troughs) generally contain Levantine Intermediate Water.

#### IV. STRAIT OF SICILY

##### A. PHYSIOGRAPHY AND GEOLOGY

The Strait of Sicily is a body of water which lies between the Island of Sicily and the African Continent (Fig. 1, Plate I). From the viewpoint of marine geology, the sea floor beneath the strait is a topographic high that separates the Ionian Basin to the east from the Tyrrhenian and Algerian Basins to the west. From a plate tectonic point of view, the floor of the strait is generally considered to be a submerged portion of the African Plate. The tectonics of the Strait of Sicily itself appear to be mostly in the form of vertical movements, probably resulting from isostatic adjustment following the main Alpine orogeny and tension resulting from bending of the downgoing plate near the zone of subduction. The major structural trends are oriented northwest-southeast and form a channel which separates the shelf regions of Sicily and Tunisia (Fig. 3).

In the central part of the strait are three elongate troughs: the Linosa, Malta, and Pantelleria Troughs. These structural grabens have marginal faults that parallel the structural trends of the strait. Structural highs are present in the form of horsts and fault-controlled volcanoes; these are the islands of Malta, Grozo, Linosa, Pantelleria and Medina Bank. Almost one-half of the strait is the shallow (>200 m) water of the Tunisia Shelf and the Sicilian Shelf (including Malta and Adventure Banks).

The eastern end of the strait is bounded by the north/south-striking Malta Escarpment, where the depth increases rapidly to the floor of the Ionian Basin. The western, or northern, end of the strait is highly influenced by the plate boundary (Fig. 3). Skeri Bank and Ustica Trough are examples of fault-controlled northeast/southwest-trending topography in the vicinity of the plate boundary. This end of the strait is formed by the east/west-trending continental margin of Tunisia and Sicily, where depth increases to the floor of the Tyrrhenian Basin.

This general discussion of the Strait of Sicily was paraphrased from Maldonado and Stanley (1976), which also contains a good bibliography for more detailed study. Much of the later discussion on sediment distributions in the strait is also taken from this important paper.

## B. SEISMIC STRATIGRAPHY

Before discussing the specific geographic area of interest, some general comments on seismic stratigraphy should be made. The terminology of deep-sea seismic interpretation is not well-developed, is often confusing, and usually has sedimentological connotations. In recent years there has been considerable work on continental shelf seismic stratigraphy (Sheriff, 1980, and Payton, 1977), but deep-sea seismic stratigraphic classifications are quite limited (Ballard, 1979). Deep-sea stratigraphic interpretations based upon 3.5 kHz profiles, however, have been made by a number of investigators (Damuth, 1980).

Extensive seismic interpretations will not be presented in this report nor will echo character maps be presented. The considerable amount of seismic and sediment core data already interpreted and published in the literature will merely be summarized and illustrated with selected, heretofore unpublished, seismic records and 3.5 kHz profiles. These records will be discussed within the framework of the Damuth (1980) and Ballard (1979) classification schemes and lithologic interpretations will be made. Although echo character is not mapped here in detail, its regional distribution in the area is discussed and utilized in determining acoustic provinces.

Seismic reflection data from the Strait of Sicily is discussed in Finetti and Morelli (1972, 1973). The continuous reflection profiles presented are 12- and 24-fold CDP stacks that show a thick sequence of sediments (sometimes in excess of 3.5 seconds of two-way travel time below the strait's floor). Within this thick sequence of sediments are a number of prominent and persistent reflecting horizons, which are continuous from Sicily to Tunisia.

Wide-angle reflection data collected with sonobuoys indicate an upper layer of unconsolidated sediment (velocities less than approximately 1700-1800 m/s), which is interpreted to be of Quaternary-Pliocene age. Below this sequence is Horizon A, which marks its base. The next lower sequence is composed of carbonates characterized by low-velocity layers (2000-3000 m/s) interbedded with high-velocity layers (3500-4000 m/s). In some places this pre-Pliocene section has consistent high velocities of 4500-5800 m/s. Within this sequence two prominent reflecting horizons have been named: Horizon B, which is in the Upper Miocene, and Horizon C, which is in the Eocene. The bottom of this sequence is marked by Horizon K, which is the top of the Mesozoic. The sediments below Horizon K are limestones and dolomites of Cretaceous, Jurassic, and Triassic age with interval velocities in the 5500-6200 m/s range. These boundaries are marked by Horizons E and F. The preceding lithologic interpretations of seismic reflection horizons were made by tracing the horizons from petroleum drill holes on the Ragusa platform (Finetti and Morelli, 1973).

In the published seismic profiles of the Strait of Sicily, the Quaternary-Pliocene unconsolidated sediment layer varies in thickness from 0.0 to 1.7 sec of two-way travel time, which roughly corresponds to actual thicknesses to 2890 m. Below Horizon A is the highly faulted pre-Pliocene sequence of carbonates whose structure determines the topographic configuration of the strait. The most active phase of faulting ended before commencement of Pliocene deposition, but some of the faults remain active to the present day. This continuation of faulting during the Quaternary-Pliocene period has produced some minor disruption of the upper sediments by faulting, and has caused some variation in water depths during the time of deposition, including some platform emergence. Vulcanism in the western portion of the strait is also felt to be related to large fault systems that are still active (Pantelleria and Linosa).

The thick Tertiary-Mesozoic sedimentary section of the strait is illustrated in the seismic line drawing of Figure 6. This section is on the edge of the Tunisian Shelf and is relatively free of faults. The enhancement resulting from multichannel digital recording and processing provides data deep in the section. The processing has also eliminated water multiples and source signature effects, allowing study of shallow stratigraphic relationships. The layering between Horizons A and F is essentially conformal, but the Quaternary-Pliocene section above Horizon A shows distinct off-lap at the shelf edge.

Figure 7 shows an interpreted single-channel analog seismic reflection profile southeast of Malta on an extension of the north wall of the Malta Trough. The faulting of pre-Pliocene sediments is characteristic of much of the central portion of the strait. On the left of the figure two faults extend to the water-sediment interface and have topographic expression, indicating recent activity. On the right of the figure the Quaternary-Pliocene section is seen to thin and pinch out against the shoal (marked by closure of the 200 m contour at 35-15'N and 15-00'E on Plate I).

Figure 8 is also an interpreted single-channel analog seismic reflection profile. This section is on the extension of the axis of the Malta Trough, due west of the previous section. Several large faults with topographic expression are shown. Note the marked increase in sediment thickness of the downthrown side of the faults to the left of center.

Both of these records show a post-Horizon A thickness in the trough of 0.2-0.6 seconds. This upper sequence is characterized by simple parallel reflectors which become smoother and more nearly horizontal as the water-sediment interface is approached. Parallel stratified trough fill such as this is most commonly associated with turbidite sequences. The irregularities in the stratification can be explained by faulting during the period of deposition. It should be noted that the term "turbidite sequence" is here and subsequently taken to mean: an alternating sequence of turbidity flow deposits interbedded with intervals of pelagic sediment, which together form a stratigraphic sequence in the classic sense.

Details of the near-surface soft sediment stratigraphy are best obtained from 3.5 kHz profiler data. Figure 9 shows a profile from near the axis of one of the troughs (south of Malta). Assuming a velocity of 1500 m/s, penetration is in excess of 60 m, which implies a moderately soft bottom (similar to deep ocean basin sediments). The record falls into the IB classification of Damuth (1980), which is a distinct reflection with numerous parallel subbottom reflections. This type of record is characteristic of distal abyssal plain turbidite sequences where the coarse basal turbidite layers are thin and are composed of relatively fine (silt/clays) material rather than the sand/silts of proximal turbidites.

Figure 10 illustrates a profile at the base of the southern margin of the Malta Trough. The profile shows that the reflection spacing and the total penetration are both thin but still persist up the relatively steep slopes of the trough margin. The water-sediment interface reflection is distinct, but the subbottom reflections are somewhat indistinct and discontinuous. The classification scheme of Damuth (1980) is based upon abyssal plains and deep sea fans and does not include steep slopes such as this, nor does he include convergent reflectors in his classification. Thus, the profile of Figure 10 does not fall directly into one of Damuth's categories, but is closest to category IIA. Damuth has correlated category IIA with turbidite sequences having thicker basal layers composed of coarser material than the distal turbidites associated with category IB (Fig. 9). The slope of the upper portion of

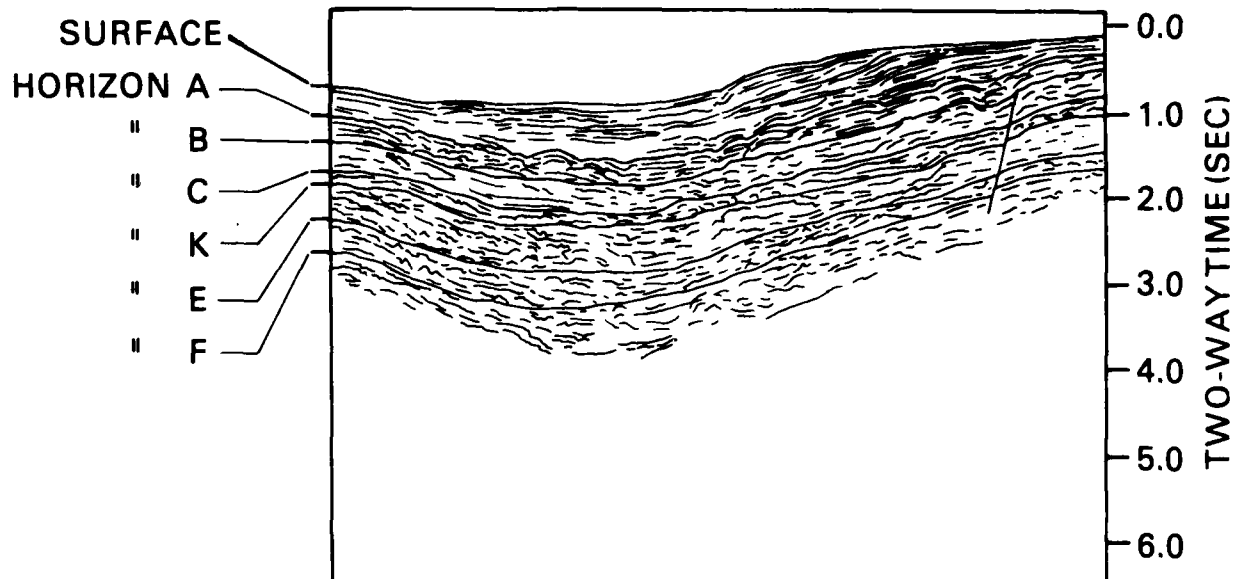


Figure 6. Line drawing of a 24-fold seismic reflection profile southeast of Lampedusa Island made from Figure 3 in Finetti and Morelli (1973). The digitally processed section shows layered sediments to the top of the Triassic (Horizon F), as well as eliminating multiples to show off-lap on the edge of the shelf.

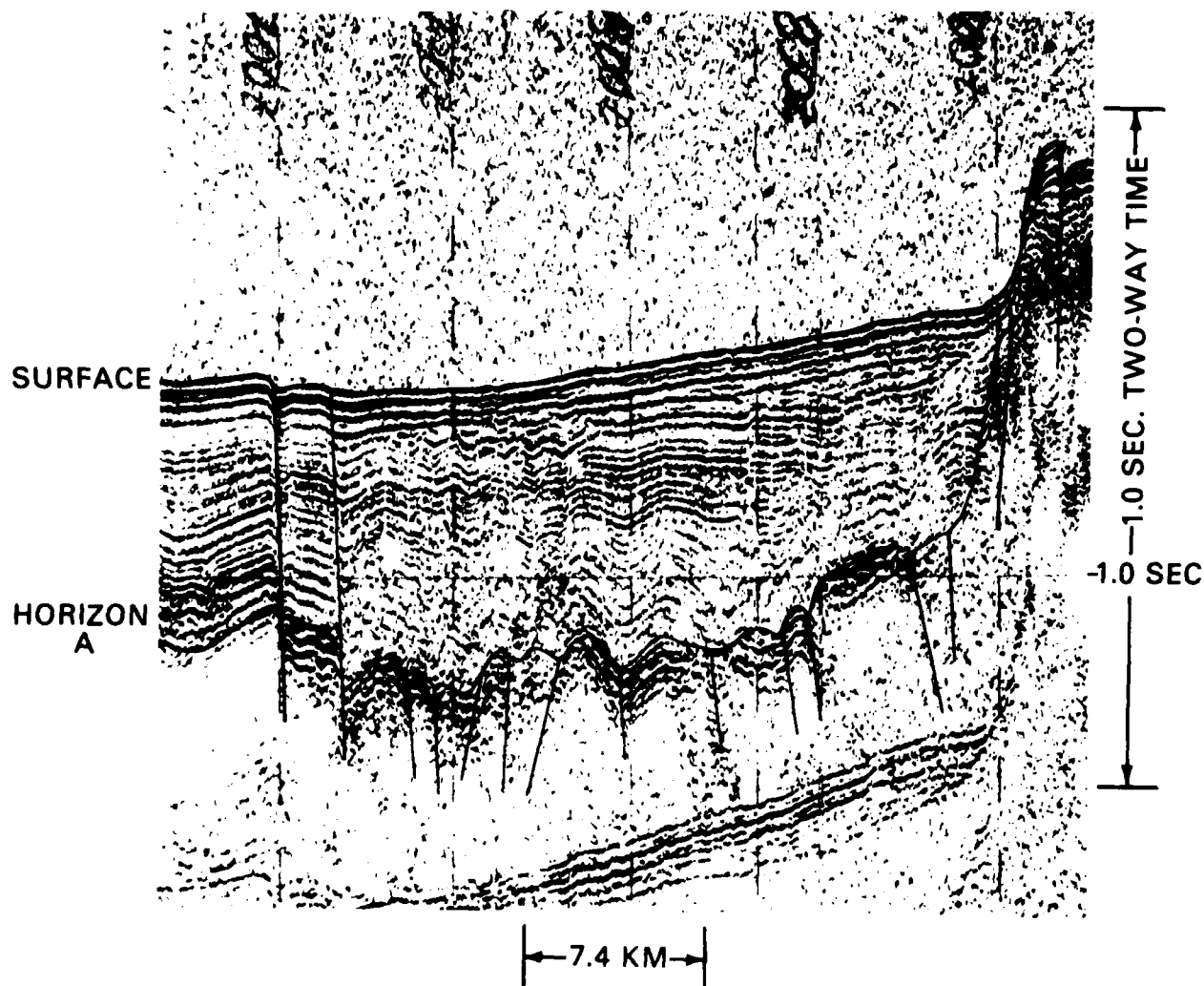


Figure 7. Interpreted continuous seismic reflection profile collected by USNS WILKES (Naval Oceanographic Office Cruise 708002) utilizing a 30 kilojoule sparker source. On this section, southeast of Malta, note the extensive faulting of the pre-Pliocene section below Horizon A, and that only a few of the faults have remained active to Recent times. Also note how Quaternary-Pliocene sediments thin and pinch out against the base of the shoal.

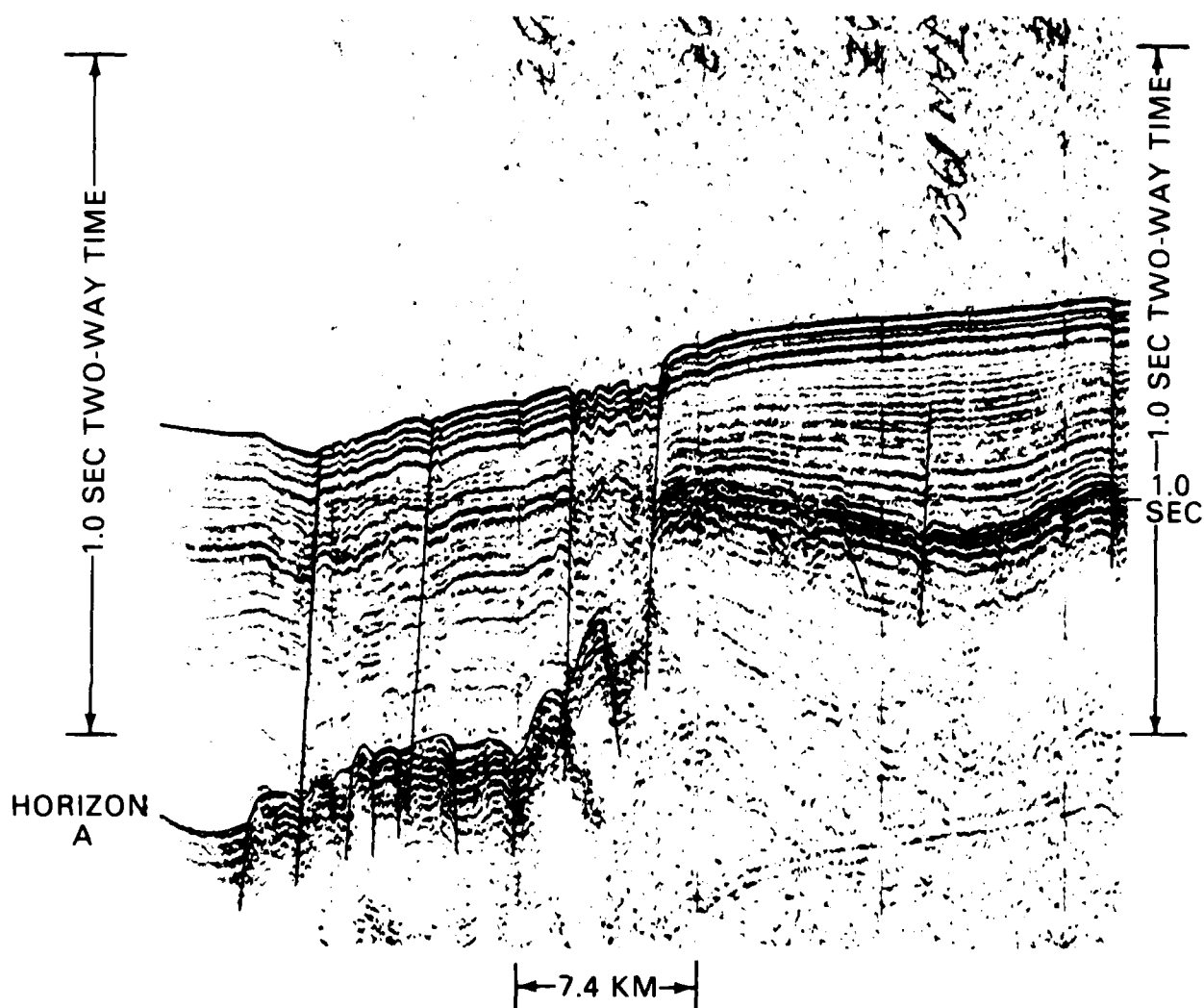


Figure 8. Interpreted continuous seismic reflection profile collected by USNS WILKES (Naval Oceanographic Office Cruise 708002) utilizing a 30 kilojoule sparker source. On this section south of Malta, note the faulting has remained active through Quaternary-Pliocene time, as evidenced by the increased sediment thickness on the downthrown side of the fault.

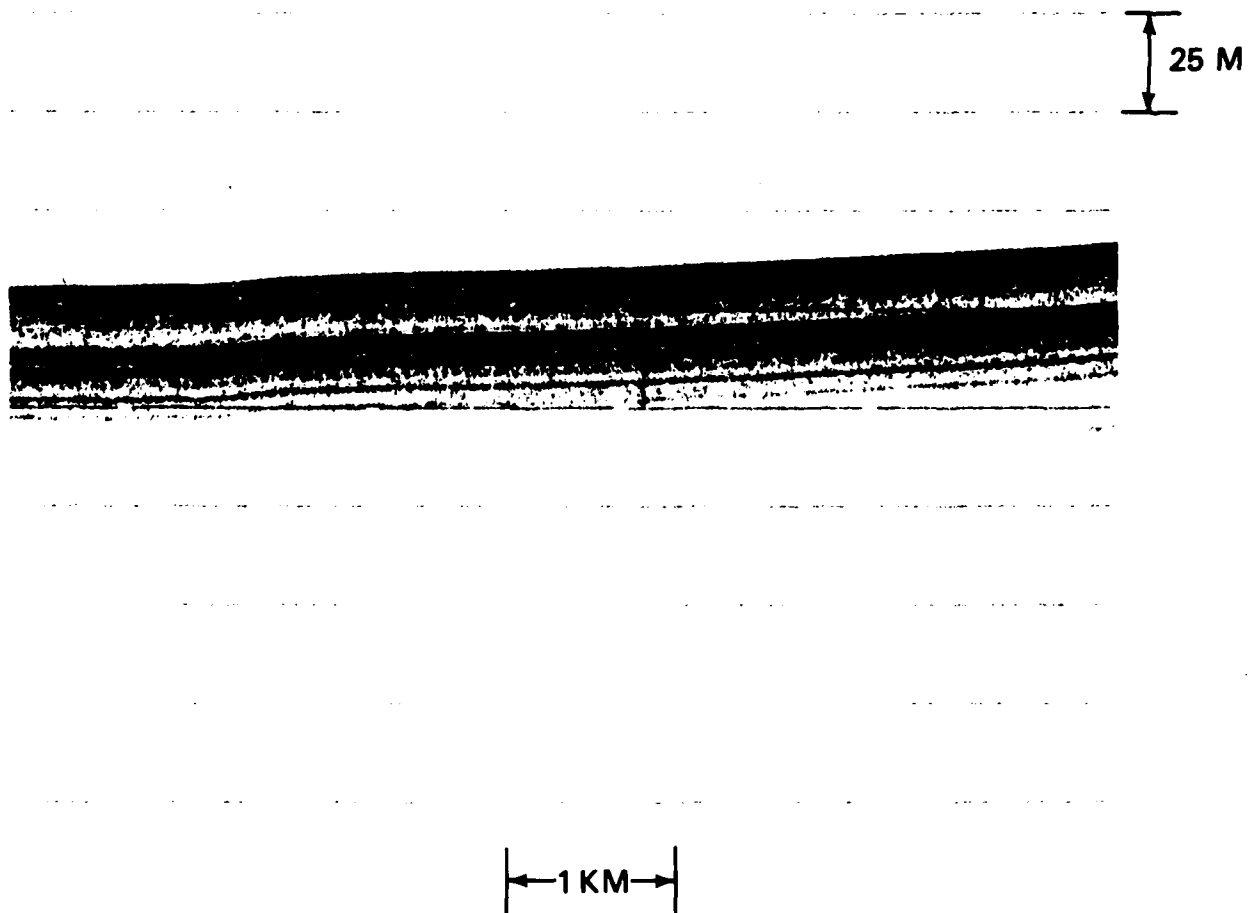


Figure 9. 3.5 kHz profiler record collected by USNS WILKES (Naval Oceanographic Office Cruise 708002). This record (south of Malta in the extension of the Malta Trough) shows well-stratified sediments, probably turbidites, with penetration in excess of 50 meters.

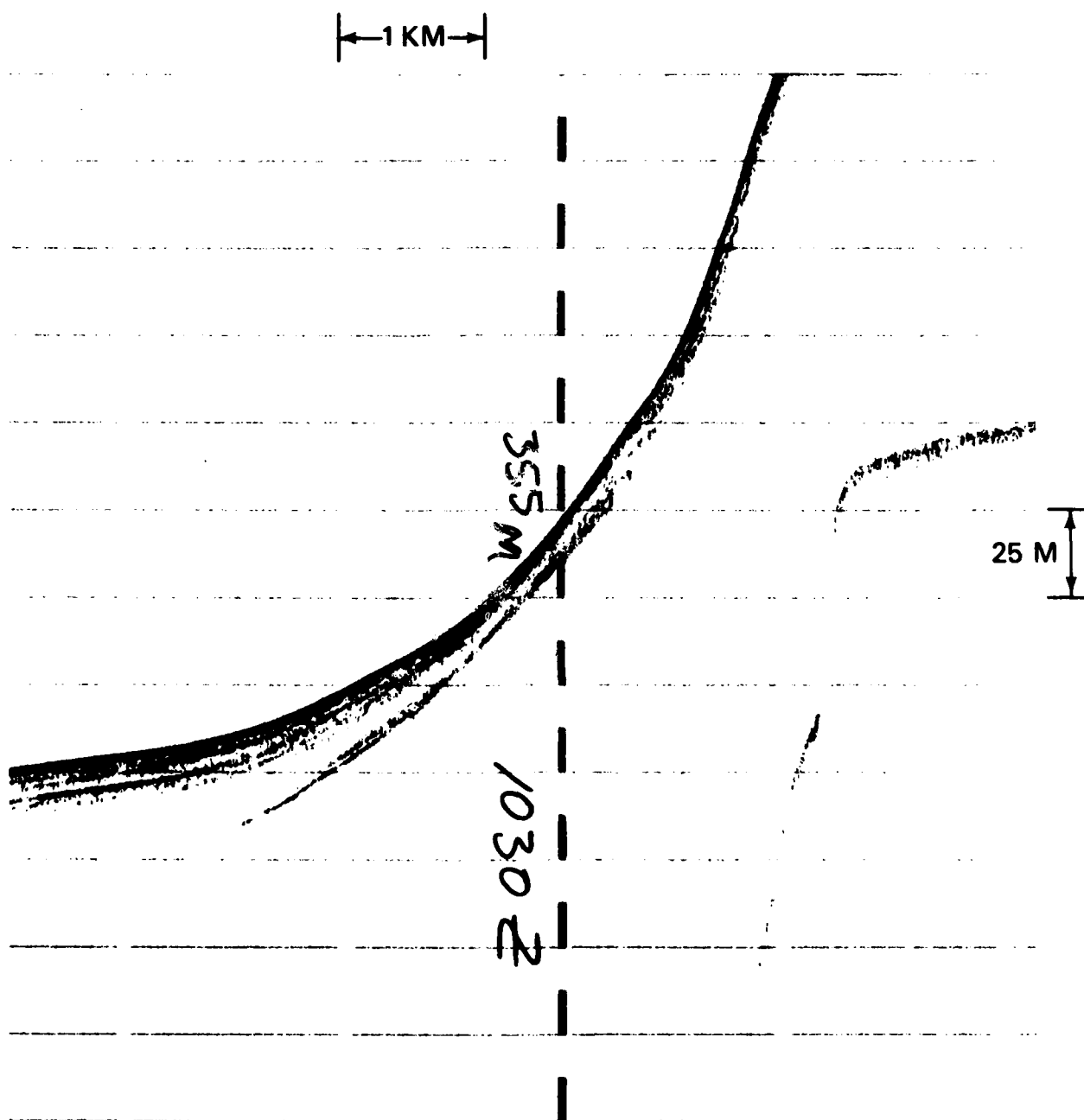


Figure 10. 3.5 kHz profiler record collected by USNS WILKES (Naval Oceanographic Office Cruise 708002). This record, collected at the base of a bank on the south edge of the Malta Trough, shows sediment thinning on the steep slopes, but the subsurface layering persists.

the record is  $5.9^\circ$ , which is rather steep for turbidity flow deposition. The subbottom reflections must therefore result from a geologically different sediment, but one with a similar acoustical signature at 3.5 kHz. The first sea floor multiple reflection of the trough rim can be seen in the lower right portion of the figure. It shows the continuation of the steep slope with virtually no subbottom penetration and an abrupt slope break at approximately a 100 m depth.

Figure 11 is a record from the area southeast of Medina Bank in 300 m of water. It is a good example of a Damuth class IA record and has a distinct reflection from the water-sediment interface with no subbottom reflections. This is characteristic of coarse sediment at the water-sediment interface and yields no information about the subsurface.

Figure 12 is a record from the same track as that of Figure 11, but is slightly farther from Medina Bank and is in 350 m of water. It shows a slope of  $0.1^\circ$ , indistinct subbottom reflections that are divergent downslope and somewhat intermittent, and a distinct reflection from the water-sediment interface. Total penetration also increases downslope. Such a record does not fit Damuth's classification, but is similar to the IIA category. The record is quite similar to that of Figure 10, which is at a similar water depth, but with significantly more slope.

Figure 13 is also a record from the same east-west track as those of Figures 11 and 12, but was taken farther east, just over the edge of the Malta Escarpment in 1200 m of water. The reflection from the water-sediment interface is distinct while subbottom reflections are less distinct, but are parallel and are fairly continuous (with amplitude fluctuations). On the far left portion of the record, all reflections become less distinct, intermittent, and nonparallel with less subbottom penetration. The right three-fourths of this record is somewhere between Damuth's classes IB and IIA, while the left one-fourth is between a IIA and IIB. Without additional profiles one can only speculate, but the indistinct reflections and irregular subbottoms of the left portion of the record may be related to mass-wasting (a small slump or debris flow). The average  $1.4^\circ$  slope of the section is more than adequate for gravity-induced sediment mass movement.

Seismic data indicate a thick sequence of sediment in the Strait of Sicily. The Quaternary-Pliocene sediments (down to Horizon A) are unlithified and generally lie conformably upon the older material. The deeper the water and flatter the bottom, the more distinct the internal layering and the deeper the acoustic penetration shown on the 3.5 kHz profiler records. As water depth decreases in the strait, the sediment layers thin and 3.5 kHz penetration decreases. As shoals and banks are approached (approximately 300 m of water) the water-sediment interface becomes quite reflective, and no subbottom penetration is seen on 3.5 kHz profiler records.

Below Horizon A the sediments are at least semi-lithified (velocities in excess of 2000 m/s) and consist of Miocene and older chinks, limestones, and dolomites. After the deposition of Horizon A, these older sedimentary rocks were subjected to extensive normal faulting, forming the graben and horst structures that control the bathymetry of the strait. Some of these faults and fault systems have remained active to Recent times, causing some present-day seismicity, some disturbance of the Quaternary-Pliocene sediments, and probably controlling Quaternary vulcanism in the strait.

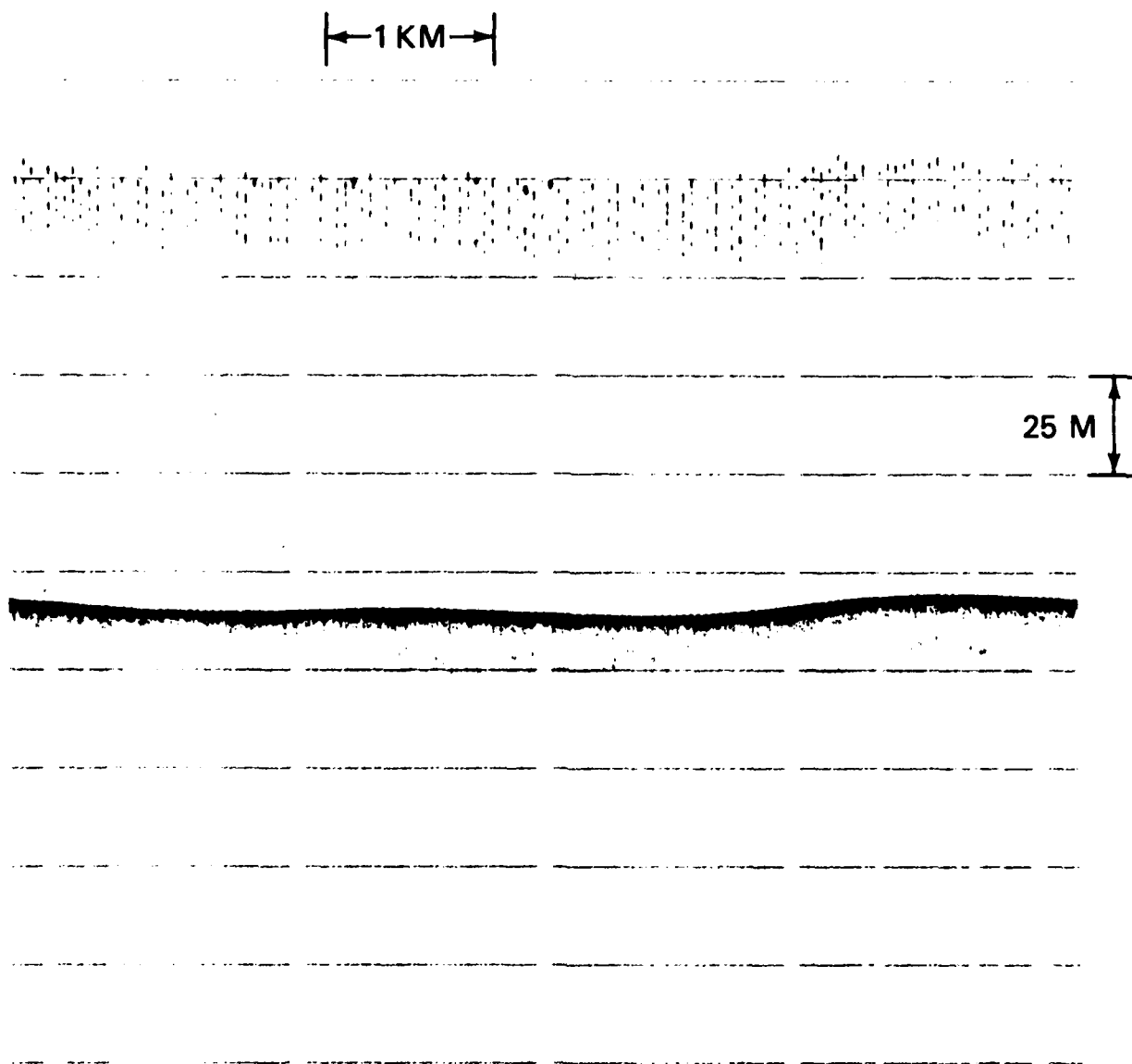


Figure 11. 3.5 kHz profiler record collected by USNS WILKES (Naval Oceanographic Office Cruise 708002). This record, taken southeast of Medina Bank in 300 meters of water, shows the water-sediment interface to be a very good reflector, with no subbottom penetration.

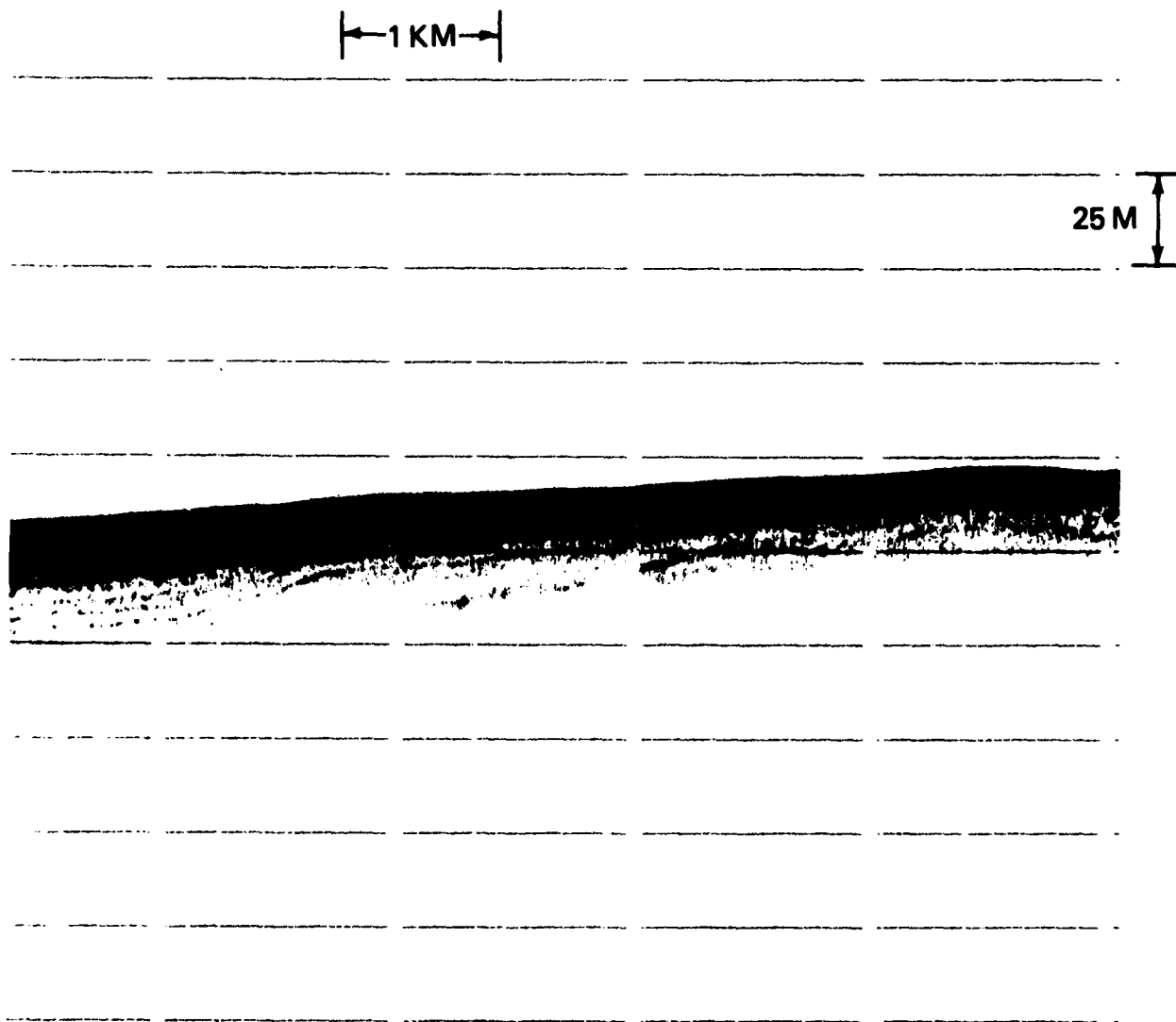


Figure 12. 3.5 kHz profiler record collected by USNS WILKES (Naval Oceanographic Office Cruise 708002). This record, taken southeast of Medina Bank in 350 meters of water (southeast of record in Fig. 7), shows a thickening of layered sediment and increasing penetration to the southeast.

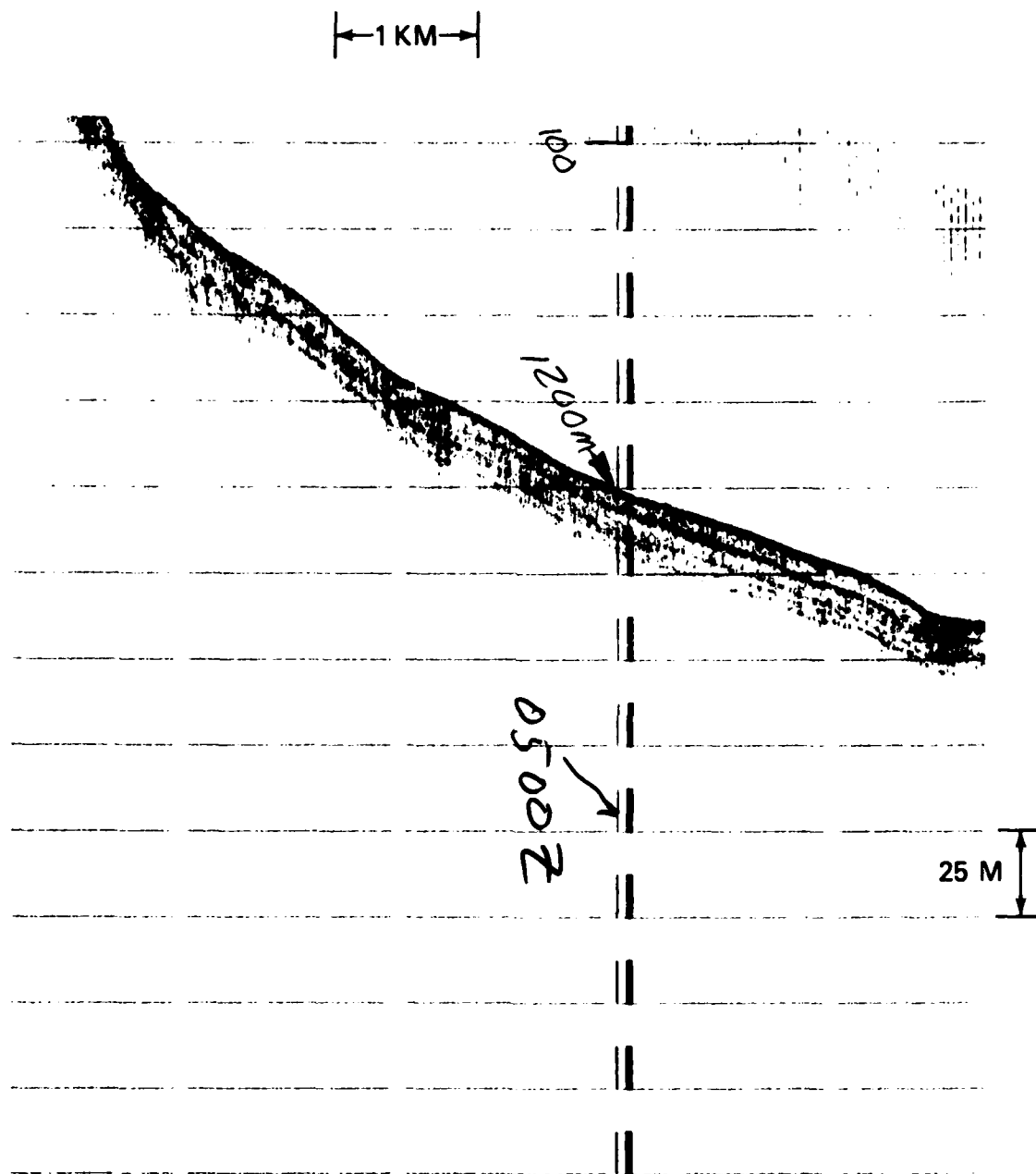


Figure 13. 3.5 kHz profiler record collected by USNS WILKES (Naval Oceanographic Office Cruise 708002). This record taken in over 1000 meters of water on the steep slope leading down to the Sicilian Basin (Ionian Sea) at the eastern end of the Strait of Sicily, shows well-stratified sediments and penetration in excess of 25 meters.

### C. DISTRIBUTION OF QUATERNARY-PLIOCENE SEDIMENTS

The previous section presented seismic and 3.5 kHz profile records and suggested a correlation between sediment type and water depth. Such a general relationship has also been proposed on the basis of core data by Emelyanov (1972), Akal (1972), and Maldonado and Stanley (1976). Before discussing these papers, however, it should be noted that the Emelyanov paper uses the Russian grain-size terminology and classification, which differs from the Wentworth system commonly used in most English language publications. In the Russian system the boundary between sand and aleurite is approximately a phi size of 3 (fine sand in the Wentworth system), while the boundary between aleurite and pelite is approximately a phi size of 7 (fine silt in the Wentworth system).

Emelyanov (1972) has mapped surface sediment properties for the entire Mediterranean Sea and has indicated the following distributions: (1) foraminiferal calcareous pelitic\* mud in the Tyrrhenian Basin, Ionian Basin and deep troughs of the Strait of Sicily; (2) shelly to foraminiferal, calcareous to highly calcareous sands on the shelves; and (3) shelly to foraminiferal, calcareous to high calcareous aleurites to aleuritic-pelitic mud in the mid-depth regions of the Strait of Sicily. The shelves are reported to be covered with coarse "lag" fragments of shell, coral, algae and foraminifera with some fine pelites, while the deeper water regions of the strait contain pelites which are winnowed from the shallow water regions, along with turbidity flow deposits, slump material and pelagic material.

Akal (1972) has summarized the sediment distribution of the strait in a single paragraph, which is quoted as follows. "Sand and silt spread over the western Sicilian and Tunisian continental shelves and extend towards the north-western flanks of the northern continental borderland. Generally, except in the southern part of the Tunisian shelf, this sand and silt is mixed with mud; over the northern borderland it is mixed with calcareous oozes. Rock and gravel patches occur over near-shore regions and over the banks. Mud and clay cover the rest of the northern continental borderland, some parts of the plateau, and the eastern parts of the southern Sicily shelf. The middle part of the strait and the northern part of the northern borderland are covered with calcareous oozes."

Maldonado and Stanley (1976) also base their discussion on core analysis, but go into considerably more detail in the area of sediment stratigraphy rather than simply grain size and chemical composition.

In their core analysis, four major sediment classes were described: (1) coarse calcareous sand plus shallow water mud, (2) hemipelagic mud, (3) turbiditic mud, and (4) sand-silt and turbiditic sand. Sedimentary environments or "sequences" are then identified and discussed on the basis of the percentages of these sediment classes found in a given core. In Figure 36 of their paper (Maldonado and Stanley, 1976) the percentage and cumulative percentage of these sediment types are plotted versus water depth. Virtually all coarse calcareous sand and shallow water mud (type 1) is found in water depths of less than 300 m. The remaining three sediment types are found in the deeper water and show a marked correlation with depth. At a water depth of 500 m, the average sediment was 97.7% hemipelagic mud and 1.2% turbiditic sand and mud, while at a 1600 m depth (the deepest depth in the strait) the average

\*NOTE: The terms sand, aleurite, and pelite are used in the Russian literature to denote sediment grainsize. A pelite is approximately equivalent to clay (lutite) and fine silt, and aleurite is approximately equivalent to medium silt through fine sand, while the Russian sand is roughly analogous to a "western" medium sand.

sediment content was 77.9% hemipelagic mud and 16.6% turbiditic sand and mud. The hemipelagic mud is by far the dominant constituent of sediments found below a water depth of 500 m. The sand and turbiditic sands were not found at depths shallower than 950 m, although the turbiditic muds were found at all depths below 500 m. In a more qualitative sense, turbidites were found in all of the trough floor sediments, while highly bioturbated and structureless hemipelagic mud covered the slopes between the banks and trough floors.

The coarse, calcareous sands on the banks are in good agreement with the strong, sharp 3.5 kHz reflections from the water-sediment interface as illustrated in Figure 11. The trough floor turbidites are in good agreement with the well-stratified 3.5 kHz record of Figure 9. The problem lies in the distinct stratification of the slope sediments illustrated in Figures 10, 12, and 13, where structureless hemipelagic mud is predicted by the core data. The sediment versus depth correlations showed that the turbiditic mud extends to shallower depths (500 m) than the turbiditic sands (950 m); however, deposition of turbidites on the slopes and trough sides is contrary to our current understanding of turbidity flows. Thus, there is a question as to the origin of these reflecting horizons. It should be noted, however, that acoustic stratification is a common feature of hemipelagic continental slope sediments. Internal stratification of these sediments possibly, results from erosion/deposition fluctuations or cycles, variations in the sediment source, and even climate change or storm activity. In this specific region wind-blown sediment from North Africa may also play a significant role in this structure.

#### D. GEOACOUSTIC MODELS

There is very little direct and detailed compressional wave velocity versus depth data available for the Strait of Sicily sediments. However, in the previous sections a geologic description of the strait was developed. From this description and from empirical data on average sediment properties, it is possible to develop geoacoustic models for the region. These models are constructed in the manner of Hamilton (1979a, 1980) and represent the "state of the art"; however, it should be kept in mind that the models in this report are based upon average sediment properties, not direct measurements in the area of interest.

At frequencies above 50 Hz, acoustic energy relevant to sonars probably does not interact with materials more than a few hundred meters below the water-sediment interface. Thus, the zone of primary interest in the present study is the Quaternary-Pliocene unconsolidated sediment above seismic Horizon A. The lithified Miocene and older sediments below Horizon A represent acoustic basement. The later distribution of sediment types within the upper zone are: (1) carbonate sands and shallow water muds on the banks, (2) turbidite sequences in the troughs, and (3) hemipelagic but acoustically stratified sediments in the regions between.

The carbonate sands covering the banks produce a hard, reflective water-sediment interface with no subbottom penetration on either the 3.5 kHz profiler or the sparker (approximately 50-150 Hz) records. These areas are characterized by simple interface reflection, i.e., "Rayleigh" reflection, which is frequency independent. The sea floor can thus be treated as a semi-infinite half-space. Table 3 is a geoacoustic model considered to be representative of such an environment. It is labeled Model I - Carbonate Banks and is felt to be applicable to water depths shallower than 300 m. The bottom water velocity is an average value for a 300 m water depth (unpublished data utilized by the author), while the sea floor properties are average properties for a sand (see footnotes to Table 3).

TABLE 3. GEOACOUSTIC MODEL I - Carbonate Banks

Layer Material	Thickness m(1)	Depth m	Velocity (m/s) Vp(2) Vs(3)		Attenuation kp(4) ks(5)		Density $\rho$ (g/cc)(6)
Sea Surface-----							
Bottom Water		300	1514.5				1.03
Sea Floor-----							
(half-space)		0	1681.	129.	.5	6.6	1.81
Carbonate clay, silt & sand							

## NOTES:

- (1) Thickness - Thickness of the sediment layer is assumed infinite.
- (2) Vp - Compressional wave velocity is an average value for a continental terrace sediment with a mean grain size between that of a very fine sand and a silty sand (Hamilton, 1980). This is confirmed by velocity measurements on four cores (Akal, 1972) which yielded velocities in the 1600-1700 m/s range.
- (3) Vs - Shear wave velocity is for a shallow water sand (Hamilton, 1979a).
- (4) kp - Compressional wave attenuation constant was scaled from Hamilton (1980).
- (5) ks - Shear wave attenuation constant is that of a sand and is taken from Hamilton (1980).
- (6)  $\rho$  - Sediment bulk density is an average value for a continental terrace sediment with a mean grain size of a silty sand (Hamilton, 1980).

Turbidites, which cover the trough floors, are known to have compressional wave velocities which increase with depth at rates of  $1.0-1.5 \text{ s}^{-1}$  (Hamilton, 1979b). They are characterized by well-defined stratification which produces marked reflection patterns on 3.5 kHz and seismic records (Fig. 9). The slope sediments between the banks and trough floors pose some as yet unanswered stratigraphic questions. On the basis of seismic and 3.5 kHz records; however, the slope sediments appear to have an acoustic response similar to turbidites but with slightly weaker subsurface reflections and less subsurface penetration. For the purpose at hand, this sediment regime must be considered "acoustically" equivalent of the trough turbidite sequences. In the absence of area-specific velocity-depth data, the average turbidite compressional wave velocity versus depth function of Hamilton (1979b) is assumed for all sediments in the Strait of Sicily, with the exclusion of the carbonate banks. Compressional wave velocity measurements from three cores taken from near the central axis of the strait yielded an average relative velocity of 0.99 (Matthews, 1981). Once a compressional wave velocity function is established, other geoaoustic model parameters can be estimated (Hamilton, 1980).

Current estimates of low-frequency compressional wave attenuation have unexplained order of magnitude discrepancies. Hamilton (1972) summarized the then-published compressional wave attenuation data for marine sediments. In that paper he suggested three important relationships: (1) compressional wave attenuation in marine sediments is a near first-power function of frequency, (2) attenuation could be estimated from grain size (or porosity) data, and (3) attenuation in deep sea sediments probably increased with depth to a maximum, then decreased with depth. Since that paper was published, there have been only two published experiments dealing with *in situ* measurement of low-frequency compressional wave attenuation in deep sea sediments. Mitchell and Focke (1980) used a velocity-depth function based upon historical data provided by Hamilton and used bottom loss data to estimate attenuation as a function of depth. They found an attenuation maxima, but their estimates were an order of magnitude less than that predicted by Hamilton. Dorman and Jacobson (1981) and Jacobson et al. (1981) applied inverse theory to solve for velocity and attenuation as a function of depth in an experiment designed expressly for that purpose. They also found the predicted attenuation maxima, and their absolute values were in agreement with those of Hamilton. The differences between these two experimental results have not been reconciled.

The preponderance of data is in favor of the Hamilton-Jacobson values; however, the Mitchell and Focke values yield plane wave bottom loss calculations in closer agreement with measured bottom loss values. The discrepancies could result from differences in measurement or analysis techniques, or they may represent actual variation in attenuation with sediment type. Because of these unexplained differences in the attenuation coefficient, two geoaoustic models are presented for this sediment province. Both have the same velocity-depth function (and density-depth function), but have two different attenuation-depth functions for compressional wave attenuation. Shear wave attenuation is taken to be proportional to compressional wave attenuation (Hamilton, 1980) and therefore also differs in the two models. These geoaoustic models are labeled Low and High Attenuation Models and are presented in Tables 4 and 5, respectively. Because the lower attenuation values seem to produce the most realistic bottom loss computations for abyssal plain turbidites (which is usually near-zero loss at grazing angles below  $20^{\circ}$ - $30^{\circ}$ ), Table 4, Geoaoustic Models IIA, for silty clays and clayey silts (Low Attenuation Model), is recommended for acoustic calculations. Density is in g/cc and  $V_p$  is in km/s.

TABLE 4. GEOACOUSTIC MODEL IIA - Silty clays & clayey silts (Low Attenuation Model)

Layer Material	Thickness s(1) m(2)	Depth m	Velocity (m/s) Vp(3) Vs(4)		Attenuation kp(5) ks(6)		Density $\rho$ (g/cc)(7)
Sea Surface-----							
Bottom Water		600	1517.5				1.03
Sea Floor-----							
Sediment (clay-silt and silty-clay)	T=.5z=500.	0	1502.	116.	.0045	15.0	1.52
		25	1534.	232.	.0060	20.0	1.55
		50	1552.	301.	.0075	25.0	1.57
		75	1596.	333.	.0090	30.0	1.62
		100	1625.	365.	.0110	36.7	1.65
		125	1653.	395.	.0120	40.0	1.69
		150	1680.	409.	.0130	43.3	1.72
		175	1706.	424.	.0140	46.7	1.75
		200	1731.	438.	.0150	50.0	1.78
		250	1778.	467.	.0170	56.7	1.83
		300	1820.	495.	.0190	63.3	1.88
		350	1857.	525.	.0195	65.0	1.92
		400	1889.	554.	.0190	65.3	1.95
		500	1937.	612.	.0160	53.3	2.01
Acoustic Basement-----							
Consolidated Sediment (Limestone and chalk)			2200.	1578.	.02	.07	2.16

NOTES:

- (1) Thickness - The thickness of the upper sediment layer is highly variable. The indicated thickness is a mean for the region in two-way seismic travel time in seconds.
- (2) Thickness - The thickness in meters is computed from the mean two-way travel time and the velocity depth function (3).
- (3) Vp - Compressional wave velocities were computed from the equation

$$V_p = 1.502 + 1.304z - .741z^2 - .257z^3$$

which is taken from Hamilton (1979b), where Vp is in km/s and z is depth in km. A water depth of 600 m was used for this computation; for other water depths the initial velocity (Vp at z=0) should be changed to 0.99 times the bottom water velocity. The velocity for limestone was taken from Finetti and Morelli (1972).

- (4) Vs - Shear wave velocities were computed from the below equations taken from Hamilton (1979a).

$$\begin{array}{ll} V_s = 116. + 4.65z & 0. < z < 36. \\ V_s = 237. + 1.28z & 36. < z < 120. \\ V_s = 322. + .58z & 120. < z < 650. \end{array}$$

Vs is in m/s and z is depth in meters. The shear velocity of limestone was computed using a Vp/Vs ratio of 1.9, for chalk, after Hamilton (1979c).

- (5) kp - Compressional wave attenuation constant was scaled from the "low" attenuation profile (Mitchell and Focke, 1980). The attenuation in limestone is taken to be 0.02, similar to basalt.
- (6) ks - Shear wave attenuation constant starts with an initial value of ks=15. at z=0, and varies with depth as a proportion to the compressional wave attenuation in the manner of Hamilton (1980).

$$k_s(z) = 15.k_p(z)/k_p(z=0)$$

- (7)  $\rho$  - Sediment bulk density was computed from the compressional wave velocity by the equation

$$\rho = 1.135V_p - .19$$

where Vp is the compressional wave velocity in km/s after Hamilton (1978). The density of limestone was also computed from the compressional wave velocity using the Hamilton (1978) equation shown below

$$\rho = 2.351 - 7.497 V_p^{-4.656}$$

Density is in g/cm<sup>3</sup> and Vp is in km/s.

TABLE 5. GEOACOUSTIC MODEL IIB - Silty clays & clayey silts  
(High Attenuation Model)

Layer Material	Thickness s(1) m(2)	Depth m	Velocity (m/s) Vp(3) Vs(4)		Attenuation kp(5) ks(6)		Density $\rho$ (g/cc)(7)
Sea Surface-----							
Bottom Water		600	1517.5				1.03
Sea Floor-----							
Sediment (clay-silt and silt-clay)	T=.4z=360.	0	1502.	116.	.0270	15.0	1.52
		25	1534.	232.	.0285	15.8	1.55
		50	1552.	301.	.0295	16.4	1.57
		75	1596.	333.	.0305	16.9	1.62
		100	1625.	365.	.0315	17.5	1.65
		125	1653.	395.	.0320	17.8	1.69
		150	1680.	409.	.0325	18.1	1.72
		175	1706.	424.	.0335	18.6	1.75
		200	1731.	438.	.0340	18.9	1.78
		250	1778.	467.	.0345	19.2	1.83
		300	1820.	495.	.0340	18.9	1.88
		350	1857.	525.	.0320	17.8	1.92
		400	1889.	554.	.0295	16.4	1.95
		500	1937.	612.	.0235	13.1	2.01
Acoustic Basement-----							
Consolidated Sediment (Limestone and chalk)			2200.	1578.	.02	.07	2.16

NOTES:

- (1) Thickness - The thickness of the upper sediment layer is highly variable. The indicated thickness is a mean for the region in two-way seismic travel time in seconds.
- (2) Thickness - The thickness in meters is computed from the mean two-way travel time and the velocity depth function (3).
- (3)  $V_p$  - Compressional wave velocities were computed from the equation

$$V_p = 1.502 + 1.304z - .741z^2 - .257z^3$$

which is taken from Hamilton (1979b), where  $V_p$  is in km/s and  $z$  is depth in km. A water depth of 600 m was used for this computation; for other water depths the initial velocity ( $V_p$  at  $z=0$ ) should be changed to 0.99 times the bottom water velocity. The velocity for limestone was taken from Finetti and Morelli (1972).

- (4)  $V_s$  - Shear wave velocities were computed from the below equations taken from Hamilton (1979a).

$$\begin{array}{ll} V_s = 116. + 4.65z & 0. < z < 36. \\ V_s = 237. + 1.28z & 36. < z < 120. \\ V_s = 322. + .58z & 120. < z < 650. \end{array}$$

$V_s$  is in m/s and  $z$  is depth in meters. The shear velocity of limestone was computed using a  $V_p/V_s$  ratio of 1.9, for chalk, after Hamilton (1979c).

- (5)  $k_p$  - Compressional wave attenuation constant was scaled from Hamilton (1972). The attenuation in limestone is taken to be 0.02, similar to basalt.
- (6)  $k_s$  - Shear wave attenuation constant starts with an initial value of  $k_s=15.0$  at  $z=0.0$  and varies with depth as a proportion to the compressional wave attenuation in the manner of Hamilton (1980).

$$k_s(z) = 15.k_p(z)/k_p(z=0)$$

- (7)  $\rho$  - Sediment bulk density was computed from the compressional wave velocity by the equation

$$\rho = 1.135V_p - .19$$

where  $V_p$  is the compressional wave velocity in km/s after Hamilton (1978). The density of limestone was also computed from the compressional wave velocity using the Hamilton (1978) equation shown below

$$\rho = 2.351 - 7.497 V_p - 4.656$$

Density is in g/cm<sup>3</sup> and  $V_p$  is in km/s.

## V. STRAIT OF SARDINIA-TUNISIA PHYSIOGRAPHY AND GEOLOGY

### A. PHYSIOGRAPHY AND GEOGRAPHY

The Strait of Sardinia-Tunisia is a body of water which lies between the Island of Sardinia and the African Continent (Fig. 1 and Plate I) and connects the Algerian Basin to the Tyrrhenian Basin. Although it is referred to here as a "strait" for convenience, it is deeper and wider than the connotation would generally imply (170 km wide), and has a sill depth of approximately 2000 m. From plate tectonic theory the strait is believed to represent either (1) a zone of convergence of the African and Sardinian (formerly part of the European Continent) continental margins, or (2) the remnant of a body of water that existed prior to the opening of the western Mediterranean Sea by rifting. The present-day plate boundary (Fig. 3) passes from Sicily to Tunisia across the western end of the Strait of Sicily, just south of Skerki Bank. This position places Sardinia, the Sardinia-Tunisian Strait, and the Tellian Atlas Mountains on the north coast of Tunisia on the same present-day crustal plate (Fig. 3).

The physiography of the strait is simple. The strait is essentially V-shaped in north-south cross section, with the deepest point about midway between Sardinia and Tunisia. The southern margin of Sardinia falls off steeply from the edge of the shelf (200 m depth) to a depth of 1000 m, then more gradually to the center of the strait. The only anomalous topographic feature of the Sardinian side of the strait is the Carbonaia Ridge. The remainder of the Sardinia margin falls off rather steeply to the Strait of Sardinia-Tunisia or the Algerian and Tyrrhenian Basins.

Stanley (1977) defines the Sardinia margin as an intermediate and locally abrupt Mediterranean margin. Faulting, tilting of fault blocks, and sediment ponding produce the steplike appearance characteristic of the intermediate type margin. However, occasional faults are large enough to produce significant topography and discontinuity of seismic reflections which are characteristic of the abrupt type of margin. Detailed discussions on the origin of Carbonaia Ridge (38°-30'N to 39°N and 9°-30'E to 9°-45'E), are not available, but it is quite possibly a large block of Sardinia which has been broken off by faulting.

The African side of the strait has two rather distinct types of physiography. One is the margin of Algeria/Tunisia where the depth falls off rapidly to the floor of the Algerian Basin on the western end of the strait. East of about 9°E the Tunisian margin broadens, with a wide and topographically irregular zone forming between the 200 and 1000 m depths. This zone of irregular topography extends eastward to form the northern entrance to the Strait of Sicily. The western half of the African margin is geologically similar to the Sardinian margin, with the fault blocks and sediment ponds forming a generally step-like appearance, but with some local fault scarps producing an abrupt margin.

The eastern half of the strait's southern margin has a broad zone (100 km) of irregular topography between the shelf edge and the 1000 m depth. To the east this zone is bounded to the south, not by the shelf edge but by the east/northeast-striking plate boundary across the northern entrance to the Strait of Sicily. This zone is a complex area of block faulting related to the plate boundary and extends eastward to the northern margin of the Island of Sicily. Below the 1000 m depth the margin falls off either gently to the 2000 m central axis depth of the strait or steeply to the 2600 m depth of the Orosei Terrace (the southeastern corner of the Tyrrhenian Basin).

## B. SEISMIC STRATIGRAPHY

A modest amount of single and multichannel seismic reflection data exists in the Strait of Sardinia-Tunisia, but few of these data are published. Its general regional character, however, does not appear significantly different from that of the surrounding region. Figure 14 is an interpretation modified from Finetti and Morelli (1973) of an east-west multichannel seismic profile in the western entrance to the strait, near the island of Sardinia. It shows a sequence of stratified Quaternary-Pliocene sediment above seismic Horizon A. On the western (left) end of the profile below Horizon A is Horizon B, the base of the Miocene evaporite sequence. Horizon S, which is termed acoustic basement (in the seismic reflection sense), is in evidence on the eastern end of the profile. In the vicinity of the Sardinia-Corsica block, Horizon S is interpreted to be the top of the igneous-metamorphic basement of the island blocks. Total sediment thickness generally increases with increasing water depth. When the travel time to Horizon S approaches the first multiple reflection time of the sea floor, S is lost. The evaporites are in places known to rest unconformably on pre-evaporite sequences, while in deep basin regions Horizon B is often a smooth, flat-lying interface which probably represents a facies change with no depositional hiatus. Figure 4 indicates that the central portion of the Sardinia-Tunisia Strait is underlain by a detectable thickness of evaporite. On the Sardinia margin, however, the entire Tertiary section thins and the evaporite sequence apparently pinches out. Thus, at some point Horizons A and B converge, the Quaternary-Pliocene sediments rest directly upon non-evaporite Tertiary sediments, and only Horizon A lies between the water-sediment interface and acoustic basement (Horizon S). In this area the post-Upper Miocene stratigraphy is essentially identical to that at comparable water depths of the Strait of Sicily.

Throughout the Strait of Sardinia-Tunisia region, the sediments above Horizon A have seismic interval velocities in the 1.7-2.3 km/sec range and are assumed to be Quaternary-Pliocene unconsolidated sediment. The material below Horizon A is horizontally variable, as noted. In the Tyrrhenian Basin, Algerian Basin and central Strait of Sardinia-Tunisia, Horizon A marks the top of Miocene evaporites that have an average seismic velocity of 4.4 km/sec. In the shelf regions (and in portions of the Sicily Strait) the seismic velocities of material below Horizon A average about 2.2 km/sec and are interpreted to be Upper Miocene chalk that is interbedded with limestones.

With the exception of the deep basins (Algerian and Tyrrhenian), the pre-Horizon A material is generally faulted, leaving Horizon A a rough interface upon which post-Horizon A sediments were deposited. As indicated previously in the discussion on the Strait of Sicily, some of this Upper Miocene faulting has remained active to the present time and has created post-A topography and controlled post-A vulcanism.

Records from 3.5 kHz profilers in both the Tyrrhenian and Algerian Basins at either end of the strait show flat-lying, well-stratified sediments which are interpreted as turbidites (similar to Fig. 9). The left portion of Figure 9 shows such a parallel stratified sequence in the Algerian Basin. Fabbri and Selli (1972) show similar records and interpretations from the Tyrrhenian Basin. These turbidites can also be seen in the left one-third of Figure 14. To the right of the small seamount in Figure 14, the near surface sediments no longer have the reflection character of turbidites, but still have obvious acoustic stratification. Figure 15 is a 3.5 kHz profile from the central portion of the western end of the strait. It shows the upper 50 m of sediment to have well-defined, coherent, acoustic stratification

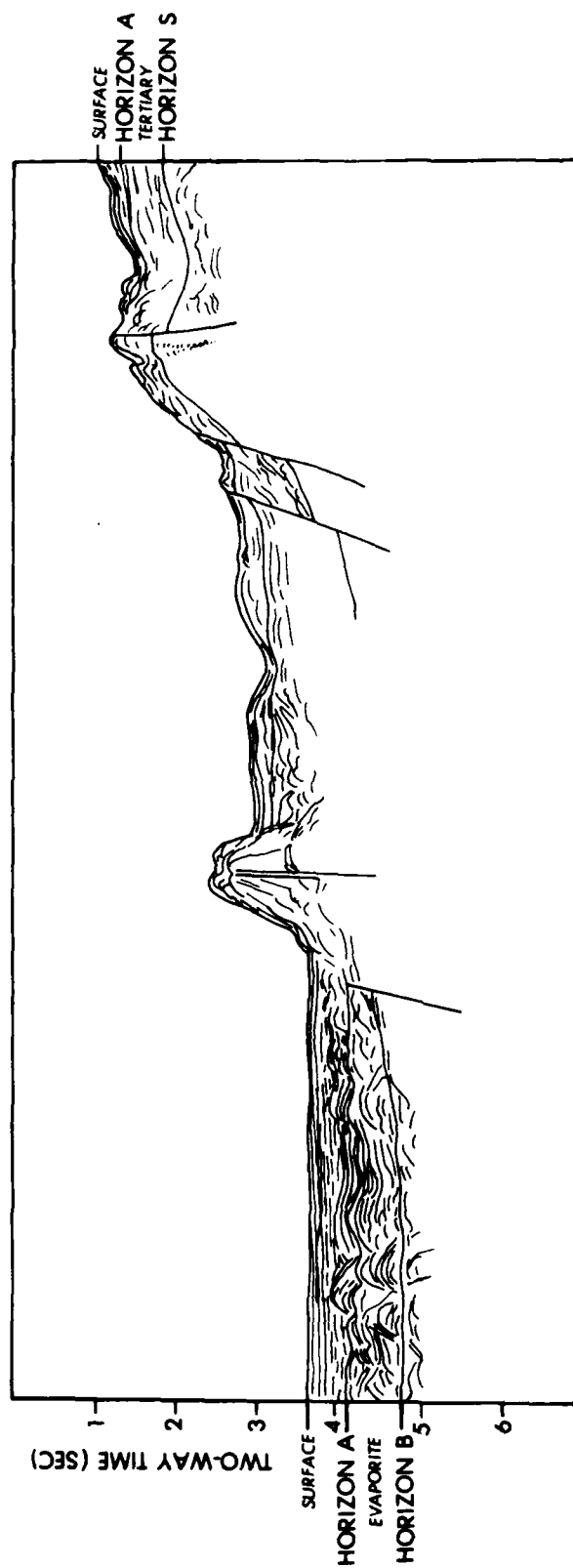


Figure 14. Line drawing of seismic reflection profile, taken from Finetti and Morelli (1973), illustrates the Algerian Basin to the left and the edge of the Sardinia Block (western entrance to the Sardinia-Tunisia Strait) to the right. In the center is a small seamount.

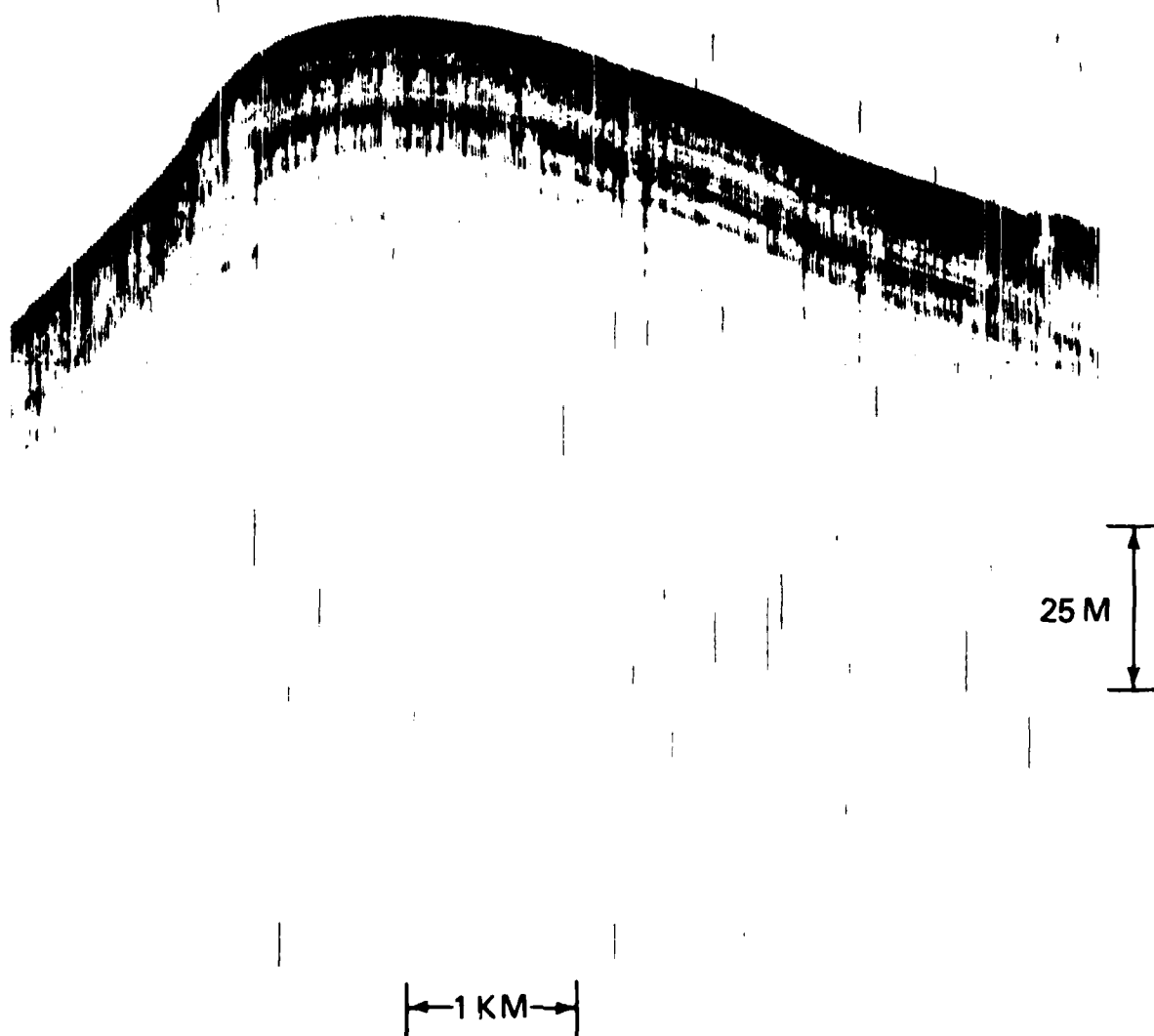


Figure 15. 3.5 kHz profiler record collected by USNS BARTLETT (Naval Oceanographic Office Cruise 1308). This record in the Strait of Sardinia-Tunisia shows uneven topography with relief in excess of 50 meters, but with good stratification and subbottom penetration in excess of 25 meters.

that is conformal to the topography. Such a record falls into Damuth's IIIB category. These sediments are not turbidites but have equally well-defined acoustic stratification at a frequency of 3.5 kHz. Coring samples indicate that these sediments are hemipelagic, have a significant calcium carbonate content, and are very similar to the sediments covering the sloping regions of the Strait of Sicily (Figs. 10, 12, 13), but with generally more distinct and continuous reflections.

Farther to the east is a region between the Tunisian Shelf and the Tyrrhenian Basin that forms part of the southern flank of the Sardinia-Tunisia Strait and the northern or western approaches to the Strait of Sicily. This area has been previously noted as having an irregular bottom and is probably best described as a continental borderland. Figure 16 shows a representative 3.5 kHz profile through this region. There is almost no discernable stratification in this record. The dark "burned" region of the record suggests a rough sea floor with an overlapping reflection hyperbolae characteristic of a Damuth class IIB. Some hint of stratification, however, can be seen on the original record. It is the author's opinion that this region is also blanketed with the same stratified hemipelagic sediment as the previous figure, but that increased surface roughness and recorder gain settings have obliterated the seismic evidence of it.

### C. DISTRIBUTION OF QUATERNARY-PLIOCENE SEDIMENTS

The Quaternary-Pliocene sediments of the Strait of Sardinia-Tunisia are represented by the soft sediment layer above seismic Horizon A. The thickness of this layer is mapped in Figure 5. The region has a significantly different pre-Pliocene history from that of the Strait of Sicily, but the post-Pliocene depositional environments have been virtually identical. A correlation between sediment type and water depth was established for the Strait of Sicily in Sections IV A and B. A similar relationship exists in the Strait of Sardinia/Tunisia. The maps of Emelyanov (1972) show the surficial sediments (0-10 cm) to be: (1) low calcareous, terrigenous, pelitic mud in the Algerian Basin; (2) foraminiferal, calcareous, pelitic mud in the Tyrrhenian Basin; (3) shelly calcareous to high calcareous sand on the shelf areas; and (4) foraminiferal, coccolithic and pteropodal; aleuritic-pelitic mud in the mid-water depth which comprise the remainder of the region. Part of this region is included in the discussion by Akal (1972). Akal refers to the area off the shelf to as the continental borderland which is covered with mud and clay mixed with some sand/silt and calcareous ooze. The northern part of the borderland (deeper water) is reported to be covered with calcareous ooze.

There is every reason to believe that the shelf areas of the Strait of Sardinia-Tunisia are essentially the same as those of the Strait of Sicily. Caulet (1972) gives a detailed discussion of sedimentation on the Algerian Shelf that is consistent with previous discussion. In the absence of specific investigations available to the author, it is here assumed that the Sardinian shelf sediments are also similar.

The uppermost stratigraphic unit in the Algerian Basin is interpreted as a turbidite sequence, based upon seismic and core data. The Tyrrhenian Basin surficial sediments are calcareous ooze (Emelyanov, 1972), but seismic records indicate that the uppermost stratigraphic unit is a turbidite sequence (Fabbri and Selli, 1972). This is a common situation, since many abyssal plains form from the influx of turbidity flows during Pleistocene sea-level lowerings, and since the last eustatic rises have reverted to a pelagic depositional environment with "red clay" or ooze covering the upper few centimeters.

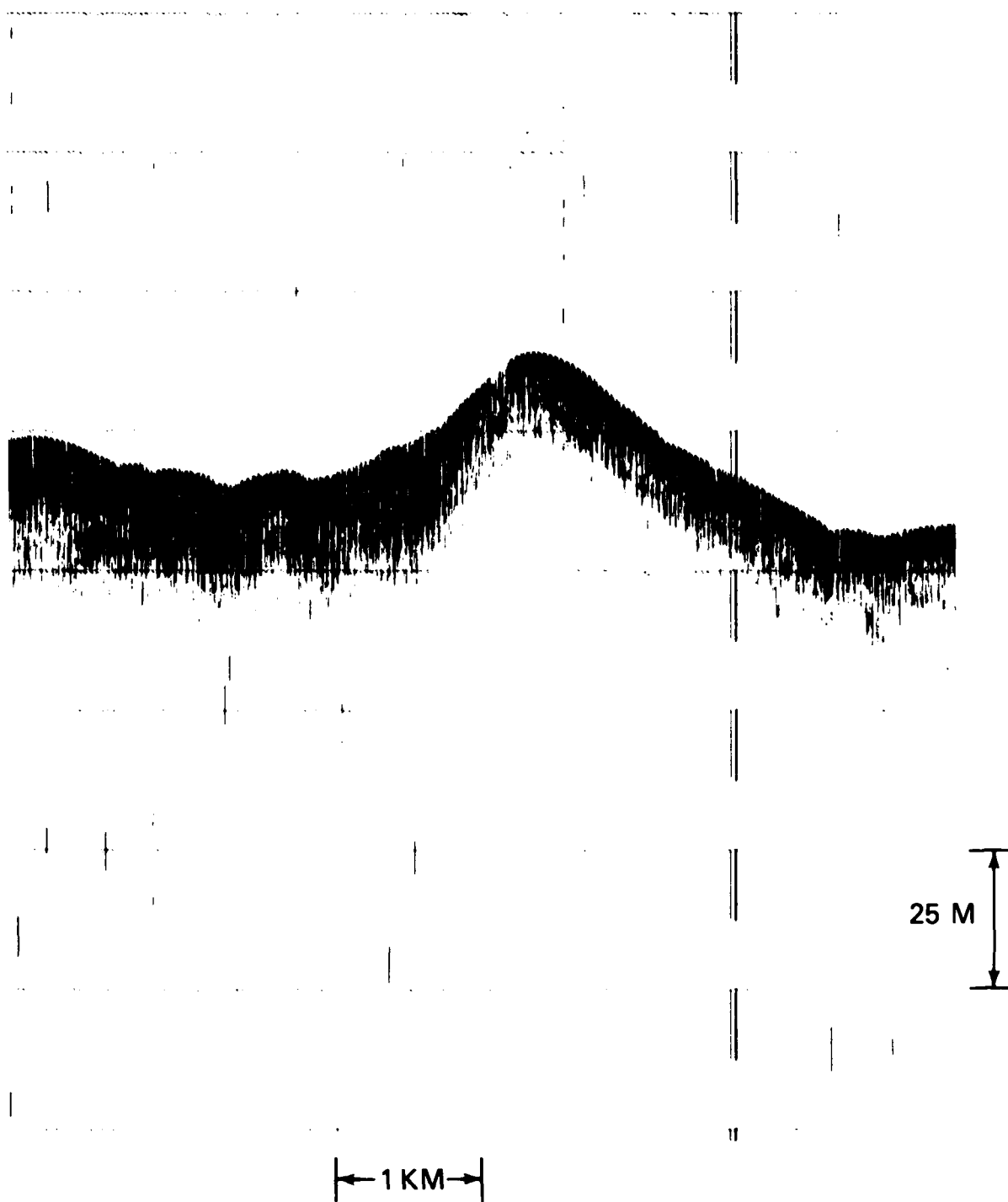


Figure 16. 3.5 kHz profiler record collected by USNS BARTLETT (Naval Oceanographic Office Cruise 1308). This record, taken in the area of irregular bottom to the north of the approaches to the Strait of Sicily, shows no discernible subbottom penetrations. The record shows an elongated bottom return.

The region between the shelf and basin floors is characterized by a sediment cover composed of a mix of pelagic and hemipelagic material with a significant calcium carbonate content. Questions remain as to the exact character of this material, but they are here interpreted to be the same as the mid-depth slope sediments found in the Strait of Sicily.

#### D. GEOACOUSTIC MODELS

In the absence of area-specific physical property data, average parameters must be used in constructing geoacoustic models for the Strait of Sardinia-Tunisia. Throughout the region of interest (Plate I) the Quaternary-Pliocene sediments in water depths greater than 300 m are typified by stratified clayey silts and silty clays. At depths shallower than 300 m, shallow-water muds with shell and reef detritus are found. Thus, the sediments in the first several hundred meters below the water-sediment interface are the acoustical equivalent of those found in the Strait of Sicily for similar water depths, and the reader is referred to Section IV.D of this report. Sediment thicknesses of the two areas are also similar, as shown in Figure 5. The only difference is in the composition of acoustic basement. Acoustic basement (for the purpose of the present study) in the Strait of Sardinia-Tunisia is principally evaporite, which has an average seismic interval velocity of 4.4 km/sec (Finetti and Morelli, 1973) and measured velocities from cores of 4.30-4.88 km/sec (Schreiber et al., 1973), as opposed to the 2.2 km/sec of chalk in the Strait of Sicily acoustic basement. This could result in some differences in acoustic propagation in areas of very thin Quaternary-Pliocene sediment cover, but the effects of a rough basement cannot be adequately dealt with in existing acoustic computational techniques. For this reason any computed basement interaction would have to be considered as highly suspect, since in reality the effects of basement roughness would probably overshadow the velocity differences.

Thus, the geoacoustic models for the two straits are essentially the same, and are dependent upon water depth (sediment type) only. Table 6 is thus identical to Table 3, while Tables 7 and 8 differ from Tables 4 and 5 only in the physical properties of acoustic basement.

#### VI. BOTTOM LOSS CALCULATIONS

The geoacoustic models of Sections IV.D and V.D represent the author's best estimate of sediment physical properties in the first few hundred meters below the sea floor. The available geological data is adequate to provide a geologic description of the area of interest, thus model uncertainties result primarily from the translation of a geologic description into quantitative estimates of sediment physical properties. Further uncertainties are introduced when the sea floor acoustic response is calculated from these geoacoustic models. The theoretical bottom loss values presented here (Figs. 17-33) represent twenty times the logarithm of the plane wave reflection coefficient, which was computed by standard seismic layered model techniques (Brekhovskikh, 1960). All computations were made at the single frequency indicated. In deep water areas, point source considerations become important, and will influence the "critical angle," but these problems are beyond the scope of this report.

The area of interest has several geologic provinces, but in terms of soft sediment physical properties, there are felt to be only two physical property provinces: (1) the shallow-water banks of Geoacoustic Model I (Table 3 and Figure 17), and (2) the "acoustically" stratified silty clays and clayey silts of Geoacoustic Model II. Because of the uncertainties in low-frequency compressional wave attenuation, Model

TABLE 6. GEOACOUSTIC MODEL I - Carbonate Banks

Layer Material	Thickness m(1)	Depth m	Velocity (m/s) Vp(2) Vs(3)		Attenuation kp(4) ks(5)		Density $\rho$ (g/cc)(6)
Sea Surface-----							
Bottom Water		300	1514.5				1.03
Sea Floor-----							
	(half-space)	0	1681.	129.	.5	6.6	1.81
Carbonate clay, silt & sand							

## NOTES:

- (1) Thickness - Thickness of the sediment layer is assumed infinite.
- (2) Vp - Compressional wave velocity is an average value for a continental terrace sediment with a mean grain size between that of a very fine sand and a silty sand (Hamilton, 1980).
- (3) Vs - Shear wave velocity is for a shallow-water sand (Hamilton, 1979a).
- (4) kp - Compressional wave attenuation constant was scaled from Hamilton (1980).
- (5) ks - Shear wave attenuation constant is that of a sand and is taken from Hamilton (1980).
- (6)  $\rho$  - Sediment bulk density is an average value for a continental terrace sediment with a mean grain size of a silty sand (Hamilton, 1980).

TABLE 7. GEOACOUSTIC MODEL IIA - Silty clays &amp; clayey silts (Low Attenuation Model)

Layer Material	Thickness s(1) m(2)	Depth m	Velocity (m/s) Vp(3) Vs(4)		Attenuation kp(5) ks(6)		Density $\rho$ (g/cc)(7)
Sea Surface-----							
Bottom Water		600	1517.5				1.03
Sea Floor-----							
Sediment (clay-silt and silty-clay)	T=.5z=500.	0	1502.0	116.0	0.0045	15.0	1.52
		25	1534.0	232.0	0.0060	20.0	1.55
		50	1552.0	301.0	0.0075	25.0	1.57
		75	1596.0	333.0	0.0090	30.0	1.62
		100	1625.0	365.0	0.0110	36.7	1.65
		125	1653.0	395.0	0.0120	40.0	1.69
		150	1680.0	409.0	0.0130	43.3	1.72
		175	1706.0	424.0	0.0140	46.7	1.75
		200	1731.0	438.0	0.0150	50.0	1.78
		250	1778.0	467.0	0.0170	56.7	1.83
		300	1820.0	495.0	0.0190	63.3	1.88
		350	1857.0	525.0	0.0195	65.0	1.92
		400	1889.0	554.0	0.0190	65.3	1.95
		500	1937.0	612.0	0.0160	53.3	2.01
Acoustic Basement-----							
Evaporite (halite, gypsum and anhydrite)			4400.	2200.			2.47

NOTES:

- (1) Thickness - The thickness of the upper sediment layer is highly variable. The indicated thickness is a mean for the region in two-way seismic travel time in seconds.
- (2) Thickness - The thickness in meters is computed from the mean two-way travel time and the velocity depth function (3).
- (3) Vp - Compressional wave velocities were computed from the equation

$$V_p = 1.502 + 1.304z - .741z^2 - .257z^3$$

which is taken from Hamilton (1979b), where Vp is in km/s and z is depth in km. A water depth of 600 m was used for this computation; for other water depths the initial velocity (Vp at z=0) should be changed to 0.99 times the bottom water velocity. The velocity for evaporite was taken from Schreiber et al. (1973).

- (4) Vs - Shear wave velocities were computed from the below equations taken from Hamilton (1979a).

$$\begin{array}{ll} V_s = 116. + 4.65z & 0. < z < 36. \\ V_s = 237. + 1.28z & 36. < z < 120. \\ V_s = 322. + .58z & 120. < z < 650. \end{array}$$

Vs is in m/s and z is depth in meters. The shear velocity of evaporite was computed using a Vp/Vs ratio of 2.0.

- (5) kp - Compressional wave attenuation constant was scaled from the "low" attenuation profile (Mitchell and Focke, 1980). The attenuation in evaporite has not been estimated due to lack of data.
- (6) ks - Shear wave attenuation constant starts with an initial value of ks=15. at z=0, and varies with depth as a proportion to the compressional wave attenuation in the manner of Hamilton (1980).

$$k_s(z) = 15.k_p(z)/k_p(z=0)$$

- (7)  $\rho$  - Sediment bulk density was computed from the compressional wave velocity by the equation

$$\rho = 1.135V_p - .19$$

where Vp is the compressional wave velocity in km/s after Hamilton (1978). The density of evaporite is an average of values measured from Mediterranean Sea DSDP Cores (Schreiber et al., 1973)

TABLE 8. GEOACOUSTIC MODEL IIB - Silty clays & clayey silts  
(High Attenuation Model)

Layer Material	Thickness s(1) m(2)	Depth m	Velocity (m/s) Vp(3) Vs(4)		Attenuation kp(5) ks(6)		Density $\rho$ (g/cc)(7)
Sea Surface-----							
Bottom Water		600	1517.5				1.03
Sea Floor-----							
Sediment (clay-silt and silt-clay)	T=.4Z=360.	0	1502.0	116.0	0.0270	15.0	1.52
		25	1534.0	232.0	0.0285	15.8	1.55
		50	1552.0	301.0	0.0295	16.4	1.57
		75	1596.0	333.0	0.0305	16.9	1.62
		100	1625.0	365.0	0.0315	17.5	1.65
		125	1653.0	395.0	0.0320	17.8	1.69
		150	1680.0	409.0	0.0325	18.1	1.72
		175	1706.0	424.0	0.0335	18.6	1.75
		200	1731.0	438.0	0.0340	18.9	1.78
		250	1778.0	467.0	0.0345	19.2	1.83
		300	1820.0	495.0	0.0340	18.9	1.88
		350	1857.0	525.0	0.0320	17.8	1.92
		400	1889.0	554.0	0.0295	16.4	1.95
		500	1937.0	612.0	0.0235	13.1	2.01
Acoustic Basement-----							
Evaporite (halite, gypsum and anhydrite)			4400.	2200.			2.47

NOTES:

- (1) Thickness - The thickness of the upper sediment layer is highly variable. The indicated thickness is a mean for the region in two-way seismic travel time in seconds.
- (2) Thickness - The thickness in meters is computed from the mean two-way travel time and the velocity depth function (3).
- (3) Vp - Compressional wave velocities were computed from the equation

$$V_p = 1.502 + 1.304z - .741z^2 - .257z^3$$

which is taken from Hamilton (1979b), where Vp is in km/s and z is depth in km. A water depth of 600 m was used for this computation; for other water depths the initial velocity (Vp at z=0) should be changed to 0.99 times the bottom water velocity. The velocity for evaporite was taken from Schreiber et al. (1973).

- (4) Vs - Shear wave velocities were computed from the below equations taken from Hamilton (1979a).

$$\begin{array}{ll} V_s = 116. + 4.65z & 0. < z < 36. \\ V_s = 237. + 1.28z & 36. < z < 120. \\ V_s = 322. + .58z & 120. < z < 650. \end{array}$$

Vs is in m/s and z is depth in meters. The shear velocity of evaporite was computed using a Vp/Vs ratio of 2.0.

- (5) kp - Compressional wave attenuation constant was scaled from Hamilton (1972). The attenuation in evaporite has not been estimated due to lack of data.
- (6) ks - Shear wave attenuation constant starts with an initial value of ks=15.0 at z=0.0 and varies with depth as a proportion to the compressional wave attenuation in the manner of Hamilton (1980).

$$k_s(z) = 15.k_p(z)/k_p(z=0)$$

- (7) ρ - Sediment bulk density was computed from the compressional wave velocity by the equation

$$\rho = 1.135V_p - .19$$

where Vp is the compressional wave velocity in km/s after Hamilton (1978). The density of evaporite is an average of values measured from Mediterranean Sea DSDP Cores (Schreiber et al., 1973).

II has two versions, a high and low attenuation case (Geoacoustic Models IIA, Tables 4, 7 and Figures 18-25; and IIB, Tables 5, 8 and Figures 26-33). As previously indicated, Model IIA is the recommended model. Model IIA and IIB differ between the Strait of Sicily and the Strait of Sardinia-Tunisia in their acoustic basement velocity; however, since existing computational techniques cannot account for a rough basement (which is the case throughout most of the area) any acoustic interaction with the basement halfspace would be improperly accounted for in the computation, and the velocity differences are thus probably not significant.

Although the region discussed in this report is often classified a shallow-water area, the dominant sediment types in water deeper than 300 m are of a deep-water variety (turbidites and hemipelagic mud). Rigidity is low in these sediments, and modeling studies have shown that shear waves are not significant (Fryer, 1978; Vidmar, 1980) to acoustic bottom interaction; hence, a fluid sediment was used for calculation. Rigidity was also neglected in the acoustic basement halfspace, since basement interactions are not adequately dealt with (rough basement) in this computation.

Two final points should be made about the bottom loss curves presented in Figures 17-33. One is their inability to account for surface roughness. Most of the area of interest has a smooth and slowly varying water-sediment interface; but the area north of Skerki Bank and the Tunisia shelf is rough and should tend to have a bottom loss above the calculated value. The second factor requiring consideration is the effect of the thin stratification of the sediments, as evidenced by the 3.5 kHz records shown in Sections IV-B and V-B. Gilbert (1980) demonstrated that layering representative of turbidites has significant effect upon reflection coefficients at frequencies above about 200 Hz. Below this frequency, the acoustic wave apparently does not "see" the thin layers as individuals. Above 200-300 Hz, however, the reflection coefficient becomes sensitive to the details of layering. This would tend to produce high variability in bottom loss and, as the kilohertz range is approached, reflection from these thin layers becomes a major bottom interaction mechanism. This is the probable explanation of the "frequency inversion" commonly noted in bottom loss measurements, where the loss at high frequency (kHz range) is less than at mid-frequencies (200-1000 Hz).

The details of sediment layering (i.e., thickness of individual turbidity deposits and intervening pelagic layers) in the area of interest were not available in the published literature. Thus, a statistical model of layering could not be developed\*. The effect of such layering (at water depths greater than 300 m) can, however, easily be demonstrated (Gilbert, 1980). Gilbert's micro-stratigraphic model was based upon layer thicknesses of an "average" turbidite sequence, consisting of thicker (0.5-1.5 m) clay layers interbedded with thinner (0.1-0.3 m) silt layers. Within these limits, he used a uniform random distribution of layer thicknesses to generate many realizations of a Monte Carlo type stochastic turbidite model. To this layering, he added a  $1.0 \text{ s}^{-1}$  velocity gradient and estimated corresponding values of compressional wave attenuation and density. For each realization, the complex reflection coefficient was computed for a variety of frequencies and grazing angles. Figures 34-41 in this report present the results of a similar computation for the frequencies of interest (Figs. 18-33), but show the ensemble average bottom loss versus grazing angle with one standard deviation above and below the average.

\*NOTE: A considerable amount of work has been done on the statistics of sediment layering (Harbaugh and Bonham-Carter, 1970).

Figure 34 depicts results very similar to Figure 18, both of which were computed for 60 Hz. However, the lower velocity gradient and higher attenuation used for Figure 34 produce a generally higher bottom loss and lower "critical angle" than in Figure 18. Similar differences are reflected at other frequencies (Figs. 19-25). Figures 26-33 use higher attenuation values and have bottom loss values comparable to Figures 34-41, but still differ in critical angle as a result of velocity gradient differences. There is, however, a significant trend in Figures 34-41 which is not present in Figures 18-25 or Figures 26-33. This phenomenon is the high frequency inversion. Instead of bottom loss increasing with frequency and grazing angle to an average saturation level of approximately 15 dB, there is a tendency for high frequency-high grazing angle bottom loss to fall significantly below this saturation level. At 840 Hz, above 40° grazing angle, even the ensemble average plus two standard deviations averages slightly less than 15 dB loss. The probable explanation is that (1) below approximately 100-200 Hz, attenuation is sufficiently low for the diving wave refraction to return the bulk of the incident energy to the water column, and the thin layers are not important as individuals, causing the sea floor to approximate a homogeneous medium, and (2) at frequencies above 300-400 Hz the thin layers become important as individuals, causing a significant return of reflected energy at high angles; but increasing attenuation has significantly diminished the importance of the diving wave arrival.

The preferred geoacoustic models of Tables 3, 4, 6, and 7 and theoretical bottom loss curves of Figures 17-25 are based upon the assumption of a homogeneous, horizontally isotropic medium. However, at frequencies above approximately 400 Hz, Figures 39, 40, and 41 imply that the predicted bottom loss will fall significantly below the 15 dB saturation level in areas where subsurface layering will have influence (water depths greater than 300 m).

Geoacoustic modeling from a statistical point of view for nonhomogeneous media has not been actively pursued. In the absence of such techniques, Figures 39-41 are recommended instead of Figures 23-25 for bottom loss at 420, 630, and 840 Hz in areas of water depths greater than 300 m in both the Straits of Sicily and Sardinia-Tunisia. As previously mentioned, the effects of a rough sea floor cannot be properly accounted for at the present time, but loss in these areas should be higher than the predictions of this report.

**BOTTOM LOSS  
GEOACOUSTIC MODEL I  
ALL FREQUENCIES**

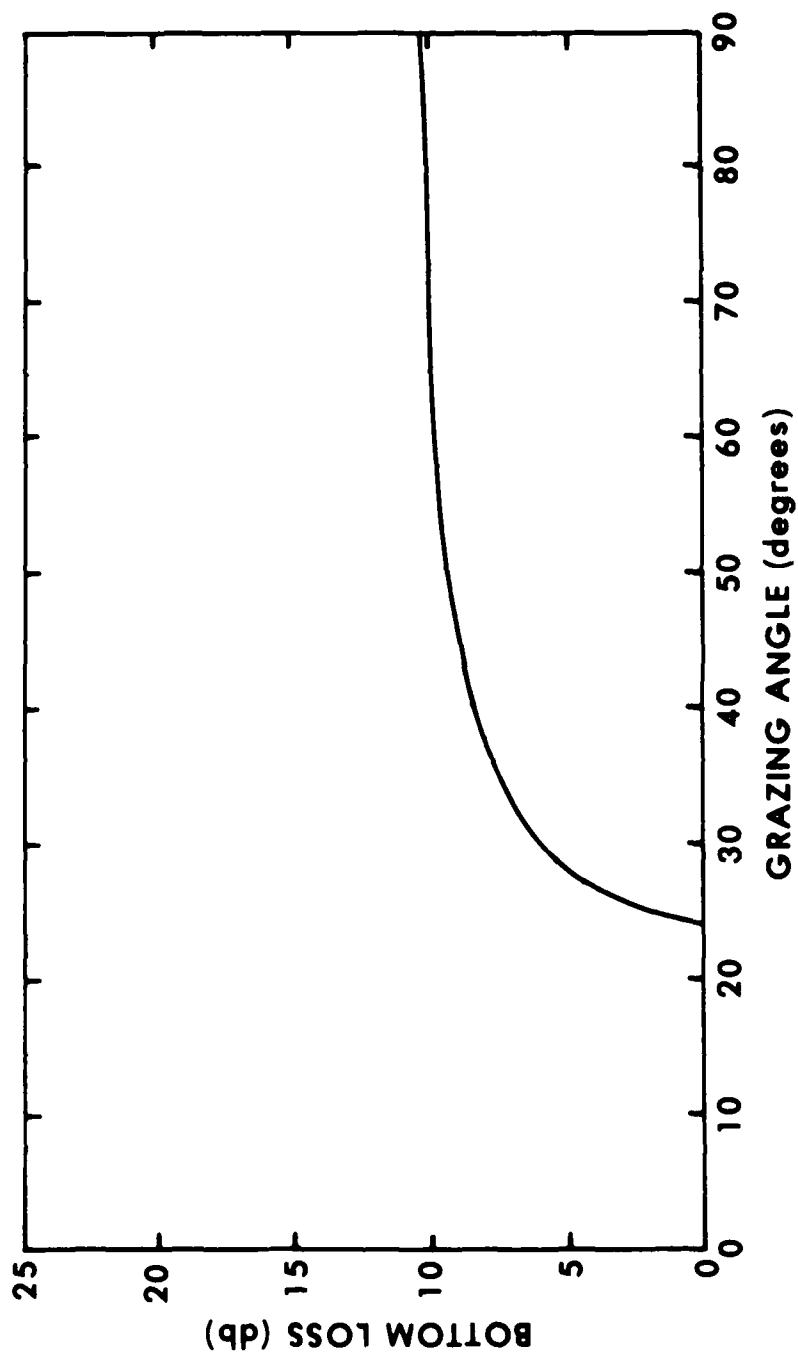


Figure 17. RECOMMENDED bottom loss curve for Model I area of Plate I

**BOTTOM LOSS  
GEOACOUSTIC MODEL IIA  
60 Hz**

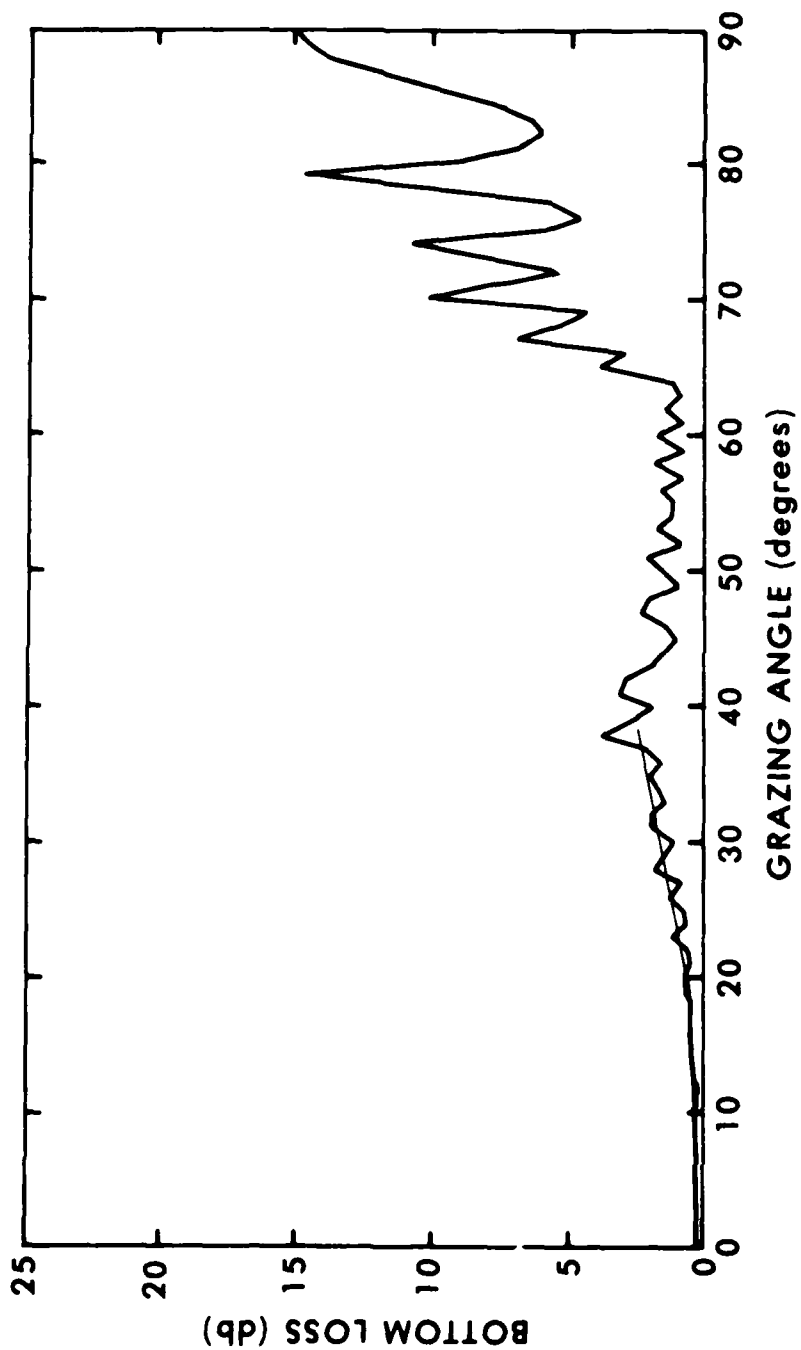


Figure 18. RECOMMENDED bottom loss curves for Model IIA area of Plate I

**BOTTOM LOSS  
GEOACOUSTIC MODEL IIA  
120 Hz**

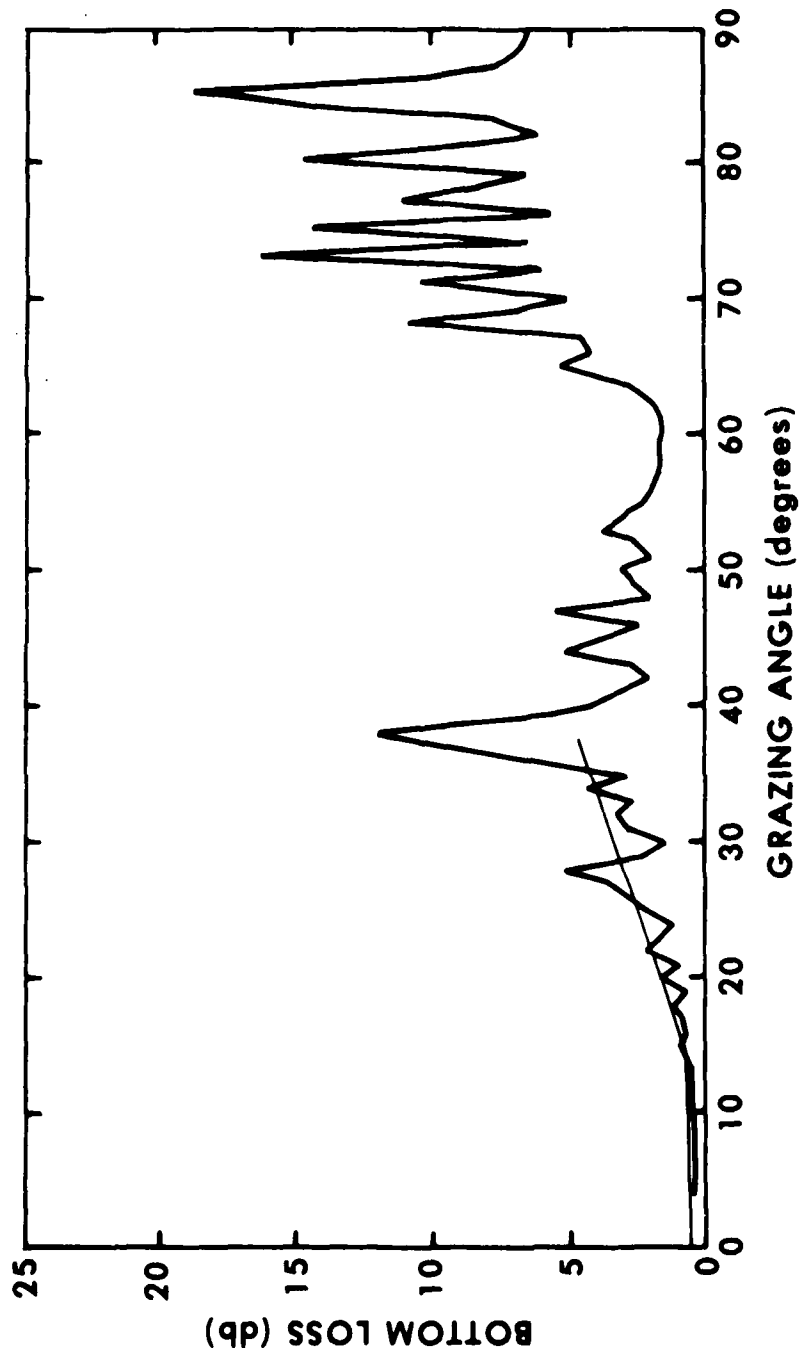


Figure 19. RECOMMENDED bottom loss curves for Model IIA area of Plate I

**BOTTOM LOSS  
GEOACOUSTIC MODEL IIA  
180 Hz**

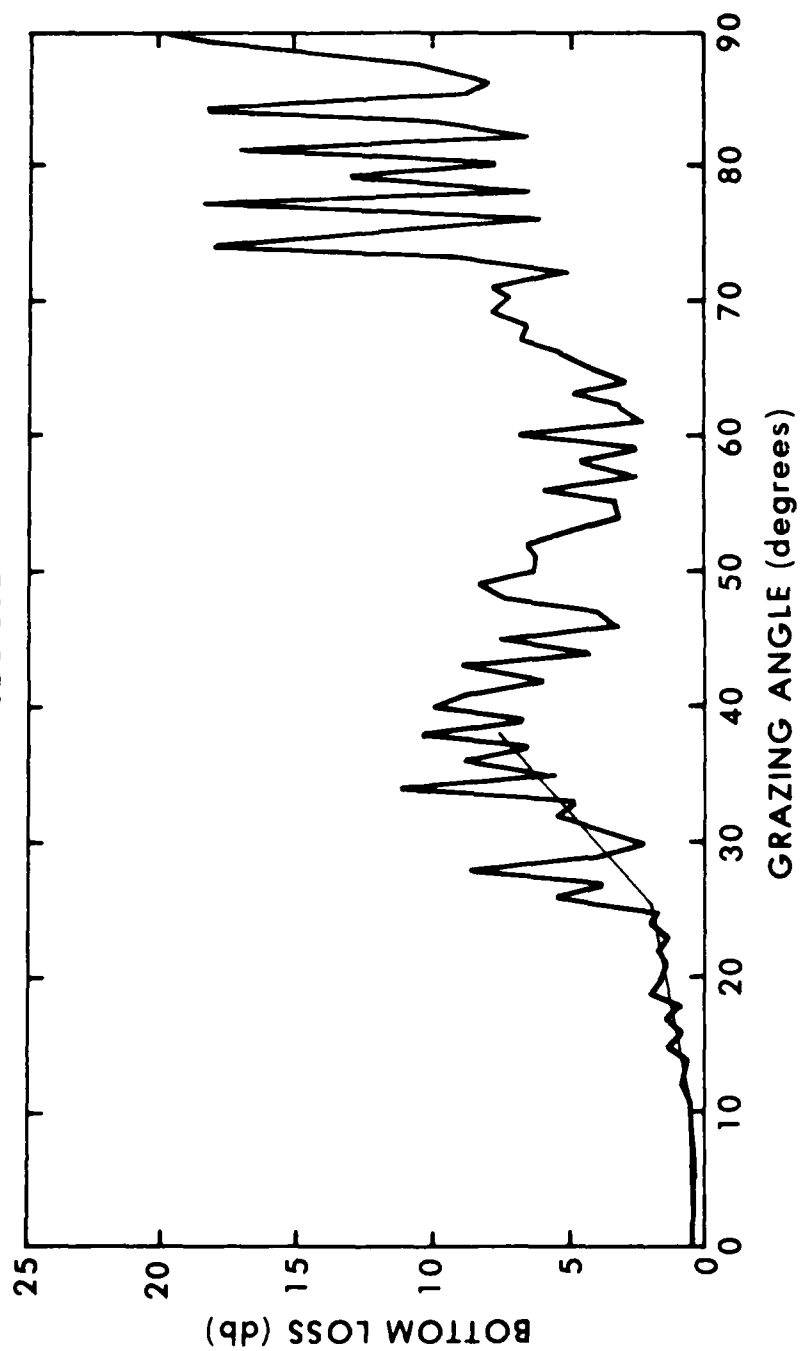


Figure 20. RECOMMENDED bottom loss curves for Model IIA area of Plate I

**BOTTOM LOSS  
GEOACOUSTIC MODEL IIA  
260 Hz**

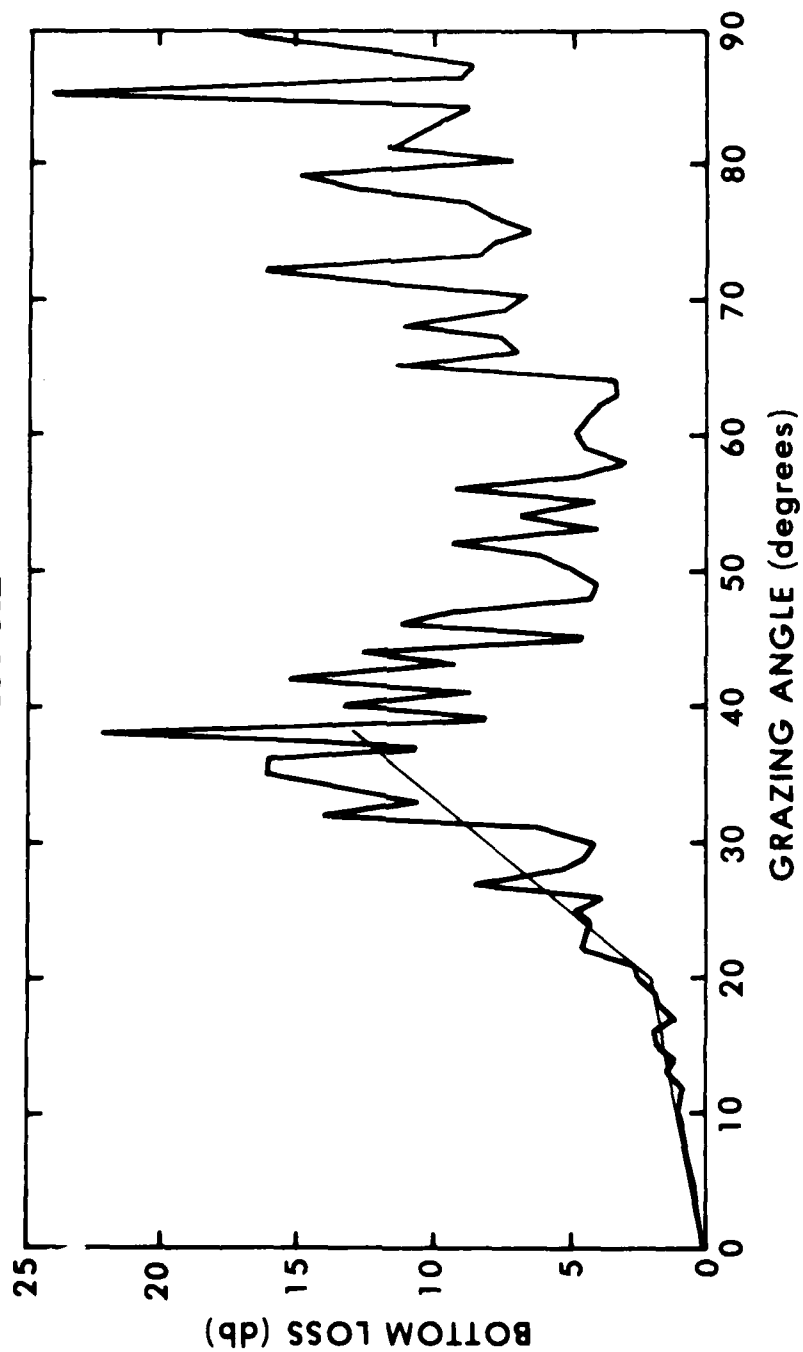


Figure 21. RECOMMENDED bottom loss curves for Model IIA area of Plate I

**BOTTOM LOSS  
GEOACOUSTIC MODEL IIA  
315 Hz**

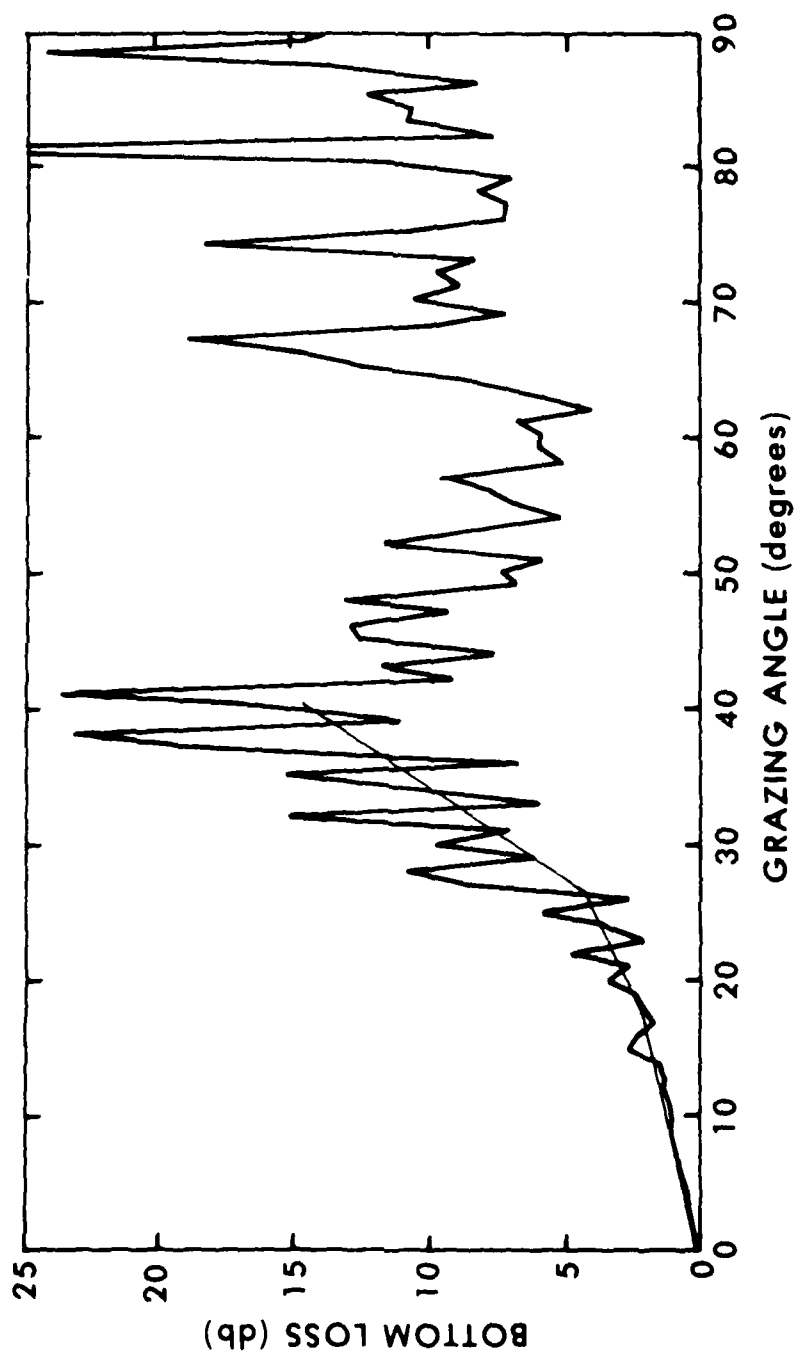


Figure 22. RECOMMENDED bottom loss curves for Model IIA area of Plate I

**BOTTOM LOSS  
GEOACOUSTIC MODEL IIA  
420 Hz**

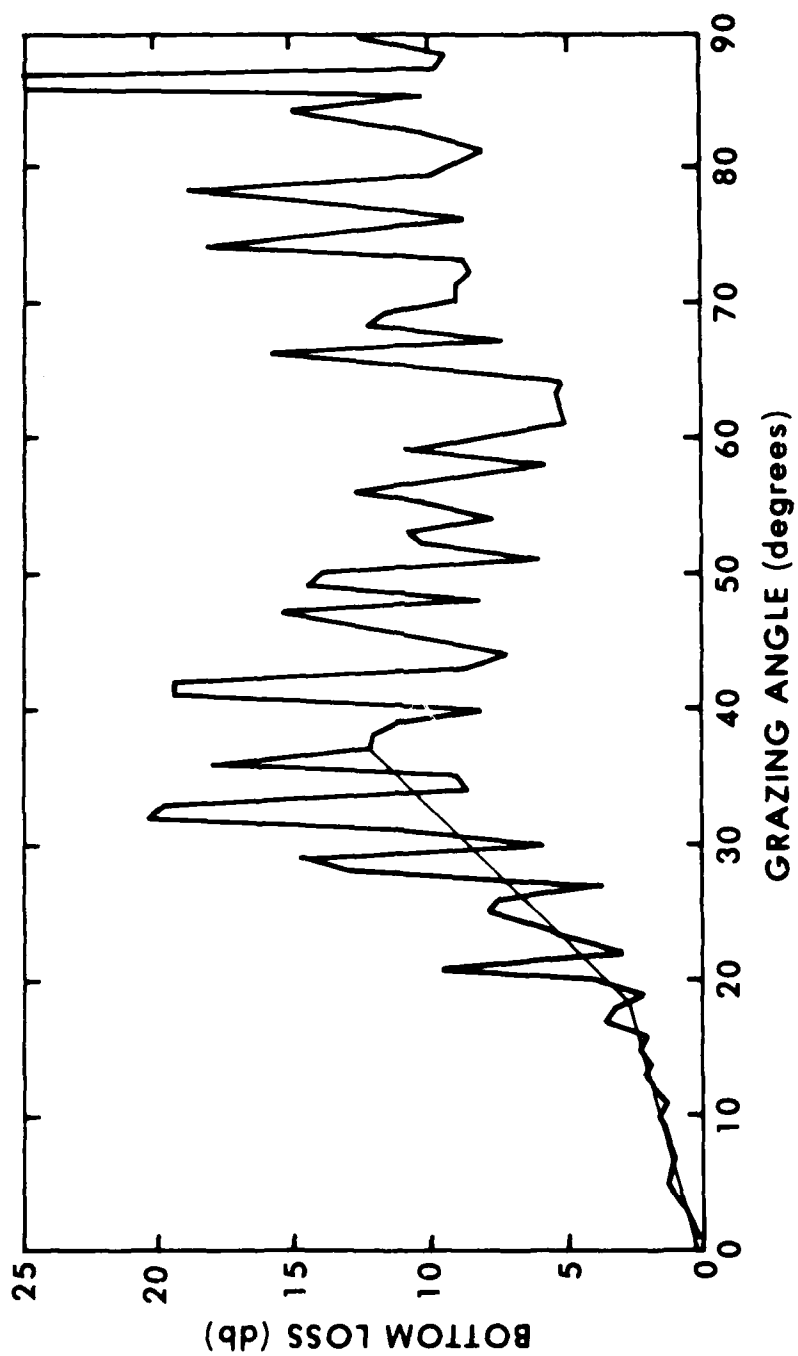


Figure 23. RECOMMENDED bottom loss curve for Model IIA area of Plate I, for ANGLES LESS THAN 30 DEGREES. For higher angles use Figure 39.

# **BOTTOM LOSS** **GEOACOUSTIC MODEL IIA** **630 Hz**

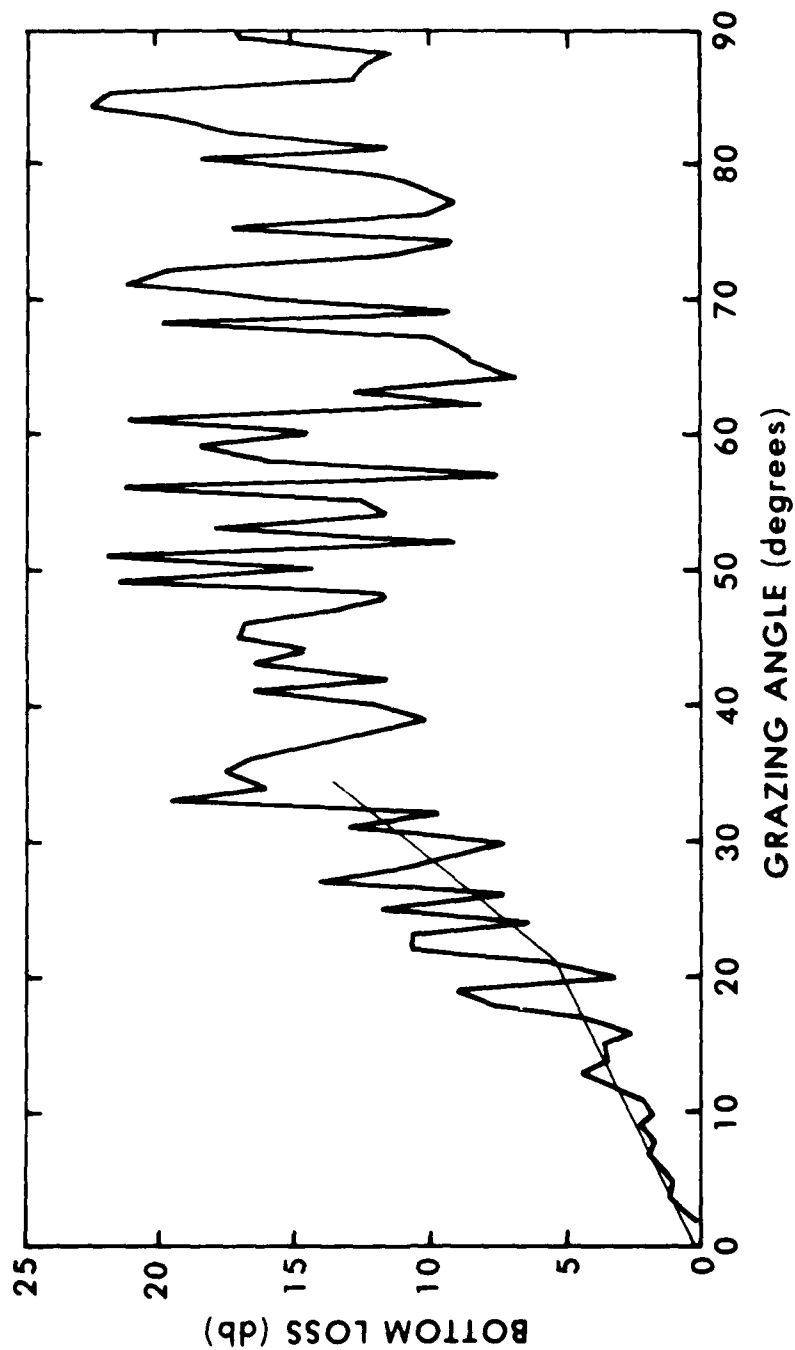


Figure 24. RECOMMENDED bottom loss curve for Model IIA area of Plate I, for ANGLES LESS THAN 30 DEGREES. For higher angles use Figure 40.

**BOTTOM LOSS  
GEOACOUSTIC MODEL IIA  
840 Hz**

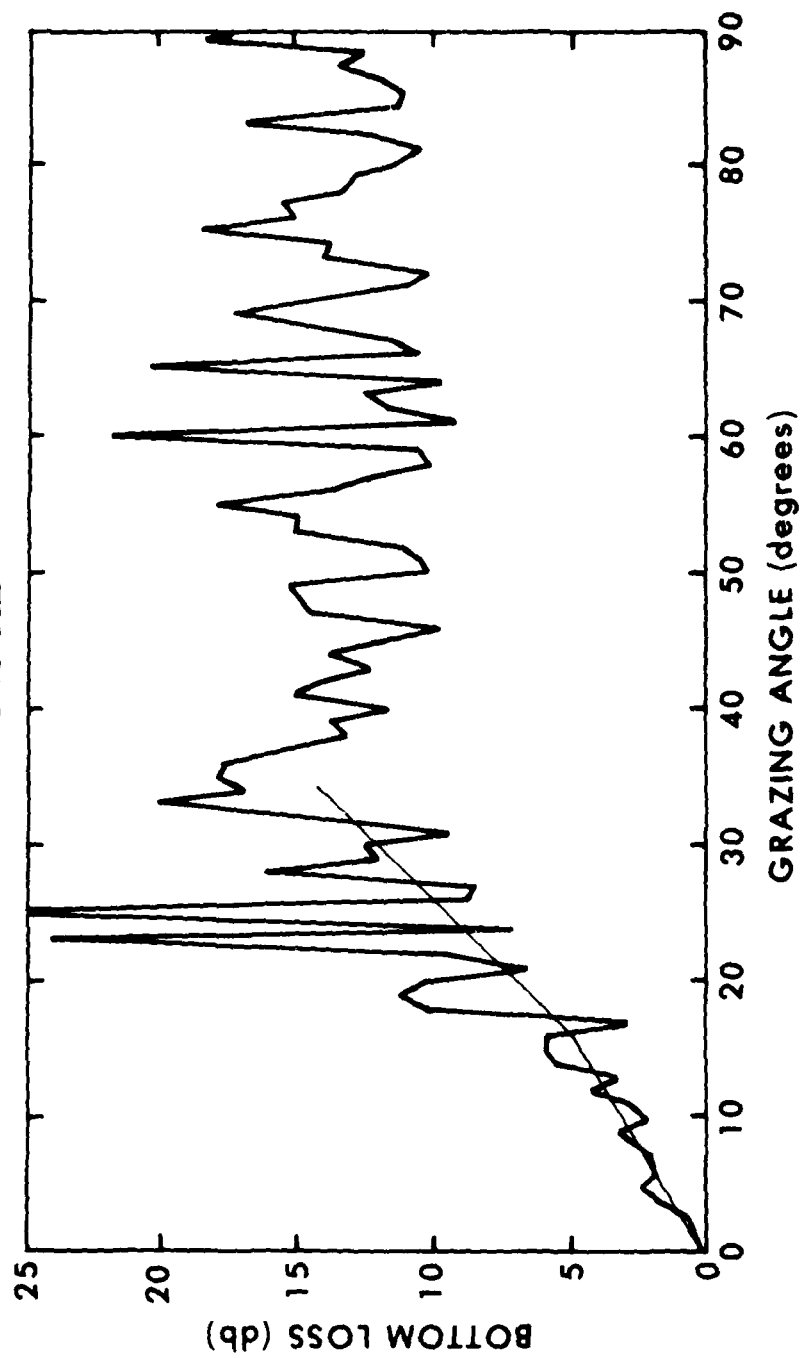


Figure 25. RECOMMENDED bottom loss curve for Model IIA area of Plate I, for ANGLES LESS THAN 30 DEGREES. For higher angles use Figure 41.

**BOTTOM LOSS  
GEOACOUSTIC MODEL IIB  
60 Hz**

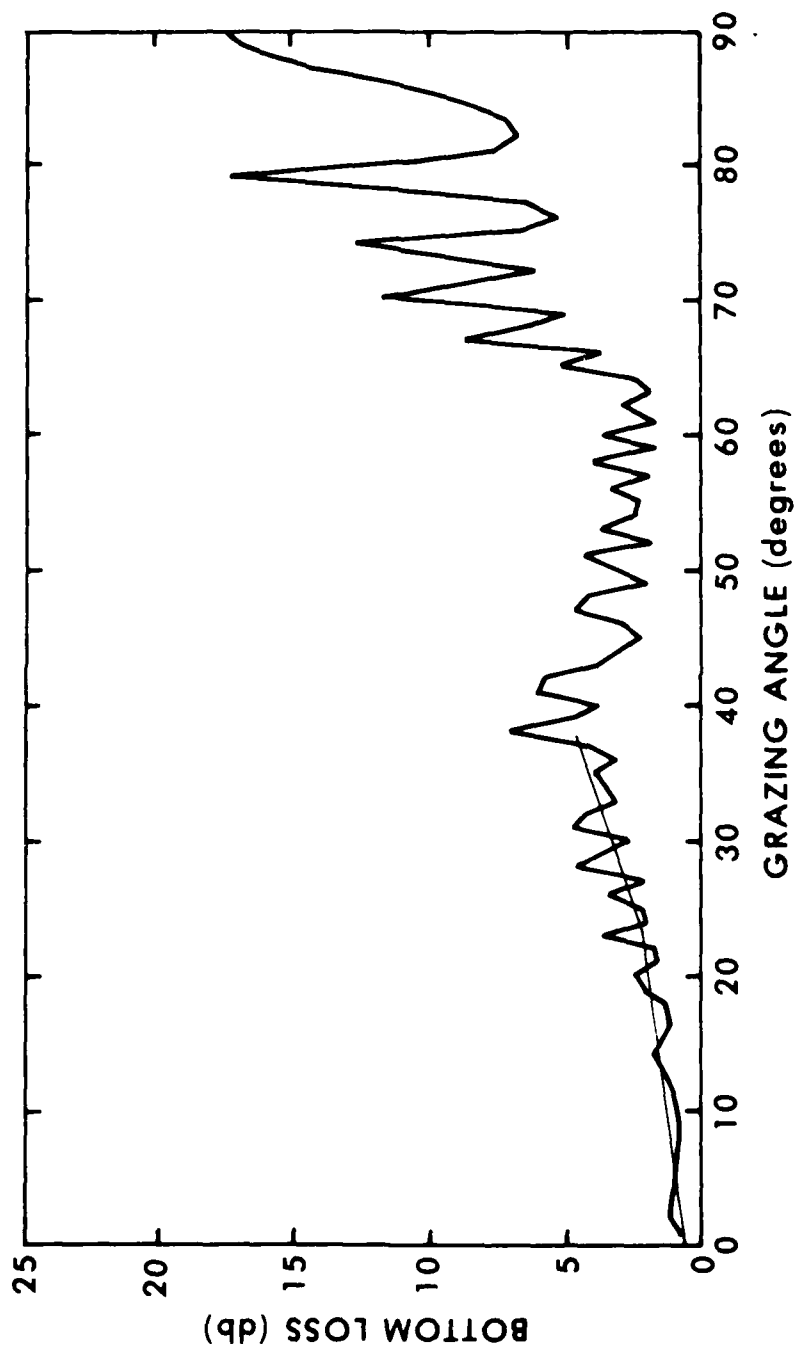


Figure 26. Estimated upper limit of bottom loss values for Model IIA area of Plate I

**BOTTOM LOSS  
GEOACOUSTIC MODEL IIB  
120 Hz**

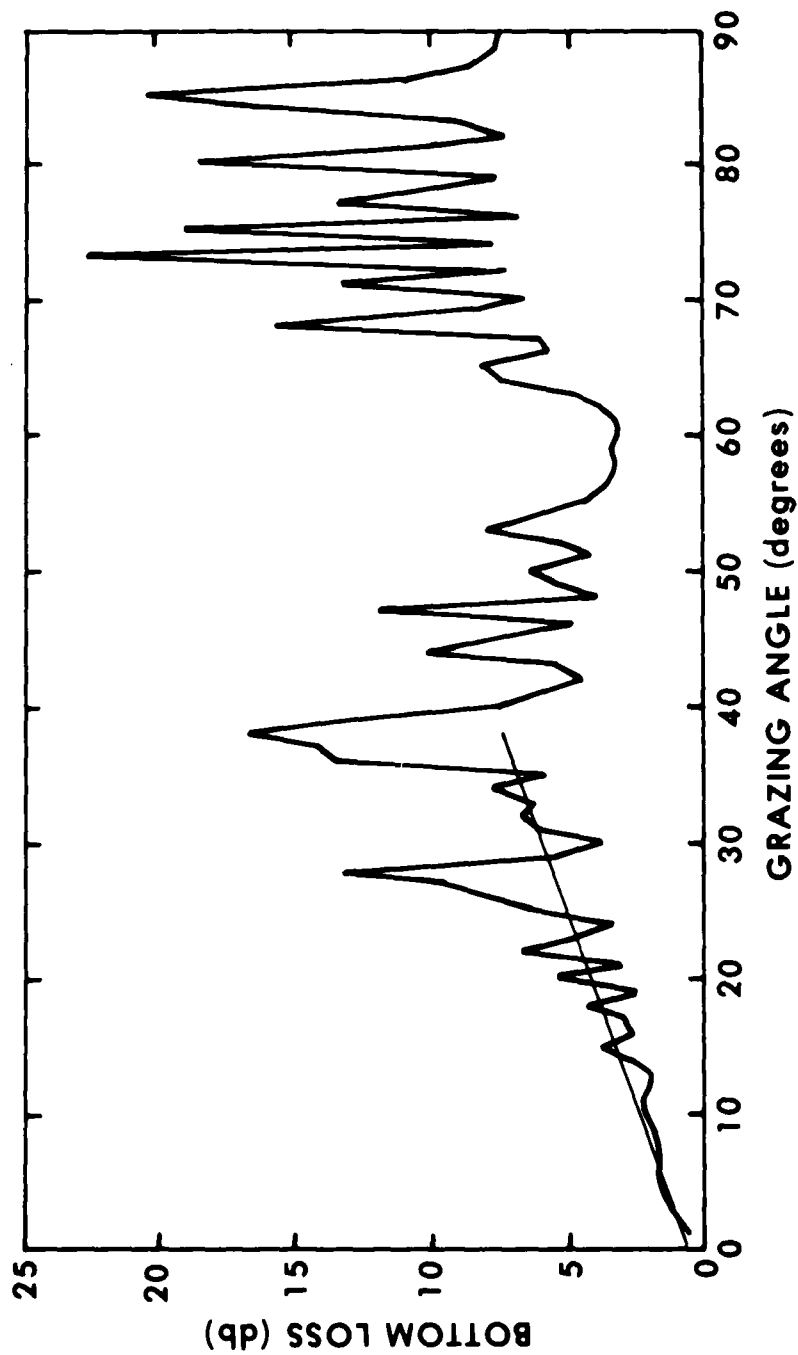


Figure 27. Estimated upper limit of bottom loss values for Model IIA area of Plate I

**BOTTOM LOSS  
GEOACOUSTIC MODEL IIB  
180 Hz**

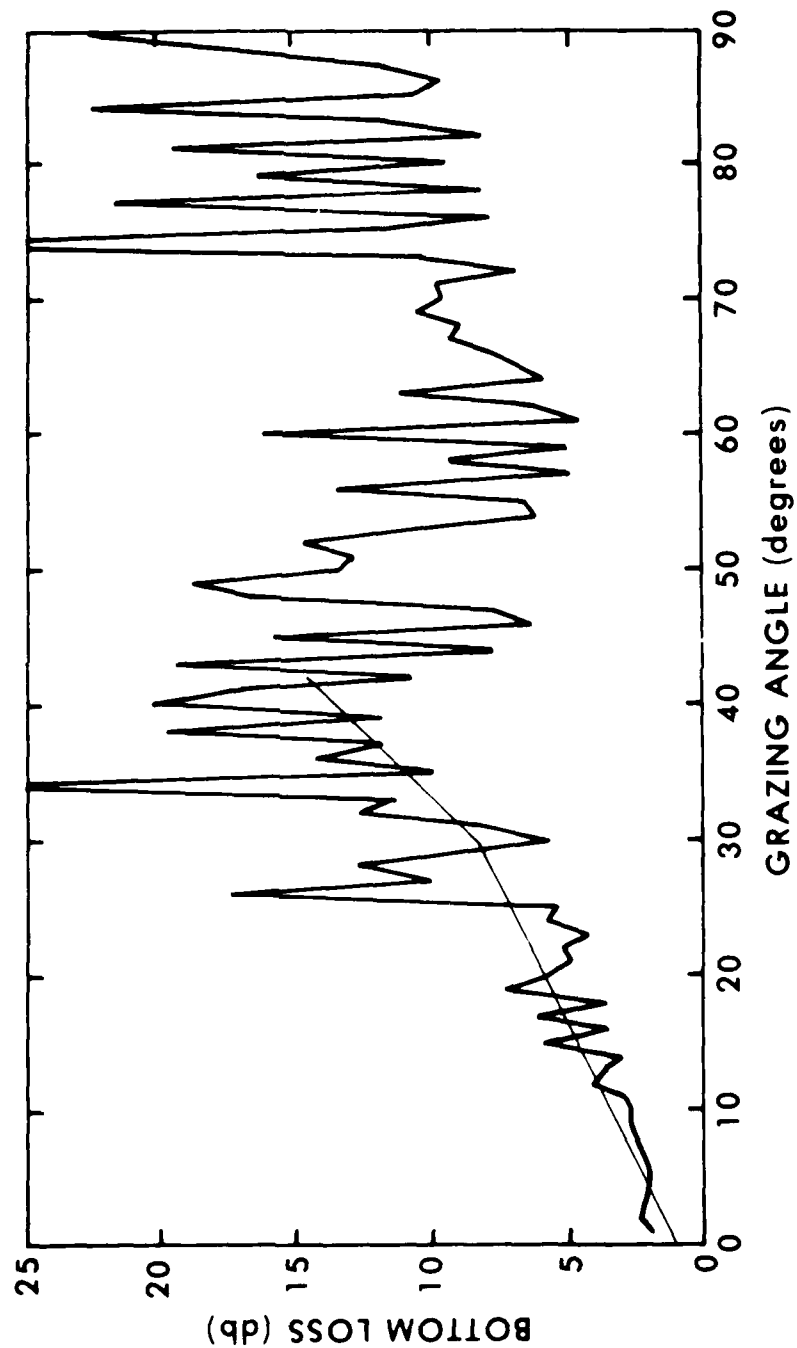


Figure 28. Estimated upper limit of bottom loss values for Model IIA area of Plate I

# **BOTTOM LOSS** **GEOACOUSTIC MODEL IIB** **260 Hz**

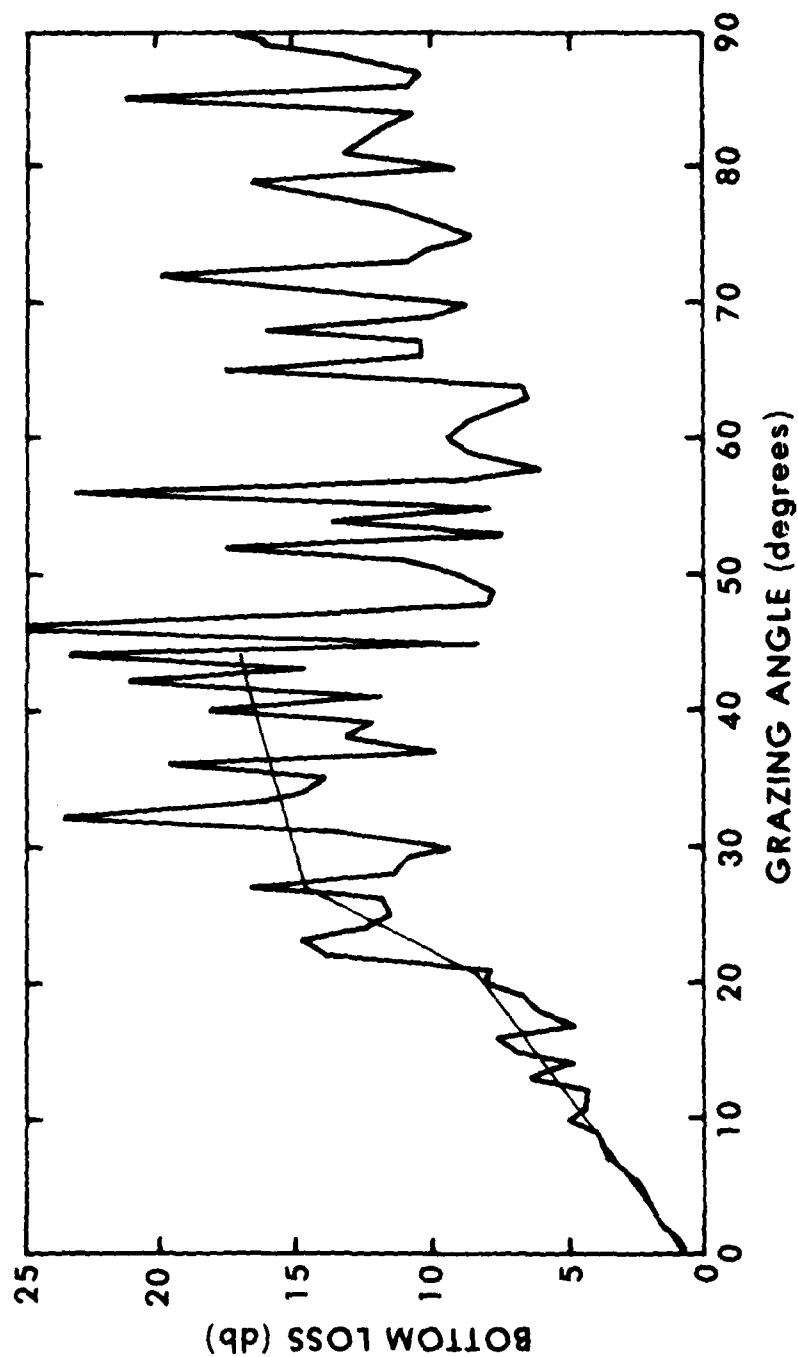


Figure 29. Estimated upper limit of bottom loss values for Model IIA area of Plate I

**BOTTOM LOSS  
GEOACOUSTIC MODEL IIB  
315 Hz**

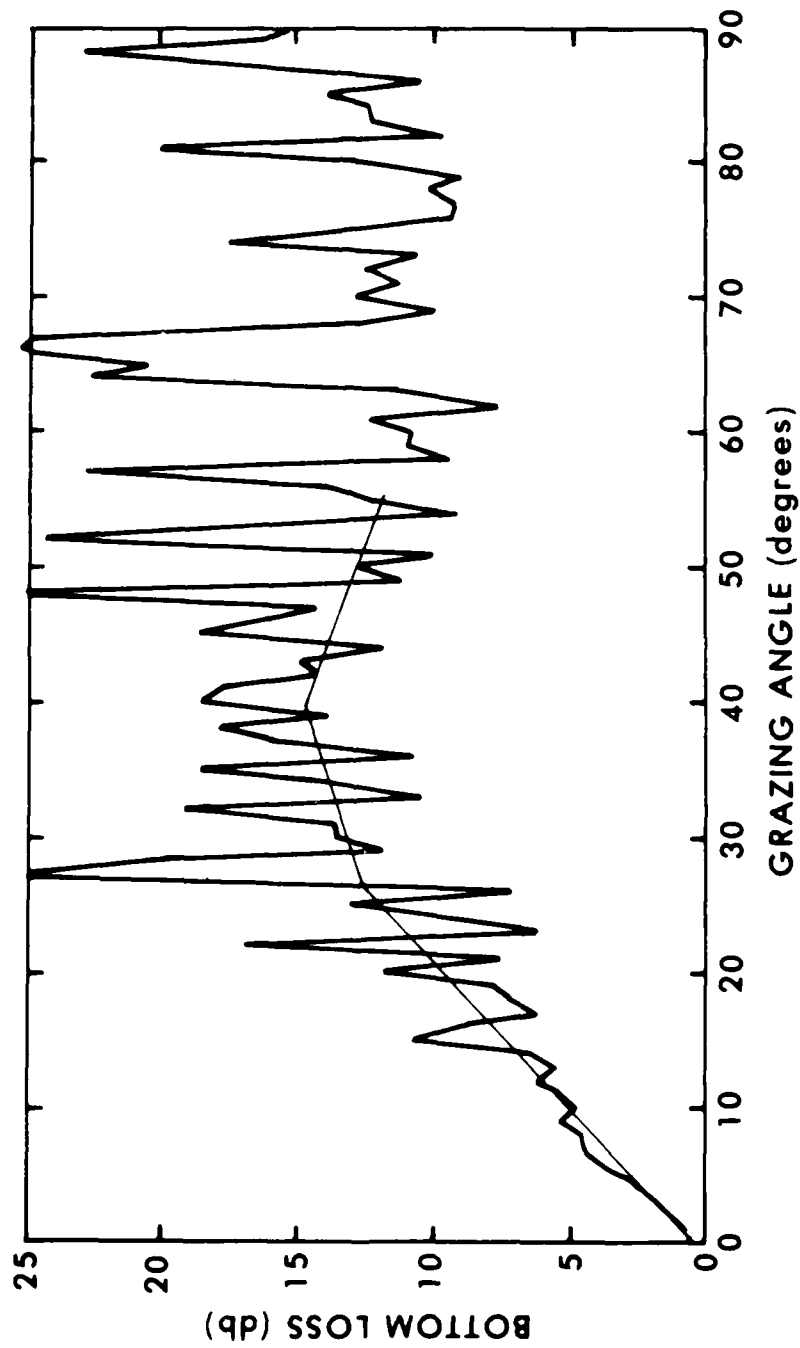


Figure 30. Estimated upper limit of bottom loss values for Model IIA area of Plate I

**BOTTOM LOSS  
GEOACOUSTIC MODEL IIB  
420 Hz**

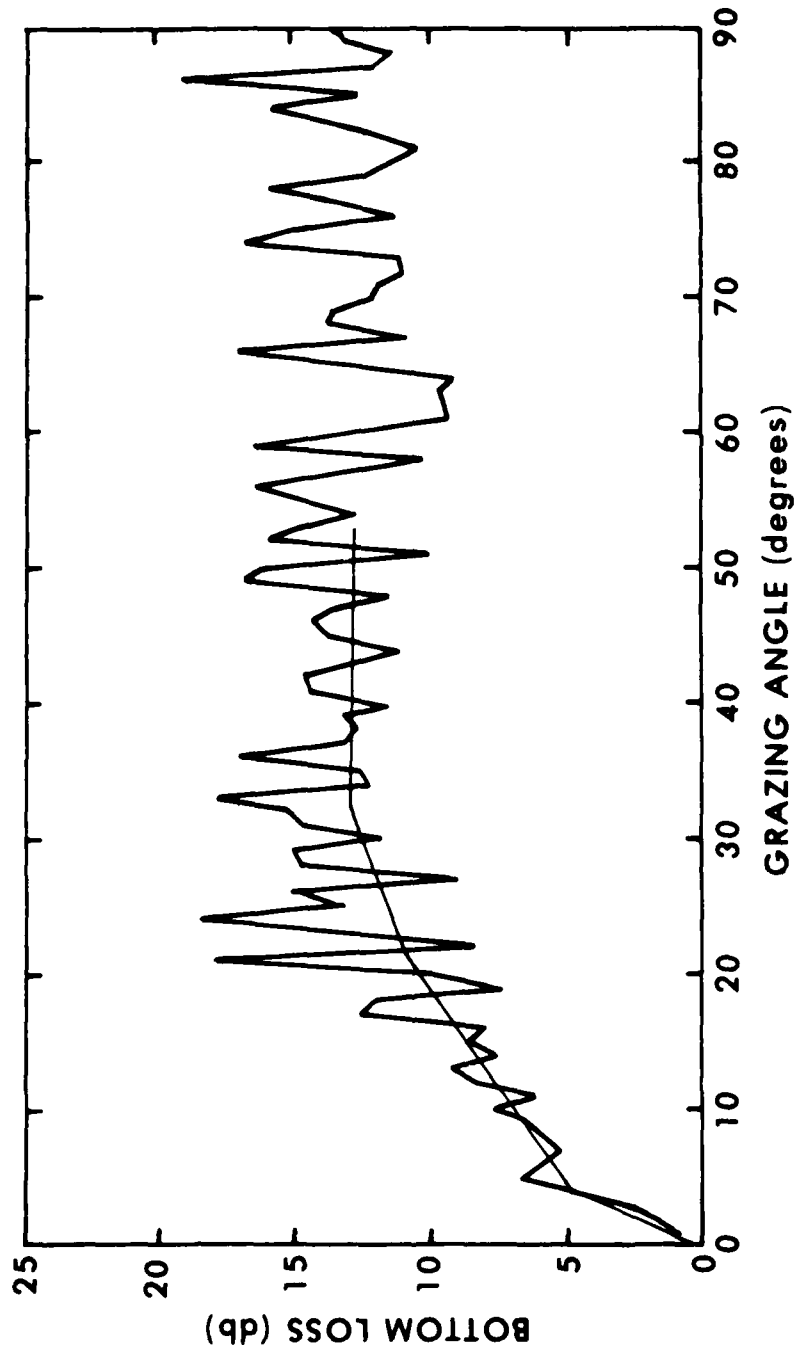


Figure 31. Estimated upper limit of bottom loss values for Model IIA area of Plate I

**BOTTOM LOSS  
GEOACOUSTIC MODEL IIB  
630 Hz**

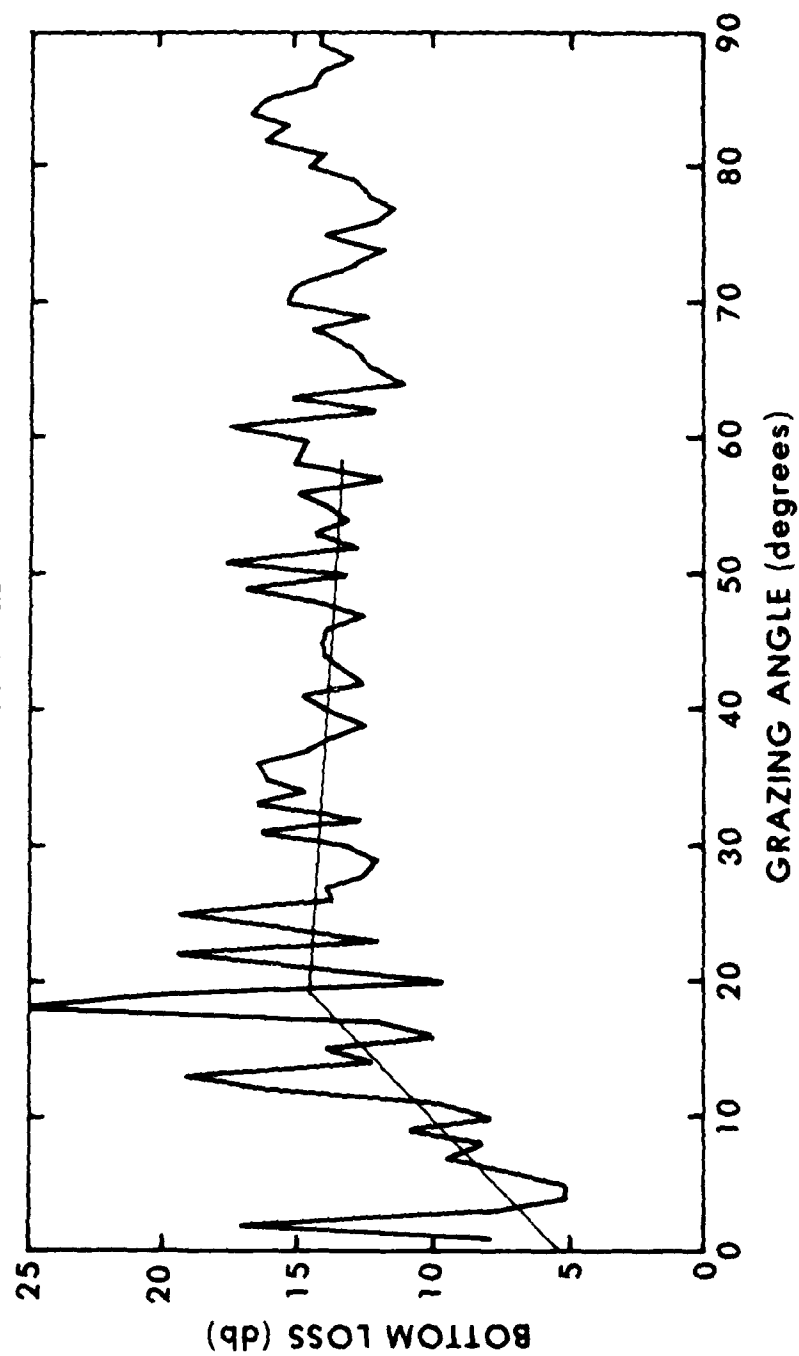


Figure 32. Estimated upper limit of bottom loss values for Model IIA area of Plate I

**BOTTOM LOSS  
GEOACOUSTIC MODEL IIB  
840 Hz**

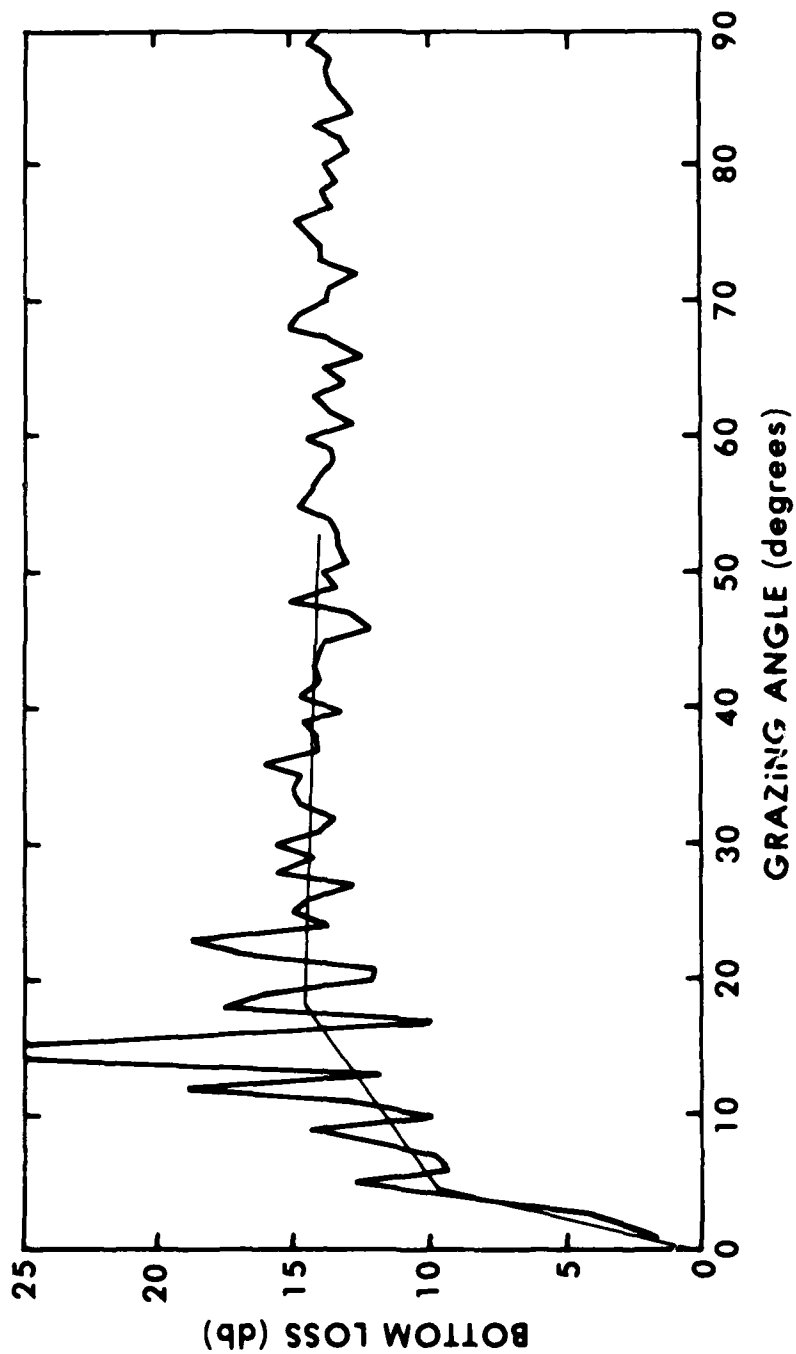


Figure 33. Estimated upper limit of bottom loss values for Model IIA area of Plate I

**BOTTOM LOSS  
RANDOMLY LAYERED SEA FLOOR  
60 Hz**

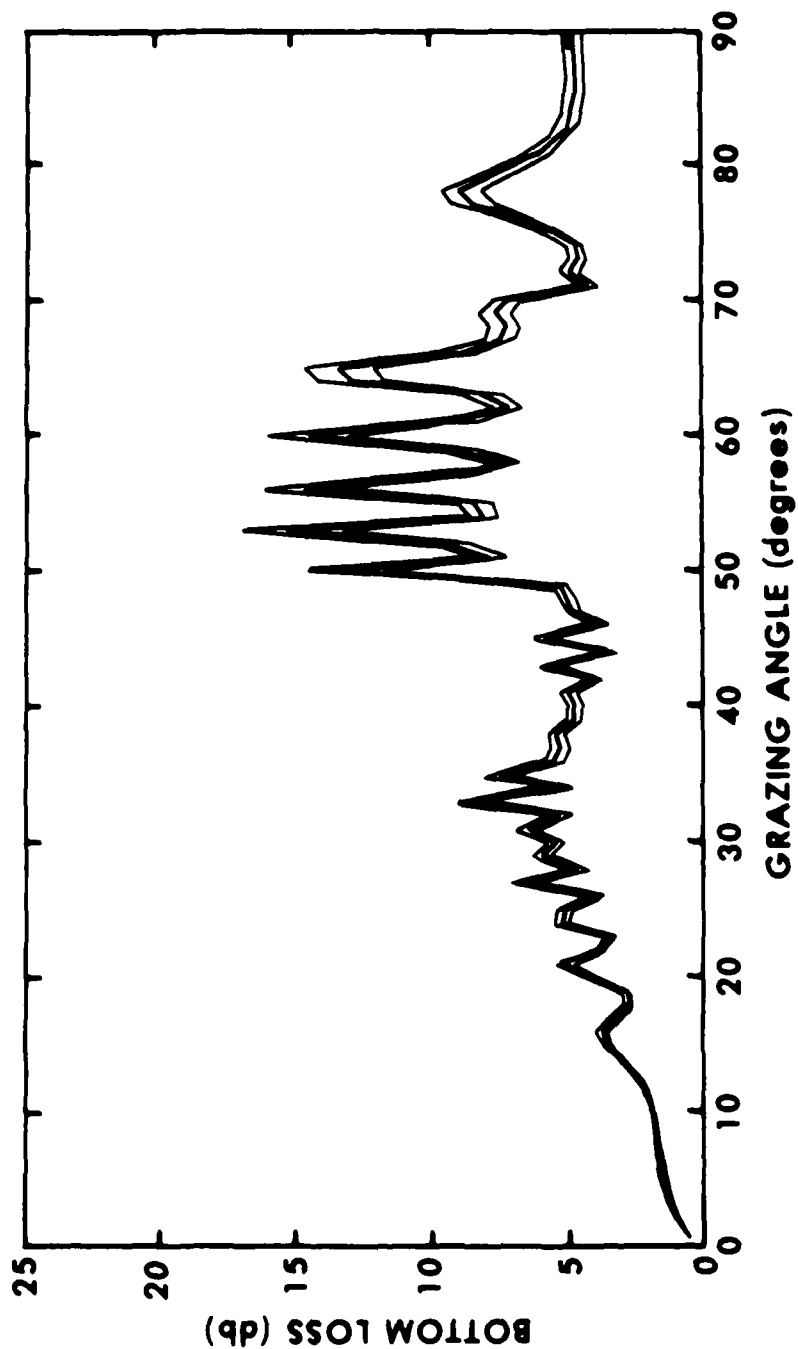


Figure 34. Bottom loss estimates of the ensemble mean plus and minus one standard deviation for a randomly layered model, after Gilbert (1980)

# **BOTTOM LOSS** **RANDOMLY LAYERED SEA FLOOR** **120 Hz**

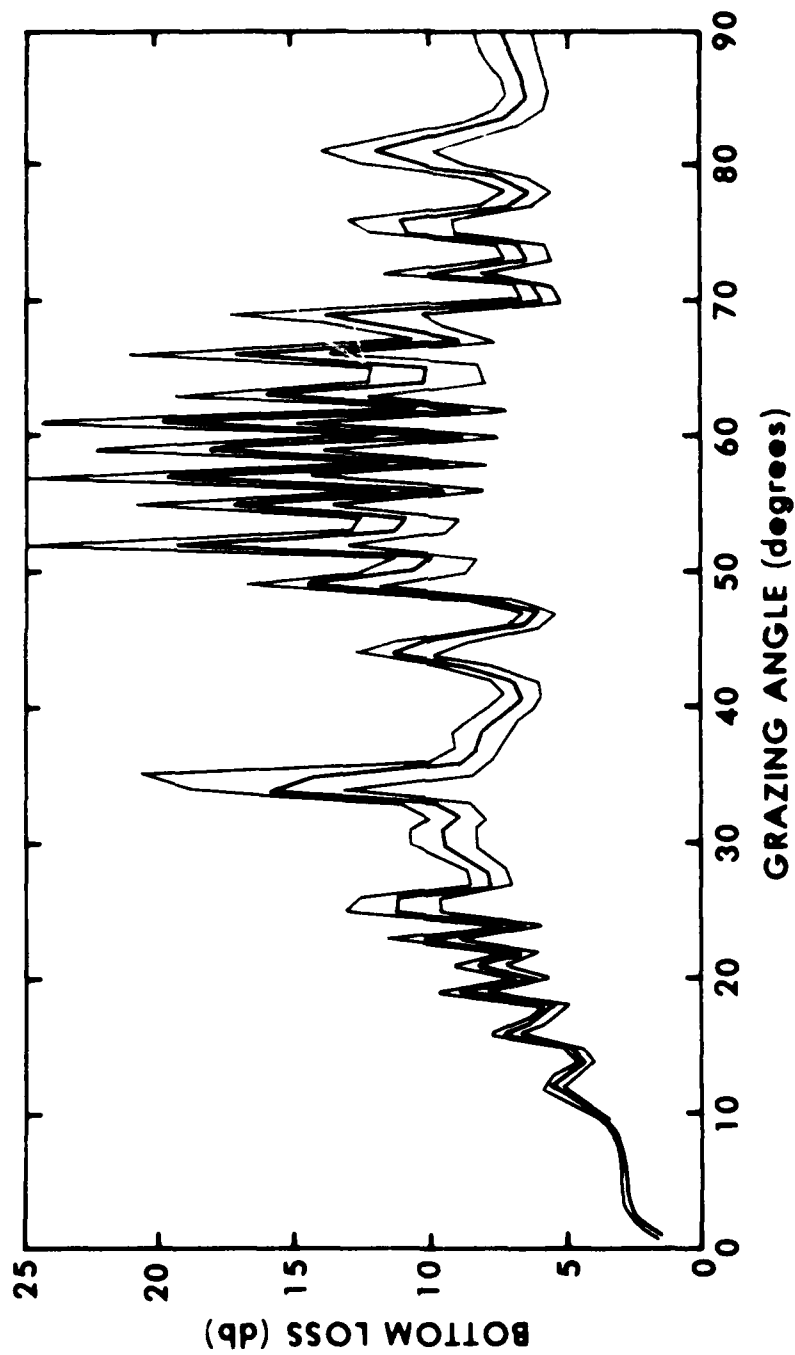


Figure 35. Bottom loss estimates of the ensemble mean plus and minus one standard deviation for a randomly layered model, after Gilbert (1980)

**BOTTOM LOSS  
RANDOMLY LAYERED SEA FLOOR  
180 Hz**

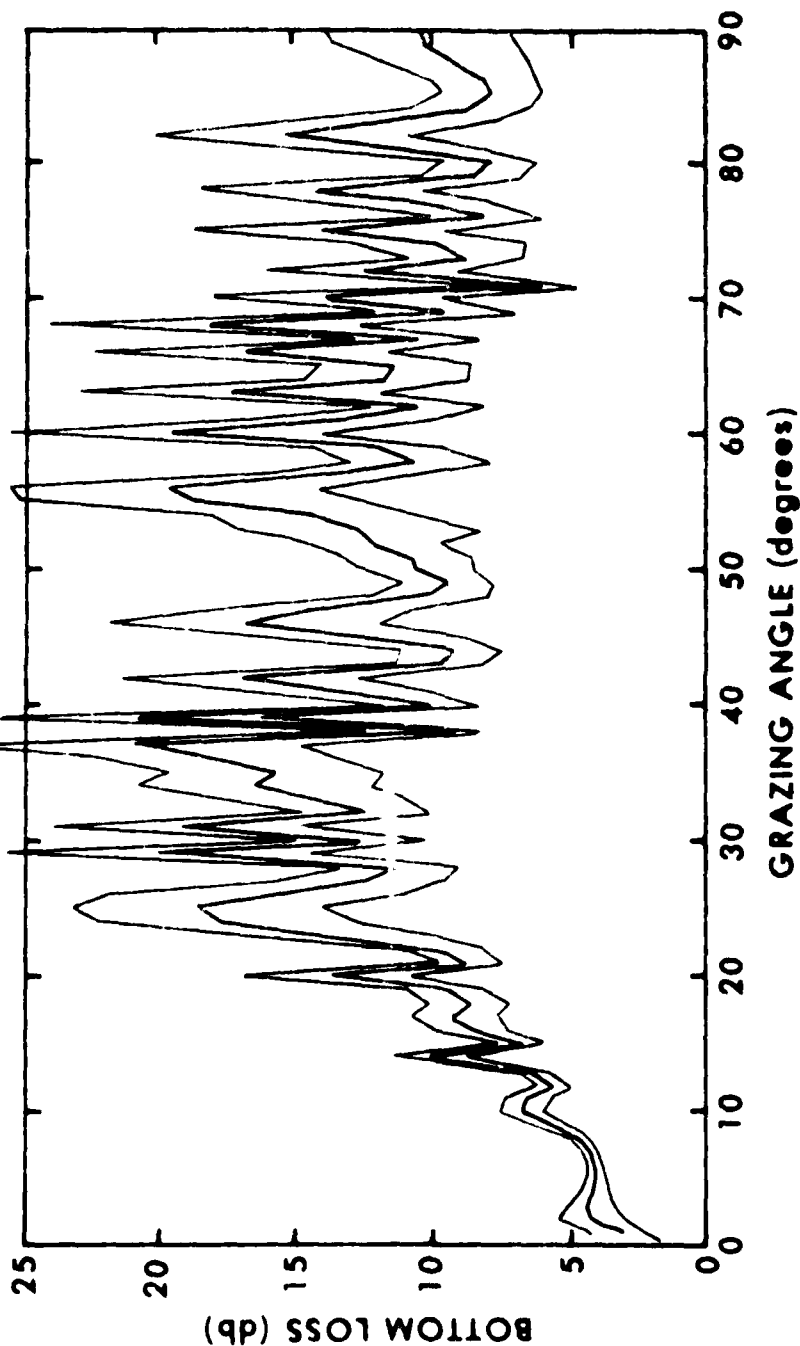


Figure 36. Bottom loss estimates of the ensemble mean plus and minus one standard deviation for a randomly layered model, after Gilbert (1980)

**BOTTOM LOSS  
RANDOMLY LAYERED SEA FLOOR  
260 Hz**

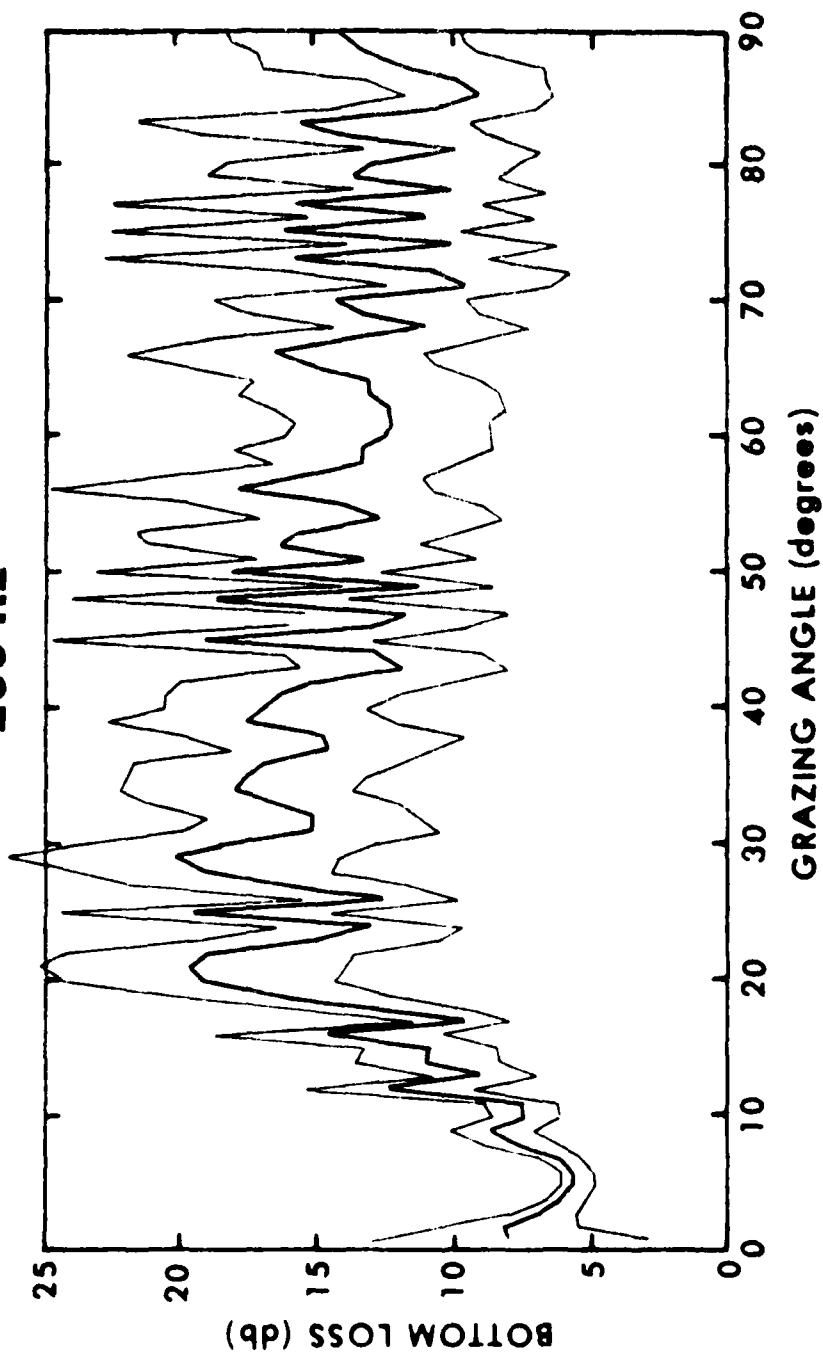


Figure 37. Bottom loss estimates of the ensemble mean plus and minus one standard deviation for a randomly layered model, after Gilbert (1980)

**BOTTOM LOSS  
RANDOMLY LAYERED SEA FLOOR  
315 Hz**

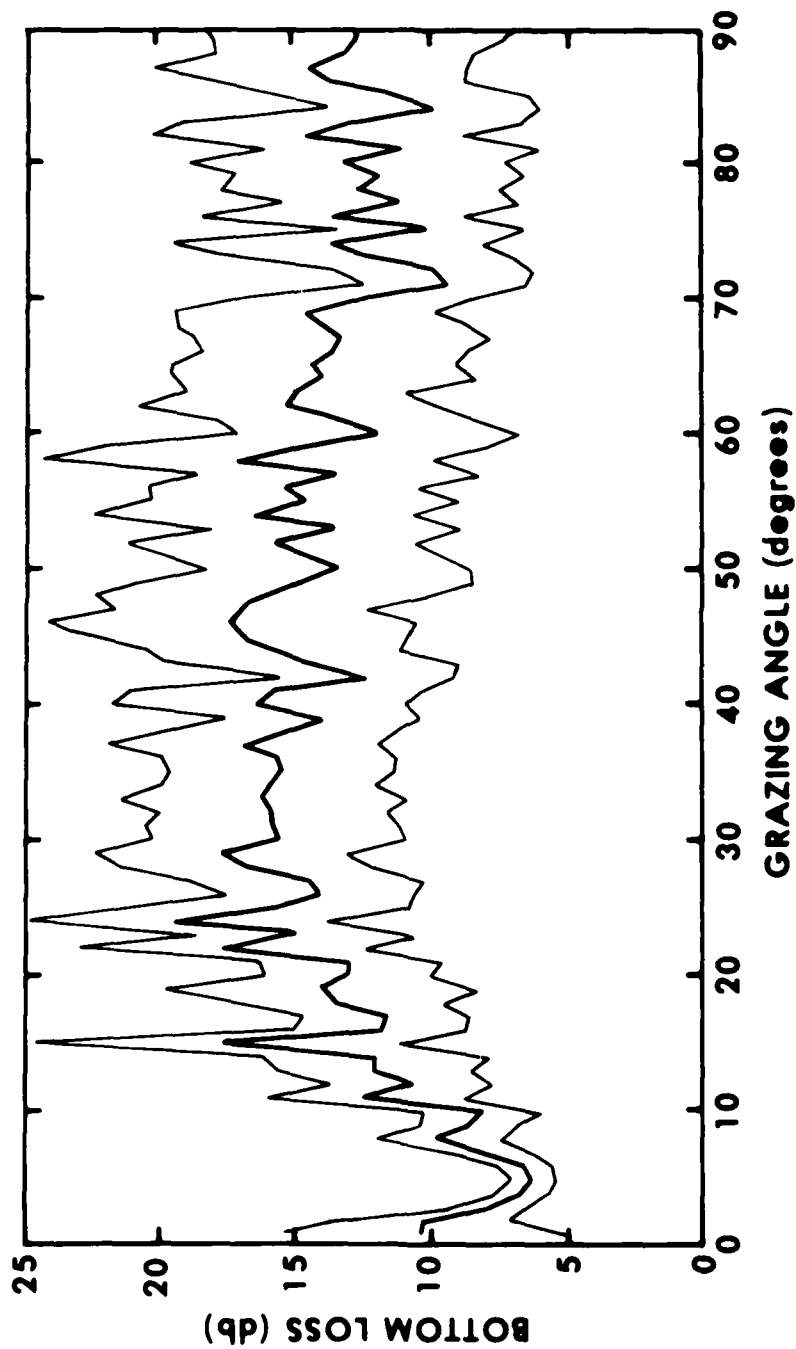


Figure 38. Bottom loss estimates of the ensemble mean plus and minus one standard deviation for a randomly layered model, after Gilbert (1980)

**BOTTOM LOSS  
RANDOMLY LAYERED SEA FLOOR  
420 Hz**

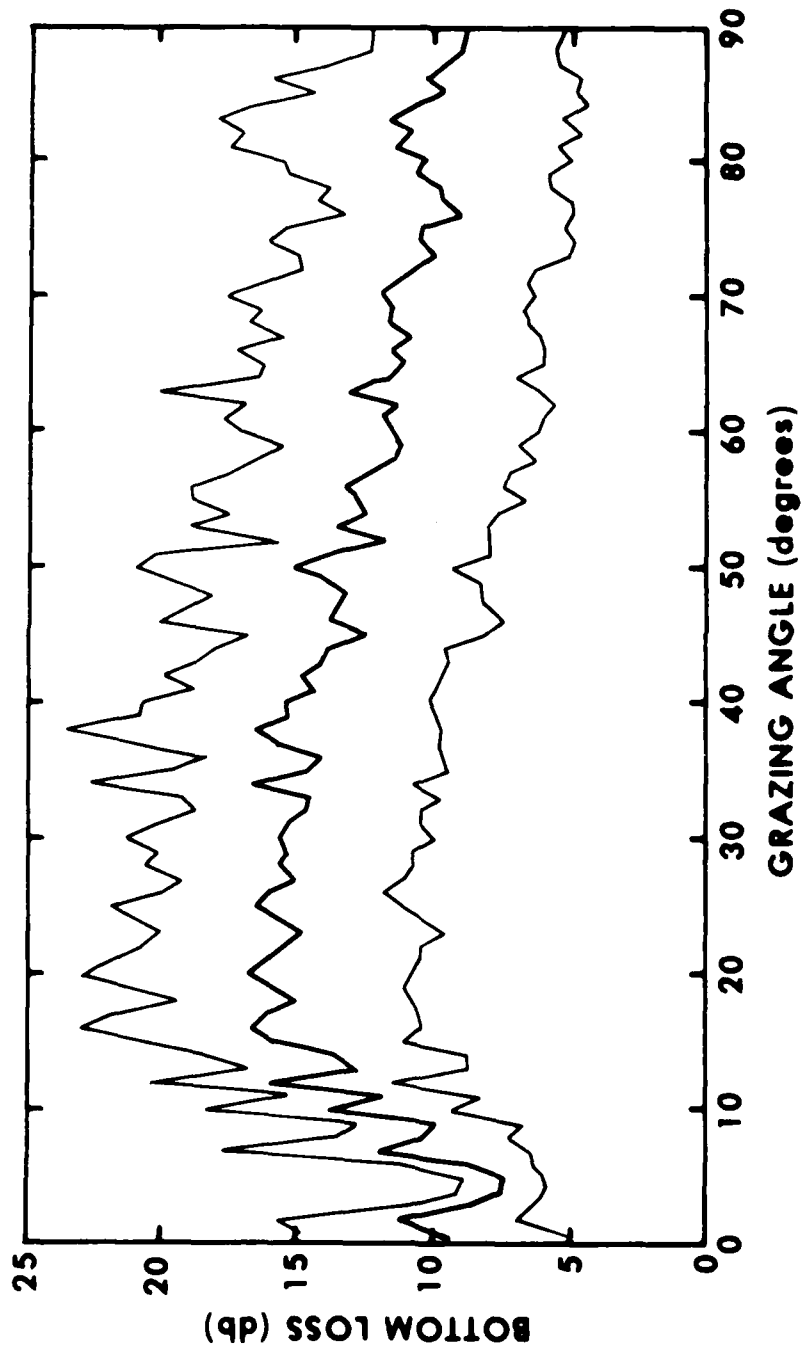


Figure 39. RECOMMENDED bottom loss curve for Model IIA area of Plate I, for ANGLES GREATER THAN 30 DEGREES. Bottom loss estimates are of the ensemble mean plus and minus one standard deviation for a randomly layered model, after Gilbert (1980).

# **BOTTOM LOSS** **RANDOMLY LAYERED SEA FLOOR** **630 Hz**

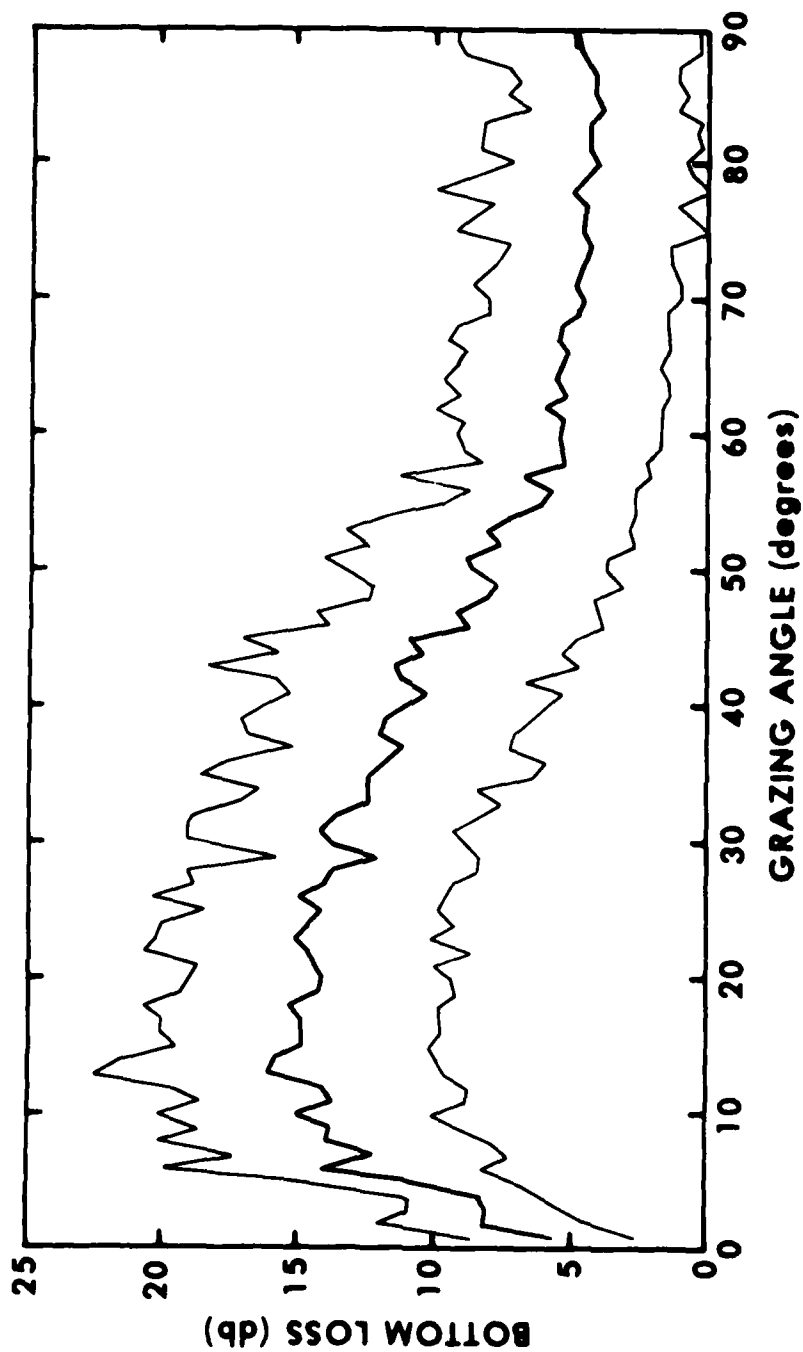


Figure 40. RECOMMENDED bottom loss curve for Model IIA area of Plate I, for ANGLES GREATER THAN 30 DEGREES. Bottom loss estimates are of the ensemble mean plus and minus one standard deviation for a randomly layered model, after Gilbert (1980)

# **BOTTOM LOSS** **RANDOMLY LAYERED SEA FLOOR** **840 Hz**

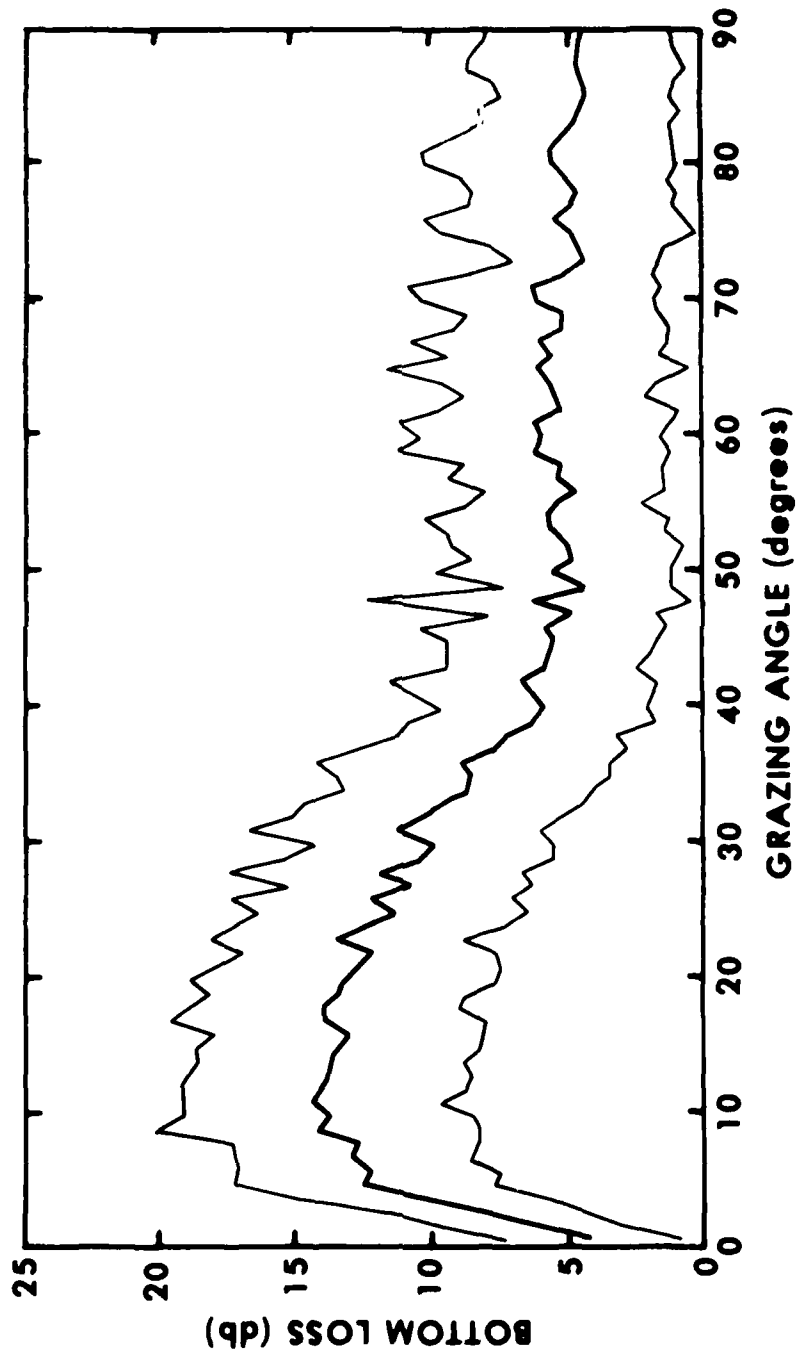


Figure 41. RECOMMENDED bottom loss curve for Model IIA area of Plate I, for ANGLES GREATER THAN 30 DEGREES. Bottom loss estimates are of the ensemble mean plus and minus one standard deviation for a randomly layered model, after Gilbert (1980)

## VII. REFERENCES

- Akal, T. (1972). The General Geophysics and Geology of the Strait of Sicily. In: Oceanography of the Strait of Sicily, ed. T.D. Allan et al., SACLANTCEN Conf. Proc. No. 7, 11-12 Apr., La Spezia, Italy, p. 177-192.
- Allen, T. D. and C. Morelli (1971). A Geophysical Study of the Mediterranean Sea. Boll. Geofis. Teor. Appl., v. 13, p. 99-142.
- Auzende, J. M., J. Bonnin, J. L. Olivet, G. Pautot, and A. Mauffret (1971). Upper Miocene Salt Layer in the Western Mediterranean Basin. Nature Phys. Sci., v. 230, p. 82-84.
- Ballard, J. A. (1979). Geology of a Stable Intraplate Region: The Cape Verde/Canary Basin. Unpublished Ph.D. Thesis, University of North Carolina, Chapel Hill, N.C., p. 78-97.
- Boccaletti, M. and P. Manetti (1978). The Tyrrhenian Sea and Adjoining Regions. In: The Ocean Basins and Margins, ed. A.E.M. Nairn, W. H. Kanes and F. G. Stehli, Plenum Press, N.Y., v. 4B, p. 149-200.
- Brekhovskikh, J. M (1960). Waves in Layered Media. Academic Press, New York, p. 15-59.
- Caulet, J. P. (1972). Recent Biogenic Calcareous Sedimentation on the Algerian Continental Shelf. In: The Mediterranean Sea: A Natural Sedimentation Laboratory, ed. D.J. Stanley, Dowden, Hutchinson & Ross, Stroudsburg, Penn., p. 75-81.
- Curzi, P., A. Fabbri, and T. Nanni (1980). The Messinian Evaporite Event in the Sardinia Basin Area (Tyrrhenian Sea). Marine Geology, v. 34, p. 157-170.
- Damuth, J. E. (1980). Use of High-frequency (3.5-12 kHz) Echograms in the Study of Near-bottom Sedimentation Processes in the Deep-sea: A Review. Marine Geol., v. 38, p. 51-75.
- Dorman, L. M. and R. S. Jacobson (1981). Linear Inversion of Body Wave Data Part I: Velocity Structure from Traveltimes and Ranges. Geophysics, v. 46, p. 138-151.
- Emelyanov, E. M. (1972). Principal Types of Recent Bottom Sediments in the Mediterranean Sea: Their Mineralogy and Geochemistry. In: The Mediterranean Sea: A Natural Sedimentation Laboratory, ed. D.J. Stanley, Dowden, Hutchinson & Ross, Stroudsburg, Penn., p. 355-386.
- Fabbri, A. and R. Selli (1972). The Structure and Stratigraphy of the Tyrrhenian Sea. In: the Mediterranean Sea: A Natural Sedimentation Laboratory, ed. D.J. Stanley, Dowden, Hutchinson & Ross, Stroudsburg, Penn., p. 75-81.
- Finetti, I. and C. Morelli (1973). Geophysical Exploration of the Mediterranean Sea. Bollettino di Geofisica, v. XV, n. 60, Osservatorio Geofisico, Trieste, Italy, p. 263-344.
- Finetti, I. and C. Morelli (1972). Regional Reflection Seismic Exploration of the Strait of Sicily. SACLANT Conference Proceedings No. 7, La Spezia Italy, 11-12 April 1972, p. 208-223.

Fryer, G. J. (1978). Reflectivity of the Ocean Bottom at Low Frequency. Jour. Acous. Soc. Amer., v. 63, p. 35-42.

Gilbert, K. E. (1980). Reflection of Sound from a Randomly Layered Ocean Bottom. Jour. Acous. Soc. Amer., v. 63, p. 1454-1458.

Hamilton, E. L. (1980). Geoacoustic Modeling of the Sea Floor. J. Acous. Soc. Amer., v. 68, p. 1313-1340.

Hamilton, E. L. and R. T. Bachman (1979a). Geoacoustic Models of the Sea Floor: Gulf of Oman, Arabian Sea, and Somali Basin. Naval Ocean Systems Center Tech. Report, NOSC TR 157, p. 1-91.

Hamilton, E. L. (1979b). Sound Velocity Gradients in Marine Sediments. Jour. Acous. Soc. Am., v. 65, p. 909-922.

Hamilton, E. L. (1979c).  $V_p/V_s$  and Poisson's Ratios in Marine Sediments and Rocks. Jour. Acous. Soc. Am., v. 66, p. 1093-1101.

Hamilton, E. L. (1978). Sound Velocity-density Relations in Sea-floor Sediments and Rocks. Jour. Acous. Soc. Am., v. 63, p. 366-377.

Hamilton, E. L. (1972). Compressional Wave Attenuation in Marine Sediments, Geophysics, v. 37, p. 620-646.

Harbaugh, J. W. and G. Bonham-Carter (1970). Computer Simulation in Geology. John Wiley and Sons, N.Y., p. 98-168.

Heezen, B. C., C. Gray, A. G. Segre and E. F. K. Zarudski (1971). Evidence of a Foundered Continental Crust Beneath the Central Tyrrhenian Sea. Nature, v. 229, p. 327-329.

Hsu, K. J. (1977). Tectonic Evolution of the Mediterranean Basins. In: The Ocean Basins and Margins, ed. A.E.M. Nairn, W. K. Kanes and F. G. Stehli, Plenum Press, N.Y., v. 4A, p. 29-75.

Jacobson, R. S., G. G. Shore, and L. M. Dorman (1981). Linear Inversion of Body Wave Data - Part II: Attenuation Versus Depth Using Spectral Ratios. Geophysics, v. 46, p. 152-162.

Lort, J. M. (1977). Geophysics of the Mediterranean Sea Basins in The Ocean Basins and Margins. Ed. A.E.M. Nairn, W. K. Kanes and F. G. Stehli, Plenum Press, N.Y., v. 4a, p. 151-213.

Maldonado, Andres and D. J. Stanley (1976). Late Quaternary Sedimentation and Stratigraphy in the Strait of Sicily. Smithsonian Contributions to the Earth Sciences No. 16, Smithsonian Institution Press, Washington, D.C., p. 1-73.

Matthews, J. E. (1981). Physical Properties of Three Sediment Cores From the Strait of Sicily-unpublished. Sediment Physics Laboratory Item 5-81, Naval Ocean Research and Development Activity, NSTL Station, Miss.

Mauffret, A., J. P. Fail, L. Montadert, J. Sancho and E. Winnock (1973). Northwestern Mediterranean Sedimentary Basin from a Seismic Reflection Profile. Bull. Amer. Assoc. Petrol. Geol., v. 57, p. 2245-2262.

- Mitchell, S. K. and K. C. Focke (1980). New Measurements of Compressional Wave Attenuation in Deep Ocean Sediments. Jour. Acous. Soc. Amer., v. 67, n. 5, p. 1582-1589.
- Morelli, C. (1975). Geophysics of the Mediterranean. Bull. Etude Commun. Medit. Monaco, Sp. Publ. No. 7, p. 27-111.
- Nairn, A. E., W. H. Kanes and F. G. Stehli (1978). The Ocean Basins and Margins, Volume 4B. The Western Mediterranean. Plenum Press, N.Y., p. 1-447.
- Nairn, A. E., W. H. Kanes and F. G. Stehli (1977). The Ocean Basins and Margins, Volume 4A. The Eastern Mediterranean. Plenum Press, N.Y., p. 1-503.
- Payton, C. E. (1977). Seismic Stratigraphy - Applications to Hydrocarbon Exploration. Amer. Assoc. Pet. Geol. Memoir 26, p. 1-516.
- Ryan, W. B. F., D. J. Stanley, J. B. Hersey, D. A. Fahlquist, and T. D. Allan (1970). The Tectonics and Geology of the Mediterranean Sea. In: The Sea. ed. A. E. Maxwell, Wiley-Interscience, N.Y., v. IV, Pt. 2.
- Ryan, W. B. F., F. Workum, and J. Hersey (1965). Sediments on the Tyrrhenian Abyssal Plains. Bull. Geol. Soc. Amer., v. 76, p. 1261-1282.
- Ryan, W. B., D. J. Stanley, J. B. Hersey, D. A. Fahlquist and T. D. Allan (1970). The Tectonics and Geology of the Mediterranean Sea. In: The Sea, ed. A. E. Maxwell, Wiley-Interscience, N.Y., v. IV, Pt. 2.
- Ryan, W. B., K. J. Hsu, W. Nesteroff, G. Pautot, F. C. Wezel, J. M. Lort, M. B. Cita, W. Maync, H. Stradner and P. Dumitrica (1973). Initial Reports of the Deep Sea Drilling Project, v. 13, Part II, p. 1447.
- Schreiber, E., P. J. Fox and J. J. Peterson (1973). Compressional Wave Velocities in Selected Samples of Gabbro, Schist, Limestone, Anhydrite, Gypsum and Halite. In: Initial Reports of the Deep Sea Drilling Project, Vol. XIII, Part 2, ed. W.B.F. Ryan et al., U. S. Govt. Printing Off., Washington, D.C., v. 13, p. 595-597.
- Sheriff, R. E. (1980). Seismic Stratigraphy. Int. Human Resources Development Corp., Boston, p. 1-277.
- Sonnenfield, P. (1975). The Significance of Upper Miocene (Messinian) Evaporites in the Mediterranean Sea. Jour. Geol., v. 83, p. 287-311.
- Stanley, D. J. (1977). Post-Miocene Depositional Patterns and Structural Displacement in the Mediterranean. In: The Ocean Basins and Margins, ed. A.E.M. Narin, W. K. Kanes and F. G. Stehli, Plenum Press, N.Y., v. 4A, p. 77-150.
- Stanley, D. J. (1972). The Mediterranean Sea: A Natural Sedimentation Laboratory. Dowden, Hutchinson Ross, Stroudsburg, Penn., p.1-765.
- Vidmar, P. J. (1980). The Dependence of Bottom Reflection Loss on the Geoacoustic Parameters of Deep Sea (Solid) Sediments. Jour. Acous. Soc. Amer., v. 68, p. 1442-1453.

UNCLASSIFIED

SECURITY CLASSIFICATION OF THIS PAGE (When Data Entered)

REPORT DOCUMENTATION PAGE		READ INSTRUCTIONS BEFORE COMPLETING FORM
1. REPORT NUMBER <b>NORDA Technical Note 99</b>	2. GOVT ACCESSION NO. <b>AD-501 301-7</b>	3. RECIPIENT'S CATALOG NUMBER
4. TITLE (and Subtitle) <b>Geoacoustic Models for the Straits of Sicily and Sardinia-Tunisia</b>		5. TYPE OF REPORT & PERIOD COVERED
		6. PERFORMING ORG. REPORT NUMBER
7. AUTHOR(s) <b>J.E. Matthews</b>		8. CONTRACT OR GRANT NUMBER(s)
9. PERFORMING ORGANIZATION NAME AND ADDRESS <b>Naval Ocean Research and Development Activity NSTL Station, Mississippi 39529</b>		10. PROGRAM ELEMENT, PROJECT, TASK AREA & WORK UNIT NUMBERS
11. CONTROLLING OFFICE NAME AND ADDRESS <b>Naval Ocean Research and Development Activity NSTL Station, Mississippi 39529</b>		12. REPORT DATE <b>April 1982</b>
		13. NUMBER OF PAGES <b>74</b>
14. MONITORING AGENCY NAME & ADDRESS (if different from Controlling Office)		15. SECURITY CLASS. (of this report)  <b>UNCLASSIFIED</b>
		15a. DECLASSIFICATION/DOWNGRADING SCHEDULE
16. DISTRIBUTION STATEMENT (of this Report) <b>Unlimited</b>		
17. DISTRIBUTION STATEMENT (of the abstract entered in Block 20, if different from Report)		
18. SUPPLEMENTARY NOTES		
19. KEY WORDS (Continue on reverse side if necessary and identify by block number) <b>geoacoustic models                      geophysics</b> <b>acoustics                                  bottom interaction</b> <b>geology                                    shallow water</b>		
20. ABSTRACT (Continue on reverse side if necessary and identify by block number) <b>This publication documents the derivation of geoacoustic models for the Straits of Sicily and Sardinia-Tunisia. The geologic description of the region is based upon published geological/geophysical papers and archive data. The zone of primary concern is the first few hundred meters below the sea floor, which, in the present case, consists of unlithified Quaternary-Pliocene sediments. Lying below this upper layer is acoustic basement, which consists of Miocene chalks and limestones or evaporites. The modeling procedures developed by E.L. Hamilton were</b>		

DD FORM 1 JAN 73 1473

EDITION OF 1 NOV 65 IS OBSOLETE  
S/N 0102-LF-014-6601

UNCLASSIFIED

SECURITY CLASSIFICATION OF THIS PAGE (When Data Entered)

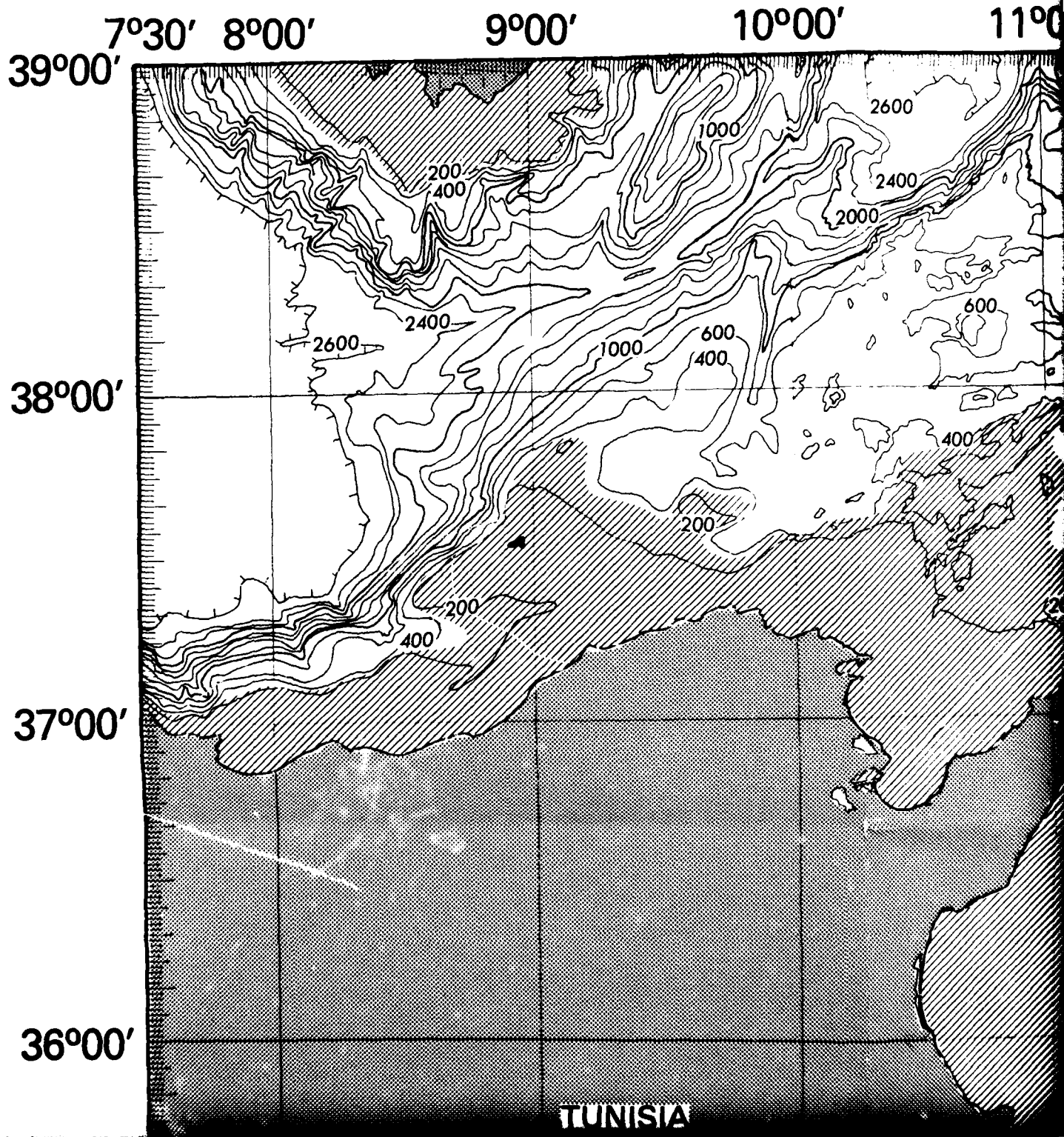
**UNCLASSIFIED**

**SECURITY CLASSIFICATION OF THIS PAGE (When Data Entered)**

then used to estimate the physical properties of these sediment types. Finally, bottom loss as a function of grazing angle at a variety of frequencies was computed for the sea floor models.

**UNCLASSIFIED**

**SECURITY CLASSIFICATION OF THIS PAGE (When Data Entered)**



**BATHYMETRY**  
**Straits of Sicily and Sardinia–Tunisia**  
with  
**Acoustic Bottom Interaction Province Classification**

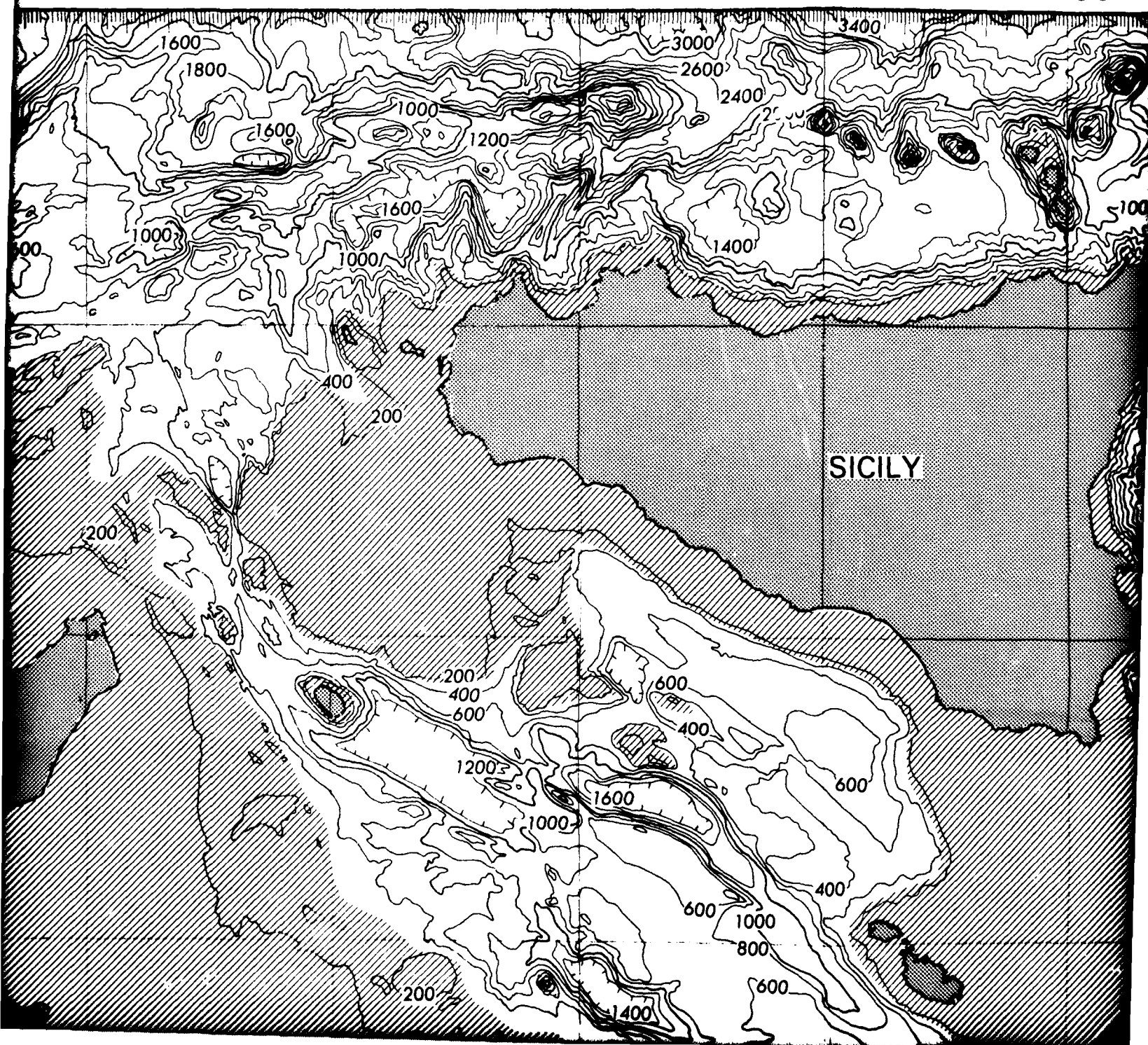
11°00'

12°00'

13°00'

14°00'

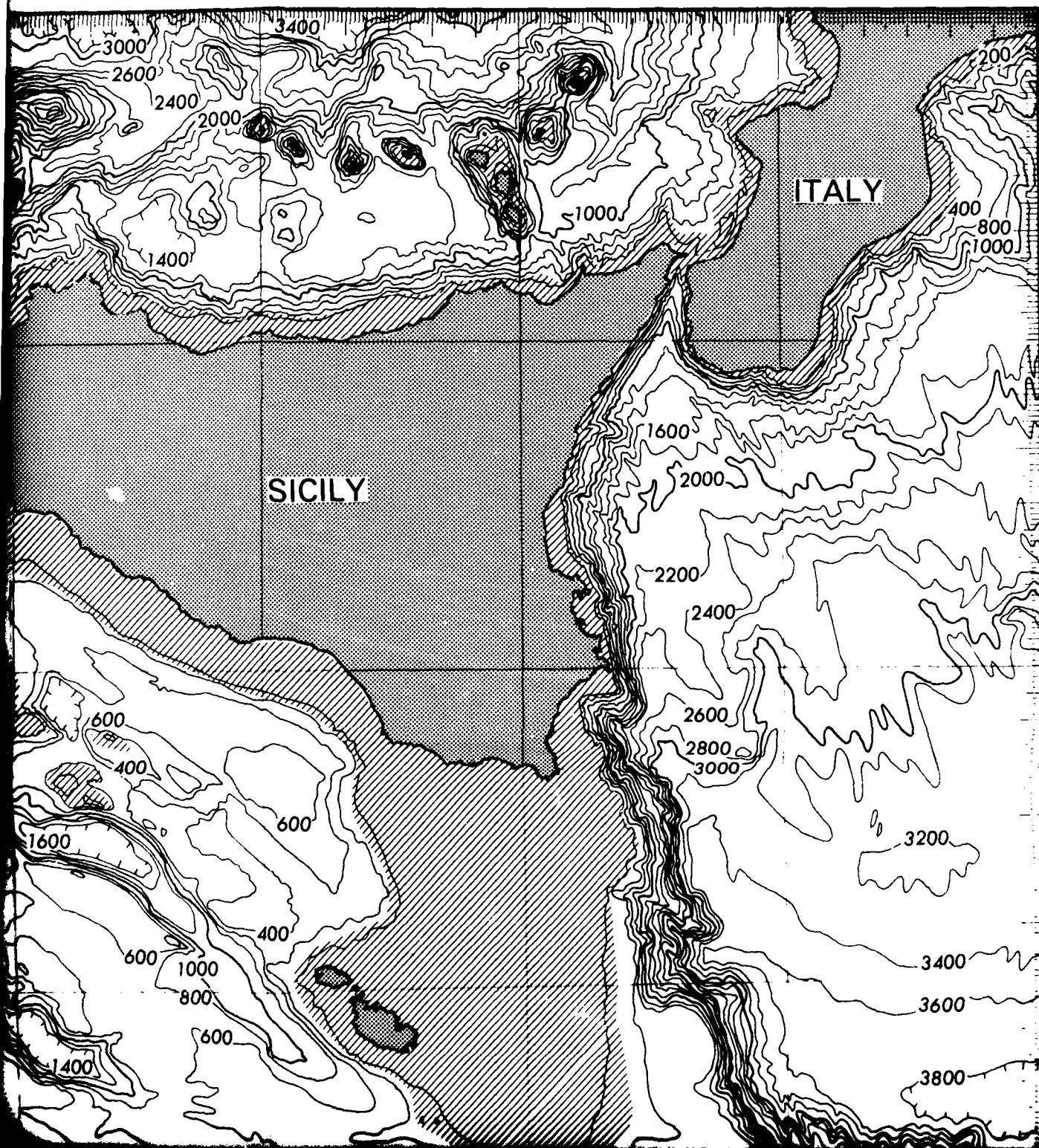
15°00'



# Tunisia

## Classification

00' 14°00' 15°00' 16°00' 17°00'



37°00'

36°00'

35°00'

34°00'

TUNISIA

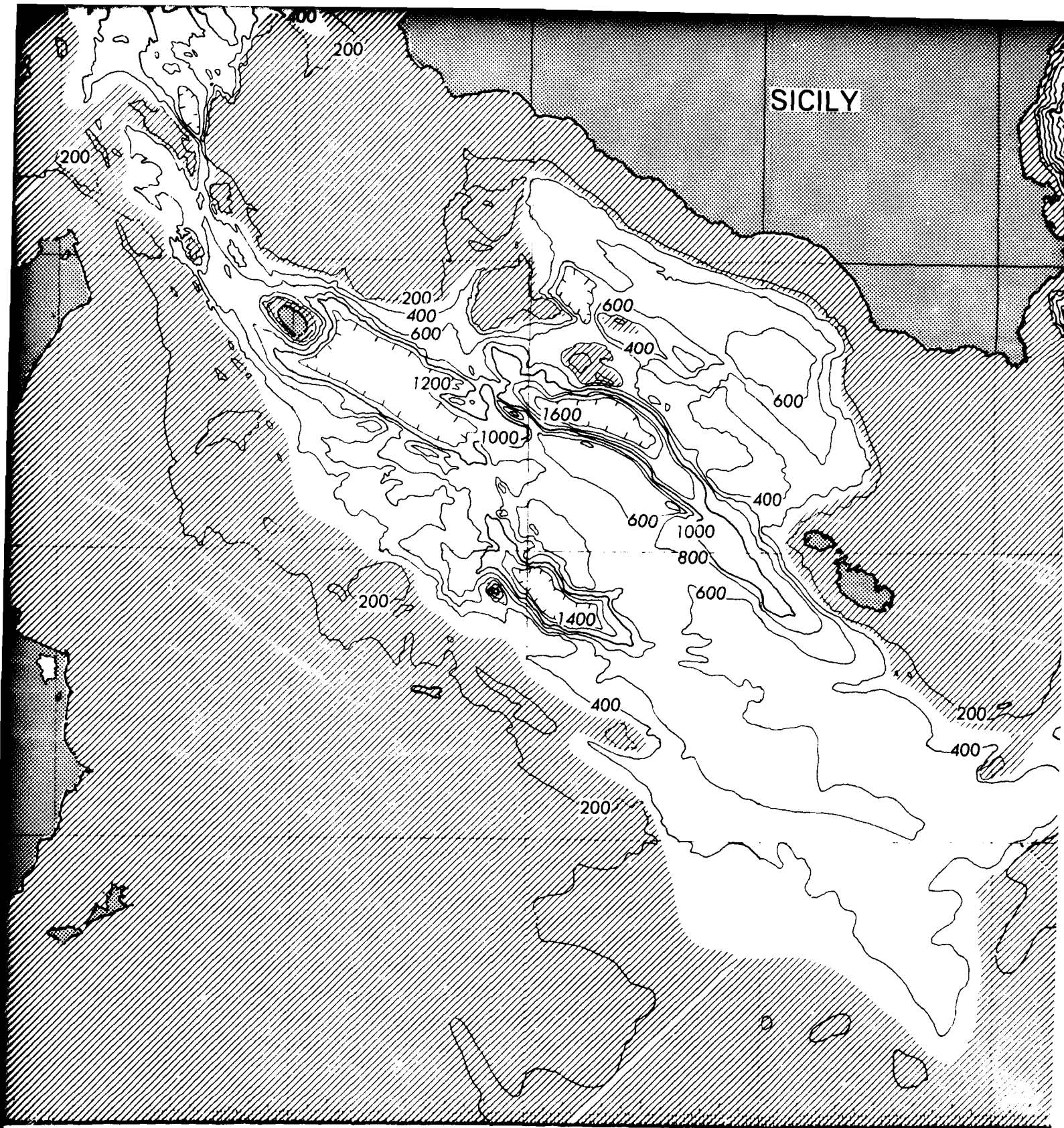
Contours based upon Sheets 3506N, 3507N, and 3607N of NOO-SP-1304 Bottom Topography of the North Atlantic and Adjacent Seas, U.S. Naval Oceanographic Office, 1975. Additions from unpublished recontouring of the original data by Messrs. F.H. Sorenson, F.L. Marchant, and T.G. Carter of the U.S. Naval Oceanographic Office. Addition of the USNS WILKES January 1980 and USNS BARTLETT July 1980 tracks, and final editing by J.E. Matthews of the Naval Ocean Research and Development Activity.

PROJECTION: Mercator

SCALE: 1° longitude = 2 inches

CONTOUR INTERVAL: 200m

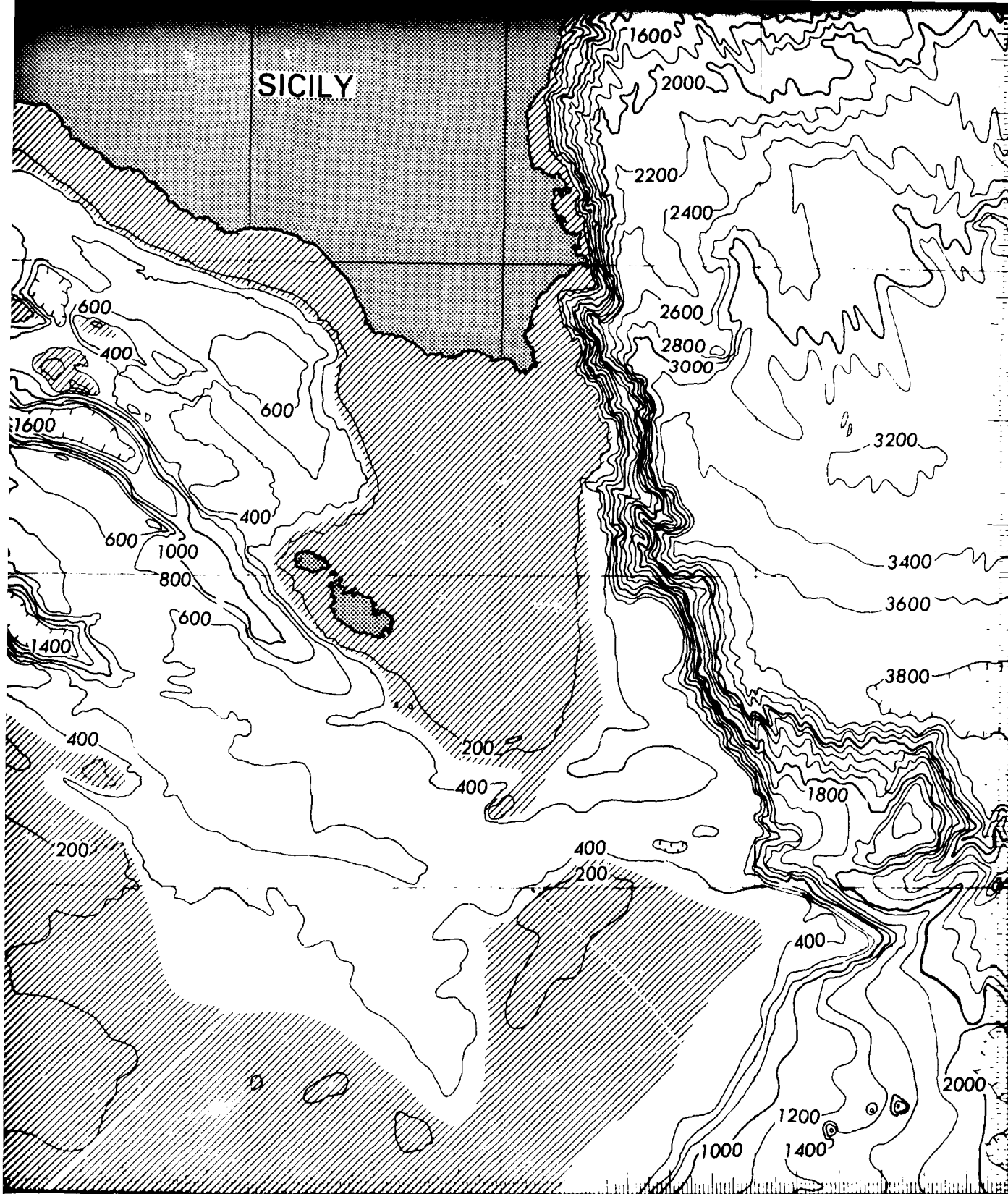
Depths in uncorrected (sonic) meters.  
assumed sound speed of 1500 m/s.



Regions where the use of Geoacoustic Model I is recommended.



Regions where the use of Geoacoustic Model IIA is recommended.



c Model I is recommended.

c Model IIA is recommended.



Sea Floor Division  
 Naval Ocean Research and Development Activity  
 Ocean Science Technology Laboratory  
 NSTL Station, Ms. 39529

